Slovak Geol. Mag., 20, 1 (2020), 49 – 84

3. Analytical Pseudo Lumped-Parameter Model for Reservoir Response and Recovery Assessment: Case Study for the Ďurkov Depression Hydrogeothermal Structure, Košice Basin, Slovakia

Fričovský Branislav, Vizi Ladislav, Fordinál Klement, Surový Martin & Zlocha Marian

State Geological Institute of Dionýz Štúr, Mlynská dolina, Bratislava, Slovak Republic, branislav.fricovsky@geology.sk

Abstract: Use of analytical and lumped parameter models (ALPMs) meets multiple limits in praxis given by many necessary assumptions and generalizations simplifying complexity of geothermal reservoir. Ability to adjust assumptions to local conditions through analytical function is, though, a robust advantage of ALPMs where relevant field production, observation and monitoring data are missing or are of unsound quality. The paper presents construction, upscaling and discussion to results of a complex ALPM model of thermal breakthrough, reservoir response and recovery estimator. A thermal breakthrough model shows a constant production of P_{th} = 38 MWth as a critical capacity to avoid cooling of production zone as long as D = 800 m and T_{inj} = 65 °C ($t_B > t_{prod}$ = 100 yrs). Introduction of tolerable cooling at a rate of $T_{wh,t(crit)} = 0.9T_{wh}$ = 122 °C so that a shut-in realizes at $t_{si} = t_{Twh,t(crit)}$ increases the capacity towards P_{th} = 51 MWth, yet more conservative proposal of P_{th} = 49 MWth is subjected to a case-study, matching results of energy balance based sustainability classification. Case studies document well a stepwise field development can reduce risks of incidental shut-in. Recovery model conservatively estimates energy recovery in a production zone as long as $T_{top,crit} \geq 80$ °C, $T_{res,t} \geq 138$ °C and $t_{reco} = t_{si} \geq 60$ yrs. Under sustainable production limitations, a system may be capable to produce $E_{TH(122)}$ = 45 – 46 TWh,th at the $t_{prod} = t_{si}$ = 100 yrs.

Key words: sustainability, reservoir response, reservoir recovery, lumped parameter models, Ďurkov Depression, Slovakia

3.1 Introduction

Geothermal energy is repeatedly reported a renewable and sustainable resource (Axelsson, 2010, 2011). Numerous examples worldwide show both can easily be exposed once excessive production is launched or maintained over a certain period of time. Concerns on sustainability and renewability resulted in a fair definition of sustainable reservoir production (Axelsson et al., 2001), according to that *"for each geothermal system and each mode of production there is a certain level of maximum energy production – E_0 below which it will be possible to maintain constant energy production for a very long time (100 – 300 years). Geothermal energy production below or equal the E_0 is termed sustainable production, while production greater than E_0 is termed excessive production"*. The frame of 100 to 300 years is further discussed in Axelsson et al., (2002, 2004); or Axelsson (2011, 2012a,b). The 100 years period is a compromise between longevity of a resource operation (meeting plural of "future generations" as defined in definition of sustainable development), and a period over which mankind development (including technologies) is somewhat predictable. This is, though, considerably longer period than that of 30 – 50 years set typically according to amortized lifetime of geothermal projects (e.g. Sanyal, 2005; Fridleifsson et al., 2008). Note the definition of sustainability addresses an impact on how a resource is used. Renewability, instead, describes a system for which "*the energy removed from the resource is continuously replaced by more energy on time scales similar to those required for energy removal and those typical of technological or societal systems*" (Rybach et al., 1999; Rybach & Mongillo, 2006; Rybach, 2007). Essentially, this rather addresses the resource characteristics and energy balance in the system, i.e. natural aspects. Conservation of renewability could, thus, be achieved through optimizing a resource production for a level a system would be capable to simultaneously (or in an equal period of time) replace removed energy, including restoration of initial state, such is distribution of heat flow anomalies, heat flux endmembers contribution etc.

Indeed, progressive growth in research, exploration and development of geothermal fields has challenged issues on a resource renewability and sustainability; crucial as long as geothermal energy is considered amongst resources to supply worldwide primary energy mixes according to a scheme of sustainable development (Stefansson, 2005; Fridleifsson et al., 2008; Rybach, 2010a,b). Numerous fields worldwide have, however, observed unexpected changes in reservoir and state conditions (e.g. cooling, phase transition, changes in chemistry), such is an example of The Geysers, Matsukawa, Laugaland, Ytri-Tjarnir or Cerro Prieto (DiPippo, 2005; Flóvenz et al., 1995, 2010; Yasukawa & Sasada, 2015; Gutiérrez & Negrín, 2005). Solutions on questionable production longevity have been approached either through contribution of reservoir engineering or energy / withdrawal or customers' policies (e.g. Flóvenz et al., 1995). These examples, amongst dozens of others, demonstrated that both, renewability and sustainability of geothermal resources can instantly be adjusted to their natural state, yet so easily can be questioned during production.

A role of geothermal reservoir engineering is, thus, not only in a design of reservoir operation, but takes significant contribution to:

- approaching a compromise between longevity and feasibility of production; and
- research and approval of capacity / deliverability a system is able to maintain for a long-term production.

Both issues can be tackled through combination of reservoir monitoring, modelling and simulations. Dozens of concepts on geothermal reservoir simulation and modeling were developed through decades that vary in magnitude of complexity, simplification, mathematical and geostatistical background (extensive reading in O'Sullivan et al., 2001; Burnell et al., 2015) or scope. Complex numerical models provide a way better screen on reservoir parameters and plausible response (e.g. Blöcher et al., 2010; Brehme et al., 2014; Bujakowski et al., 2016). On the other hand, they also require a sound input databasis from prospection and production monitoring (Axelsson, 2012b), including repeating recalibration (e.g. O'Sullivan et al., 1998), turning them time consuming. Lumped parameter or analytical models (e.g. Axelsson, 1989; Alkan & Satman, 1990; Sarak et al., 1995; Hyashi et al., 1999; Onur et al., 2008) apply robust simplifications to reservoir parameters (Sanyal & Sarmiento, 2005; Grant & Bixley, 2011). Still, they also provide a fair hint on prediction analysis especially at situations with lack of reliable or long-term monitoring data; where numerical models would yield robust uncertainties. Not regarding to what kind of model is constructed, each new data accessible subsequently urge its testing and recalibration.

Use of models (simulations) capable to predict (at a given confidence level) reservoir behavior in a response to its production is an exact example on application of modeling strategies in approaching concept of sustainable geothermal production and sustainable development. There is, however, an extensive group of models (frameworks; more reading in Shortall et al., 2015a,b) that scope sustainability of geothermal production or projects differently, e.g. through:

- balancing recent operation to probable reserves at a site – the reserve capacity ratio (Bjarnadottir, 2010; Fričovský et al., 2020a) on regional or national scales;
- evaluation of the project interaction with the environment (physical, chemical, biota) and society (economical, cultural, societal, technical); such is the rapid impact assessment matrix (Pastakia & Jensen, 1998; Ijäs et al., 2008) used in geothermal applications (e.g. Arevalo, 2003; Yousefi et al., 2009; Phillips, 2010a,b; González et al., 2015);
- thermodynamic optimization using efficiency analysis, exergoeconomics and derived indexes, i.e. the sustainability index, improvement potential etc. (e.g. Ozgener et al., 2007; Utlu & Hepbasli, 2008; Gungor et al., 2011).

The Ďurkov Depression hydrogeothermal structure (DDHS) is considered perspective since pioneering prospection on oil and gas in the Košice Basin from 70's (Vranovská et al., 1999a). Conduction of first hydrogeothermal evaluation in late 90's (Vranovská & Bodiš, 1999; Vranovská et al., 1999a,b, 2002) proved high thermal energy potential of the site, installing three geothermal wells (GTD-1 to GTD-3) to assess a potential of 41.8 MWth in overflow regime and 92.6 MWth obtainable by pumping, including need of reinjection. Applied studies emerged soon, whether aimed at heat supply for the city of Košice (e.g. Halás et al., 1999; Vranovská et al., 2000) or at possibilities on binary cogeneration cycles and working fluid selections (Popovičová & Holoubek, 2011; Kukurugyová et al., 2015a,b) and their tentative environmental impact through CO_2 emission reduction (Fričovský et al., 2013). Geothermal field and hydrogeothermics were approached through 3D (matrix driven) modelling (Pachocká et al., 2010); conceptual models on reservoir fluid origin and chemistry (Bodiš & Vranovská, 2012; Vranovská et al., 2015); crustal-scaled (Majcin et al., 2017) or regional thermal field modelling (Jacko et al., 2014); reservoir heat flow analysis (Fričovský et al., 2018b,c); or reservoir thermodynamics (Fričovský et al., 2019; Vizi et al., 2020).

A first production sustainability assessment at a site was conducted in 90's using TOUGH2 code (Giese, 1998, 1999). The model used orthogonal regular grid and borehole data, considering purely conductive environment for 2:1 producer – injector scheme scheduled to operate at a scale of 40 years and at a rate of 225 $l.s^{-1}$. Reinjection temperature was set to T_{inj} = 25 °C. A models shows no thermal breakthrough at a given capacity, implying thermal output of P_{th} = 92.6 MWth sustainable under given conditions. Recently Fričovský et al. (2019) presented results of geothermal reserves booking in combination with reserve capacity ratio (Bjarnadottir, 2010) applied to the DDHS, challenging a thermal output of P_{th} = 49 MWth as critical capacity considering reservoir production sustainability through energy balance.

The paper presents complete reconstruction and upscaling of analytical pseudo lumped-parameter models (ALPMs) at comprehensive theoretical background (Axelsson, 1989; Sarak et al., 2005; Onur et al., 2008; Tureyen et al., 2009; Satman, 2010, 2011; Tureyen & Akyapi, 2011; Satman & Tureyen, 2012) for the Ďurkov Depression hydrogeothermal structure. The entire module consists of:

- thermal breakthrough estimator using advective production-based model for doublets (Ungemach et al., 2005, 2009), involving propagation retardation through conductive effective thermal-exchange profile heating from surroundings (Sauty et al., 1980; Menjoz & Sauty, 1982);
- 1TIQ (1-tank closed ALPM with heat influx and reinjection) model for reservoir response during production since breakthrough (t_B); and
- 1TER (1-tank closed ALPM) model for energy recovery after production shut-in (t_{si}).

The entire estimator module is designed as non-linear and non-isothermal, i.e. production characteristics at time t+1 are function of a reservoir state at time t; and thermal field is subjected to plausible variation in contribution of convection and conduction, while radiogenic heat production is left constant. Both, 1TIQ and 1TER algorithms are designed to cover a desired period of production of t_{prod} = 100 yrs to match theory beyond a concept of sustainable reservoir production (Axelsson et al., 2001). Unlike apparently conventional boundary shut-

in condition given by breakthrough, the 1TIQ and 1TER work on invoking a tolerated cooling rate $T_{wh,t(crit)}$ (Tester et al., 2006; Sutter et al., 2011; Fox et al., 2013; Williams, 2007, 2014), i.e. as long as temperature at a wellhead at time t falls beneath 90 % of a steady-state, i.e. $t_{si} = t_{Twh,t(crit)}$.

In following, both algorithms are tested in a range of optional constant production scenarios P_{th} = 1 – 240 MWth, referenced to a return temperature of T_{inj} = 65 °C, as well as a case of step-wise field development is presented. Besides response of temperature, estimates on thermal field dynamics and response are presented in terms of heat flow end-members contribution and variation. This is crucial when searching for fluid phase stability during considered production.

Note that models have not been history-matched, limiting gained representativeness. Authors do not consider, however, accessible monitoring data from 21-days long pumping tests reliable, hence during production, multiple drawdowns were induced. Instead, more focus has been given to field and heat flow analysis. Use of analytical functions in a single module allow easy recalibration as long as new and sound data are available from (pre) production monitoring. Up to authors best knowledge, any other isothermal, nor non-isothermal lumped parameter modelling has been carried to study the DDHS.

Gained results must, thus, not be considered definitive. Instead, a goal of carried study is to set a baseline at given reliability level for initial production opening considerations, providing safe time span to carry sound reservoir monitoring campaign, recalibrate models, and, finally, optimize production; approaching sustainable and renewable use of a geothermal resource.

3.2 Site description

The DDHS (Fig. 3.1) represents a depressed morphostructure of multiply dissected Mesozoic carbonates underlying Neogene sedimentary fill of the Košice Basin, a NE promontory of the Pannonian Basin (Pereszlenyi et al., 1999). At an approximate area of 33.6 km^2 the system is defined structurally at subsurface extension of Neogene complexes of the Slanské vrchy Mts., whilst terminates along tectonic lines with the Bidovce depression (N), or elevated (uplifted) Mesozoic bedrock (the Vyšný Čaj – Oľšovany – Ďurďošík and Ruskov – Vyšný Čaj junction) to the W and S (Vranovská et al., 1999a, 2000).

A vertical profile (Fig. 3.2) begins with polygeneous Quaternary accumulations at small (< 10 m) thickness, essentially neglected in deep structural models.

Neogene succession reaches up to 2,000-3,000 m; with Sarmatian clays (200 to 1,200 m thick) and rare andesite to rhyolite volcanism products atop Badenian carbonate sandy clays intercalated rarely with tuffites and shales (thickness up to 1,500 m). Karpatian conglomerates that transit to carbonate clays and evaporates form a base of the profile (Pereszlenyi et al., 1999; Vranovská et al., 1999a, 2000).

Mesozoic carbonates are considered as analogue to the Krížna Nappe series of the Western Carpathians (Vranovská & Bodiš, 1999). Transiet varieties, i.e. the carbonate dolomites and dolomitic carbonates prevail. Brecciation and karstification reflects pre-Tertiary uplift and paleo-karstification (Činčura & Köhler, 1995) diminishing towards the base of the reservoir. Thickness of carbonates increases quasi-axially from peripheries (200 m) to central part of the structure (Vranovská et al., 1999a,b) (2,200 m). A top of the reservoir is at 1,660-2,600 m.b.t., a base sinks o 1,960-4,000 m (Vranovská et al., 1999; Fričovský et al., 2018a). Tectonic dissection of the morphostructure owes to three generations of faults in the SW-NE, NW-SE and N-S direction (Bodiš & Vranovská, 2012). A few is known about pre-Mesozoic basement, however, analogously to the Western Carpathians, crystalline complex (magmatites

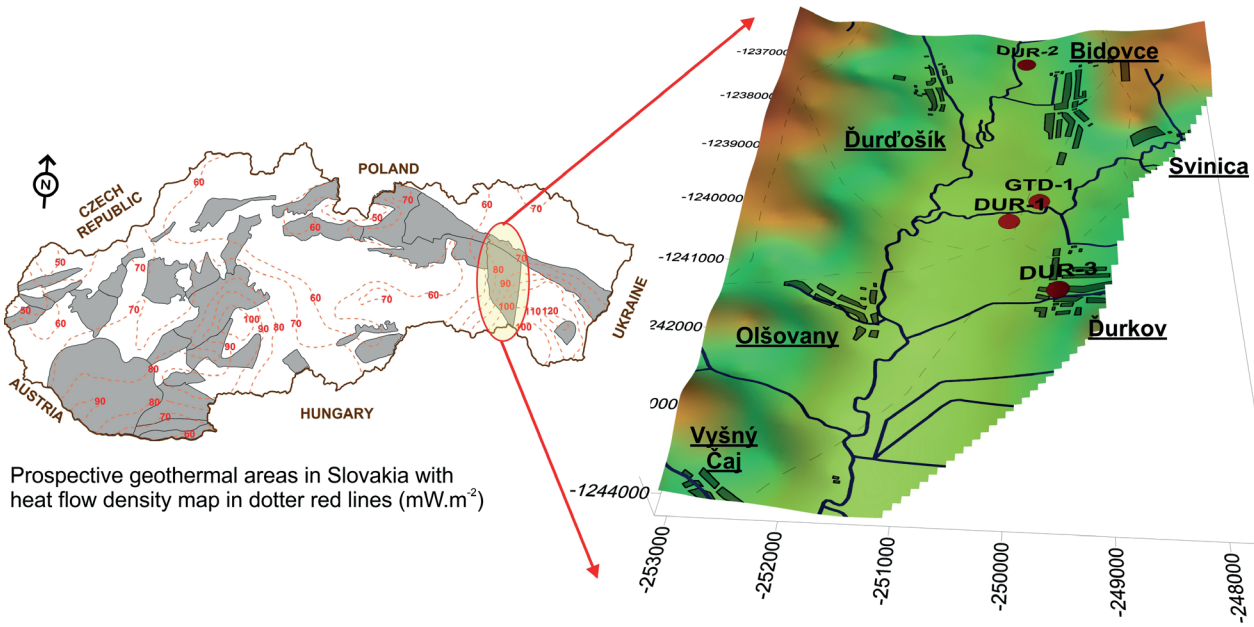

Fig. 3.1. Position of the Ďurkov Depression hydrogeothermal structure within geothermal water bodies of the Slovakia and surface heat flux density distribution. Note resolution is not enough to identify all GTD wells, too close to position of GTD-1.

and metamorphites) of the Veporic unit is expected instantly beneath (Pereszlenyi et al., 1999). The entire crust is roughly 30 km thick (Bielik, 1999).

Saturated geothermal water forms a resource of low to moderate-low thermodynamic quality, i.e. specific exergy index is estimated for SExI = 0.04-0.25 (a mean of 0.11) and moderate temperature / enthalpy, T_{res} = 80-180 °C (Vranovská et al., 1999b; Fričovský et al., 2018a) at TDS of 20.4 to 33.1 g.l^{-1} (Bodiš & Vranovská, 2012).

Geothermal brine originated as infiltrated meteoric water seeped to Neogene strata, dissolving evaporates and reacting with Hg-As-Sb type mineralization prior reaching Mesozoic carbonates. Hence signs on recent reservoir media degradation are missing, the system is generally considered closed. Brines are high in arsenic content, i.e. 19-36 mg.l^{-1} and total dissolved solids, up to 31 g.l^{-1} (Vranovská et al., 2015).

A surface heat flow density is 105-115 mW.m^{-2}. A mean geothermal gradient differs of 51.2 °C.km^{-1} for Neogene and 29.4 °C.km^{-1} for Mid Triassic horizon (Vranovská et al., 2015). Neither temperature distribution (Fig. 3.3), nor use of linear stability analysis at horizontal (Fričovský et al., 2018b; Vizi et al., 2020) or inclined (Fričovský et al., 2018c) conditions proven existence of complex convective zones. Instead, if any, stable, insulated cells may form in deepest parts of the system, limited within particular blocks, restraining progressive adiabatic boiling. Yet this system is off any geodynamically active zone, it meets concepts of conductive plays of orogenic belt type (Moeck, 2014; Moeck & Beardsmore, 2014).

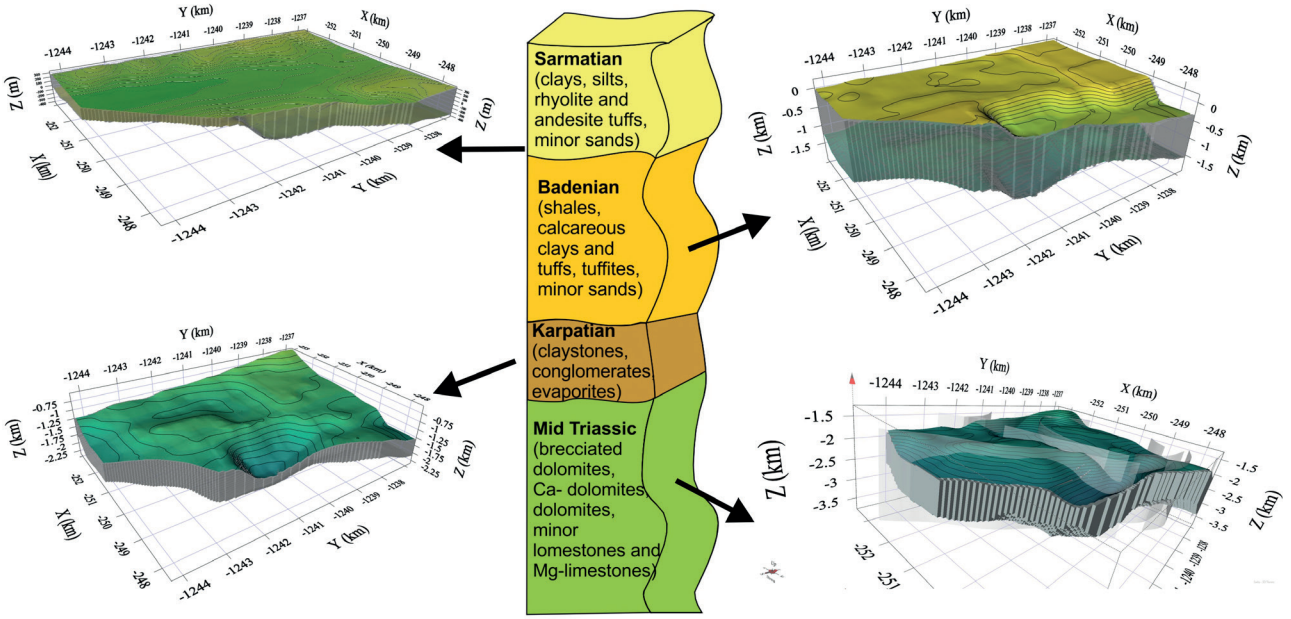

Fig. 3.2. *Deep geological profile of the Ďurkov Depression hydrogeothermal structure.*

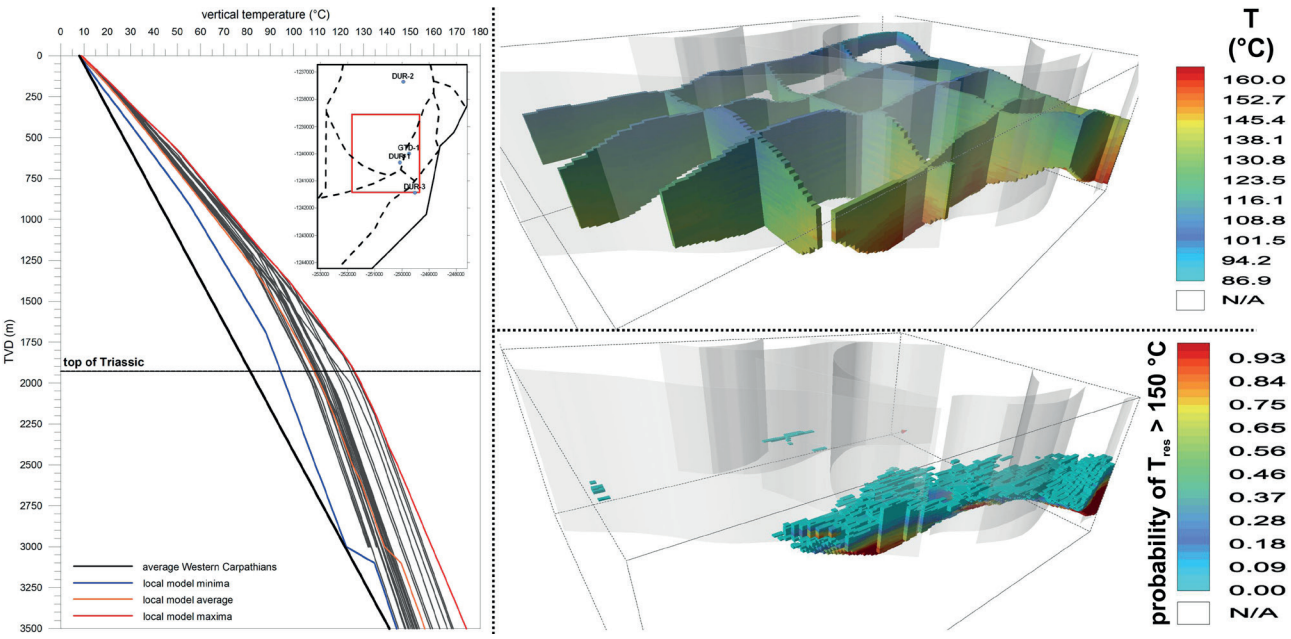

Fig. 3.3. *Horizontal and vertical temperature distribution.*

3.3 Analytical pseudo lumped-parameter model – theory beyond

Lumped parameter models (LPMs) "simplify" a hydrogeothermal system into one "tank" (1T) or multiple "tanks" representing different parts of the system or reservoir and the recharge zone connected to a constant-pressure recharge zone (open - O) or having a point-source reinjection at a margin (closed - C) – see generalized scheme on Figure 3.4.

LPMs have been developed to substitute numerical models in reservoir pressure changes simulations under a lack of adequate data that subsequently yields errors due to many necessary approximations. Early LPMs tackled simulation as an inverse problem, fitting analytical response function to observed data by non-linear iterative least-square techniques (Axelsson, 1989), later replaced by Levenberg-Marquardt method based algorithm for history matching and objection function error mitigation (Sarak et al., 2003a).

At their very beginning, LPMs assumed negligible temperature changes in reservoir, turning this approach applicable to low or moderate enthalpy systems (Onur et al., 2008). Although several non-isothermal LPMs were designed later (Onur et al., 2008; Tureyen et al., 2009, 2014; Tureyen & Akyapi, 2011), they all consider a single phase, liquid (water) dominated reservoir media. Some insights into two-phase and vapor-dominated models were carried by Alkan & Satman (1990) or Hosgor et al. (2013).

3.3.1 Model configuration (number of tanks) selection

Although multiple options were available, we consider a *one (single) closed – tank model* as representative at local conditions. The configuration is justified according to:

- closed hydrogeological character (uplift at faults is up to 400 m, no geochemical indices on chemistry degradation through natural recharges - i.e. Mg^{2+} increase or Cl^- decay); and
- necessary reinjection (producer / production well PW to injector / injection well IW distance ca. 800 m, geothermal brine chemistry).

On Figure 3.4, the reservoir represents a productive part of targeted formation at given hydraulic and geothermal conditions. Aquifer stands for distal, peripheral parts of system in connection to reservoir itself, be it, e.g. a transition zone. Both are, however, "capacitors", i.e. simulate tank with capacity to accumulate a fluid. Hydraulic "conductors" describe capacity of a system to transit the fluid from periphery (recharge zone, injector) towards producer.

3.3.2 Mass balance in one-tank closed model

The reservoir mass balance during production can be assessed through a current mass M_c equation (1) modified for the closed system equaling $M_{rech} = 0$ (2) as there is no recharge

$$M_c = M_{ini} - M_{prod} + M_{rech} + M_{inj} \tag{1}$$

$$M_c = M_{ini} - M_{prod} + M_{inj} \tag{2}$$

The fluid is a single-phase, saturated water, degassed artificially (e.g. Fričovský et al., 2018a,b), at conditions of compressed water expandable with decline in pressure (3). Differentiation of (2) and (3) to time using isothermal compressibility C_t defines the mass flow rate (Sarak et al., 2003a) in a closed tank as (4), assuming compressibility of water as a function of density (5) and compressibility of matrix (6) as function of porosity:

$$M_c = V_{res}.\phi_{res}.\rho_{w,res} \tag{3}$$

$$-\overset{\square}{m}_{prod} + \overset{\square}{m}_{inj} = V_{res}.\phi_{res}.C_{th}.\frac{dp}{dt} \tag{4}$$

$$C_{w,res} = \frac{1}{\rho_{w,res}}.\left(\frac{d\rho_{w,res}}{dp}\right)_{T_{res}} \tag{5}$$

$$C_m = \frac{1}{\phi_{res}}.\left(\frac{d\phi_{res}}{dp}\right)_{T_{res}} \tag{6}$$

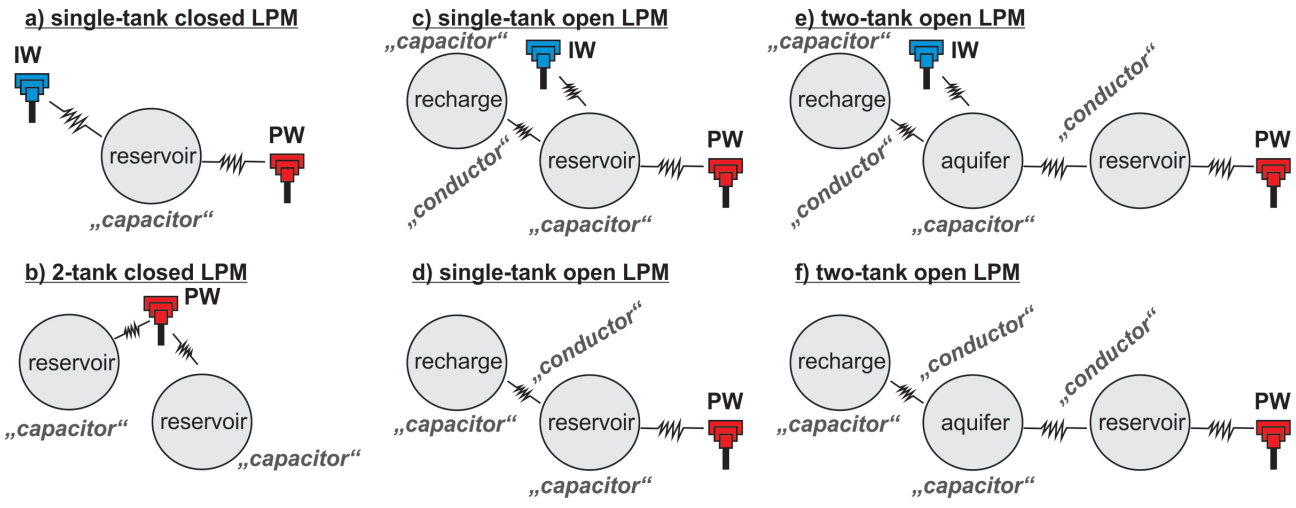

Fig. 3.4. *Schematics of lumped parameter models.*

If constant pressure boundary is assumed, the term of net production (7) characterizes a balance in reservoir mass per unit pressure change with time (8) for closed system:

$$\dot{m}_{prod} - \dot{m}_{inj} = \dot{m}_{net} \tag{7}$$

$$\dot{m}_{net} = V_{res}.\phi_{res}.\rho_{w,res}.C_t.\frac{dp}{dt} \tag{8}$$

The balance does not account for transient reservoir effects, nor extension of reinjection-induced cold-front propagation, essentially modifying reservoir matrix and media properties. Reduction of a problem to isothermal model is yet more accented as reinjection (due to robust temperature differences to the reservoir conditions) causes extensive non-isothermal changes especially when injection / production ratio is high (Sarak et al., 2005).

Now adjusting reinjection proportional to pressure difference between producer and injector (9) allows maintaining production / reinjection ratio constant and equal, so that $Q_{prod} = Q_{inj} = 1:1$, and so that net productivity (8) transforms to (10), with net reservoir storage capacity κ_{res} described as by Eq. 11 (Sarak et al., 2003a):

$$\dot{m}_{inj} = \Psi_{res}.\left(p_{inj} - p_{res}\right) \tag{9}$$

$$\dot{m}_{net} = \Psi_{res}.\left(p_{inj} - p_{res}\right).\kappa_{res}.\frac{dp_{res}}{dt} \tag{10}$$

$$\kappa_{res} = V_{res}.\phi_{res}.\rho_{w,res}.C_t \tag{11}$$

Assuming injection pressure constant (p_{inj} = const. as the $Q_{prod} = Q_{inj} = 1:1$ = const.), and pressure difference is $\Delta p = p_{inj} - p_{res}$, a first-order ordinary differential equation (Sarak et al., 2005) is obtained (12), solved according to initial conditions for reservoir pressure (13) or pressure difference (14):

$$\frac{\dot{m}_{net}}{\kappa_{res}} = \frac{d\Delta p}{dt} + \frac{\Psi_{res}}{\kappa_{res}}.\Delta p \;\Bigg|\; \begin{matrix} p_{res}(t=0) = p_{inj} \\ \Delta p(t=0) = 0 \end{matrix} \tag{12}$$

$$p_{res}(t) = p_{inj} - \frac{\dot{m}_{net}}{\Psi_{res}}.\left[1 - \exp\left(-\frac{\Psi_{res}.t}{\kappa_{res}}\right)\right] \tag{13}$$

$$\Delta p(t) = \frac{\dot{m}_{net}}{\Psi_{res}}.\left[1 - \exp\left(-\frac{\Psi_{res}.t}{\kappa_{res}}\right)\right] \tag{14}$$

3.3.3 Energy and mass flow in one-tank closed model

Alike shallow groundwater sources, the energy flux in the geothermal reservoir is of an essential importance. At initial (natural, undisturbed) conditions, the energy flow in the system is generally given by a balance between an energy inflow E_{IN} and outflow E_{OUT}. When the system is produced (Satman, 2010), the energy that is extracted through reservoir fluid removal is accounted. Rewritten to a term of cumulative energy, the balance becomes (15):

$$E_{prod} - E_{rech} - E_{inj} - E_{IN} - E_{OUT} = E_{ini} - E_{(t)} \tag{15}$$

Because $E_{IN} = -E_{OUT}$ in quasi-stable conductive environment, cumulative energy added and lost from the system are neglected in a balance. Simplification of (15) into (16) requires:

- to set energy produced E_{prod} (17) as function of a fluid withdrawal $Q_{prod,t}$ and change in wellhead temperature $T_{wh,t}$
- to mitigate natural energy recharge E_{rech} (18) to a system ($E_{rech} = 0$) as long as a tank is closed
- to adjust energy increment / removal to the system through reinjection E_{inj} (19) as function of mass withdrawal Q_{prod} and a time tprod as long as $Q_{prod} = Q_{inj}$ and T_{inj} = const. during production, or to turn $E_{inj} = 0$ after shut in as $Q_{prod} = Q_{inj} = 0$ during reclamation
- definition of initial reservoir energy content E_{ini} (20) as given by reservoir volume V_{res} and accumulated heat γ_a at initial conditions, i.e. $T_{res(t=0)}$; and
- to account an effect of reinjection on energy content and balance at time $t \neq 0$ $E_{t=i}$ as function of gradient between actual $T_{res,t}$ and reinjection T_{inj} temperature (21):

$$E_{prod} - E_{inj} = E_{ini} - E_{(t)} \tag{16}$$

$$E_{prod} = Q_{prod}.c_{w,wh}.\int_0^t \Delta T dt \tag{17}$$

$$E_{rech} = c_{w,rech}.\int_0^t Q_{rech}.\Delta T dt \tag{18}$$

$$E_{inj} = Q_{inj}.c_{w,inj}.T_{inj}.t \tag{19}$$

$$E_{ini} = V_{res}.\gamma_a.\Delta T_{t=0} \tag{20}$$

$$E_{t=i} = Q_{inj}.c_{w,inj}.\Delta T_{t=i} \tag{21}$$

Combining (16) to (21) yields different analytical models for a reservoir depending on a production management. For a *closed system with production only* (Satman, 2011) the energy – mass balance is proportional between the energy / fluid stored and its removal (22), expecting a temperature to decrease exponentially with abstraction of a heat in place (23 – 24):

$$V_{res}.\gamma_{a,res}.\frac{dT}{dt} = -Q_{prod}.c_{w,wh}.T_{wh} \tag{22}$$

$$T_{(t)} = T_{ini}.e^{-a.t} \tag{23}$$

$$a = \frac{Q_{prod}.c_{w,wh}}{V_{res}.\gamma_{a,res}} \tag{24}$$

A modification of a balance (22) can be made *adding reinjection* into a scheme (25). The reinjection

temperature T_{inj} is far less than that in the reservoir T_{res}. Fluid management balances reservoir pressure but so it induces cooling. For $Q_{prod} = Q_{inj}$ the rate of cooling (26) is proportional to a difference between $T_{res,t}$ and T_{inj} (T_{inj} = const.) during production, non-linearly increasing as cold-front propagates towards producers. At given specifications, the balance (25) and analytical functions for a single, closed tank model with reinjection are (Satman, 2011):

$$V_{res}.\gamma_{a,res}.\frac{dT}{dt} = -Q_{prod}.c_{w,wh}.T_{wh} + Q_{inj}.c_{w,inj}.T_{inj} \quad (25)$$

$$\Delta T = T_{ini} - T_{(t)} \rightarrow \Delta T = \left(T_{ini} + \frac{g}{a}\right).\left(1 - e^{-a.t}\right) \quad (26)$$

$$T_{(t)} = T_{ini}.e^{-a.t} - \frac{g}{a}.\left(1 - e^{-a.t}\right) \quad (27)$$

$$g = \frac{Q_{inj}.c_{w,inj}.T_{inj}}{V_{res}.\gamma_{a,res}} \quad (28)$$

Reservoir exploitation represents all but a natural state of a reservoir, with plausible formation of cooling-induced gradient within. A *closed system with production and heat increment model* (Satman, 2010) accounts the energy influx E_n in a general balance on a stored-heat site (29), set proportional to a heat gradient in the reservoir (30 to 32):

$$V_{res}.\gamma_{a,res}.\frac{dT}{dt} = -Q_{prod}.c_{w,wh}.T_{wh} + E_n \quad (29)$$

$$\Delta T = T_{ini} - T_{(t)} \rightarrow \Delta T = \frac{a.T_{ini} - x}{a}.\left(1 - e^{-a.t}\right) \quad (30)$$

$$T_{(t)} = T_{ini} - \frac{a.T_{ini} - x}{a}.\left(1 - e^{-a.t}\right) \quad (31)$$

$$x = \frac{E_n}{V_{res}.\gamma_{a,res}} \quad (32)$$

Essentially, the E_n substitutes the $E_{IN} - E_{OUT}$ balance. While at natural state the $E_{IN} - E_{OUT} = 0$ because $E_{IN} = E_{OUT}$, there is a heat gradient formation between the undisturbed zone (surroundings) and the effective heat-exchange profile (i.e. part of a reservoir body assumed dynamic according to pressure depression build-up and connectivity where reinjected fluid propagates to producer) during reservoir production.

Apparently, when combining equations (22), (25) and (29), an analytical model for a *single-tank, closed system with reinjection and a heat increment* is given by (33), with following functions (34 – 35) for temperature change and its function with time (Satman, 2011):

$$V_{res}.\gamma_{a,res}.\frac{dT}{dt} = -Q_{prod}.c_{w,wh}.T_{wh} + Q_{inj}.c_{w,inj}.T_{inj} + E_n \quad (33)$$

$$\Delta T = T_{ini} - T_{(t)} \rightarrow \Delta T = T_{ini}.\left(1 - e^{-a.t}\right) - \left[\frac{g'}{a}.\left(1 - e^{-a.t}\right)\right] \quad (34)$$

$$T_{(t)} = T_{ini}.e^{-a.t} - \frac{g'}{a}.\left(1 - e^{-a.t}\right) \quad (35)$$

$$g' = \frac{Q_{inj}.c_{w,inj}.T_{inj}}{V_{res}.\gamma_{a,res}} + \frac{E_n}{V_{res}.\gamma_{a,res}} \quad (36)$$

The solution of (33) to (36) (Satman, 2010, 2011) represents a general form of ALMP used to simulate estimates on reservoir response to production. A discussion on upscaling to adjust the general model to local conditions is provided in following chapter.

3.3.4 Energy recovery

In (33) to (36) the rate of reservoir cooling decreases with E_n, standing for a heat that is available in a reservoir when all its losses are subtracted from a balance (O'Sullivan & Mannington, 2006). As such, it is the sum of the heat that flows to the system, and is transported within the system by all available endmembers (37):

$$E_n = E_{CD} + E_{CV} + E_{RG} - E_{OUT} - E_{PROD} \quad (37)$$

The heat increment into produced part of a reservoir (profile of effective heat exchange) is definitely not constant. During production, the E_n increases with decline in $T_{res,t}$ and drop in temperature at top of the reservoir $T_{top,crit}$ as thermal gradient forms. At shut-in (t_{si}) the $E_{PROD} = 0$, and $T_{res,r}$ and $T_{top,r}$ starts to recover according to a state of $E_{n(t=tsi)}$. Recovery of $T_{res,r}$ and $T_{top,r}$ towards $T_{res,r} = T_{res}$ and $T_{top,r} = T_{top}$ causes an induced gradient to vanish. The E_n decreases, thus, simultaneously with approaching an initial state during reclamation (38). A rate of recovery (39) is, thus, proportional to thermal gradient ceasing, formulated as (Satman, 2011):

$$E_n = V_{res}.\gamma_{a,res}.\frac{d\Delta T}{d\Delta t} \quad \left| \begin{array}{l} \Delta T = T_{reco} - T_{top} \\ T_{top} = \text{const.} \\ T_{reco} = T_{si} \\ T_{reco} = T_{ini} \end{array} \right. \quad (38)$$

$$T_{reco} = T_{si} + x.\Delta t \rightarrow T_{si} + x.t_{reco} \quad (39)$$

Equations (32 and 39) require reservoir area and thickness equal for radiogenic heat production (E_{RG}), convection (E_{CV}) and conduction (E_{CD}). This yields a robust approximation, as e.g. in conductive low- or moderate- enthalpy basin systems convection cells may develop as insulated and limited in extension (such is a case of DDHS – Fričovský et al., 2018b,c), so that $V_{(CD)} >> V_{(CV)}$. Consequently, necessary upscaling changes a form (32) into (40) accounting on heat endmember geometry limitations:

$$\sum x = x_{(CD)} + x_{(CV)} + x_{(RG)} = \frac{E_{CD}}{A_{CD}.H_{CD}.\gamma_{a,CD}} + \frac{E_{CV}}{A_{CV}.H_{CV}.\gamma_{a,CV}} + \frac{E_{RG}}{A_{RG}.H_{RG}.\gamma_{a,RG}} \quad (40)$$

Thermal recovery terminates at thermal equilibrium, i.e. at $T_{res,r} = T_{res}$ and $T_{top,r} = T_{top}$ at a time t_{reco}, when heat flux into the system is balanced by natural heat losses such is a surface heat flux or heat transmission to surroundings

according to $E_n = E_{CD} + E_{CV} + E_{RG} \rightarrow lim\ E_{OUT}$. For closed-tank model, the analytical solution to search for a t_{reco} is (41):

$$t_{reco} = \frac{T_{ini} - T_{si}}{x} \quad (41)$$

3.3.5 Thermal breakthrough

The thermal breakthrough is an essential feature of reservoir response to production, whether considering natural recharge and/or reinjection. Selection of model to predict a breakthrough gains considerable credits in reservoir engineering especially when question of production longevity is considered, yet not necessarily causing a shut-in. Instead, a rate of cooling is questioned through concept of sustainability according to boundary conditions defined at a level of tolerable drop in reservoir / wellhead temperature (e.g. Williams, 2007).

Numerous analytical models have already been introduced in past, different in accounting heat transfer endmembers to contribute on cooling and its retardation. As based on local geothermal settings and data quality, an advective model with diffuse retardation for doublet systems (Gringarten & Sauty, 1975; Ungemach et al., 2005, 2009) was applied. The model is based on parametrical heat transfer equation (42), assuming hydraulical insulation of a reservoir at a top and a base and matrix homogeneity (Gringarten & Sauty, 1975). Cone-shaped cold-front propagation during time t_B (43) at a distance D and thickness H_{eff} (Ungemach et al., 2005) is assumed. Thermal diffusion slows cooling at a contact of injected fluid with matrix, increasing with D. A front cools the effective profile adjectively, accenting a rate of reinjection Q_{inj} at constant T_{inj}. A rate of thermal diffusion is given by a coefficient of heat exchange Λ_{CD} (44), implying minimum conductive retardation for $\Lambda_{CD} \rightarrow \lim\infty$ and rapid diffuse slowing of advective cold-front transport for $\Lambda_{CD} \rightarrow \lim 0$ (Gringarten, 1978; Sauty et al., 1980):

$$div\left(\lambda_B \nabla T\right) - div\left(\rho_{w,inj}.c_{w,inj}.v_D.T_{inj}\right) = \gamma_{a,res}.\frac{dT}{dt} \quad (42)$$

$$t_B = \frac{\pi}{3}.\frac{c_{w,inj}.\rho_{w,inj}}{\gamma_{a,res}}.\frac{Q_{inj}.H_{eff}}{D^2} \quad (43)$$

$$\Lambda_{CD} = \frac{c_{w,inj}.\rho_{w,inj}.\gamma_{a,res}}{\lambda_B.\rho_m.c_m}.\frac{Q_{inj}.H_{eff}}{D^2} \quad (44)$$

3.4 Analytical pseudo lumped-parameter model – upscaling

3.4.1 Production scheme

The model represents a one-tank closed system, localized within the Ďurkov Depression hydrogeothermal structure. In reference studies (e.g. Vranovská et al., 1999a,b; Giese, 1998, 1999), the producer – injector scheme is considered 2:1. Constructed ALPM simplifies a situation neglecting number of production and injection wells (Fig. 3.5).

The *distance D* is calculated as horizontal distance of the borehole tip in the reservoir level between GTD-2/GTD-3 (producers) and GTD-1 (injector) for D = 800 m, accounting angle of borehole inclination. A *wellhead temperature* T_{wh} is given by pumping tests (e.g. Vranovská et al., 1999a,b; Halás Sr et al., 2016) as averaged mean yearly temperature T_{wh} = 135 °C. *Reinjection temperature* T_{inj} is assumed for T_{inj} = 65 °C (Vranovská et al., 1999b) scheduled for a free-flow, however, considered reasonable according to chemistry of geothermal brine. Although lowering T_{inj} (such as T_{inj} = 25 °C calculated in Halás Sr et al., 2016) may generate ancillary benefits through building up a thermal gradient for P_{th}, subsequently requiring less yield (45), a risk of intense corrosion / scaling occurs. Maintaining the T_{inj} = 65 °C appears thus, a conservative scenario, yet more realistic.

Simulation of thermal breakthrough, reservoir response (1TIQ) and reclamation (1TER) is carried on a wide range of constant production scenarios (P_{th} = const.) obtained from combining the geothermal reserves booking (Sanyal – Sarmiento, 2005; Fričovský et al., 2019) with reserve capacity ratio classification (Bjarnadottir, 2010; Fričovský

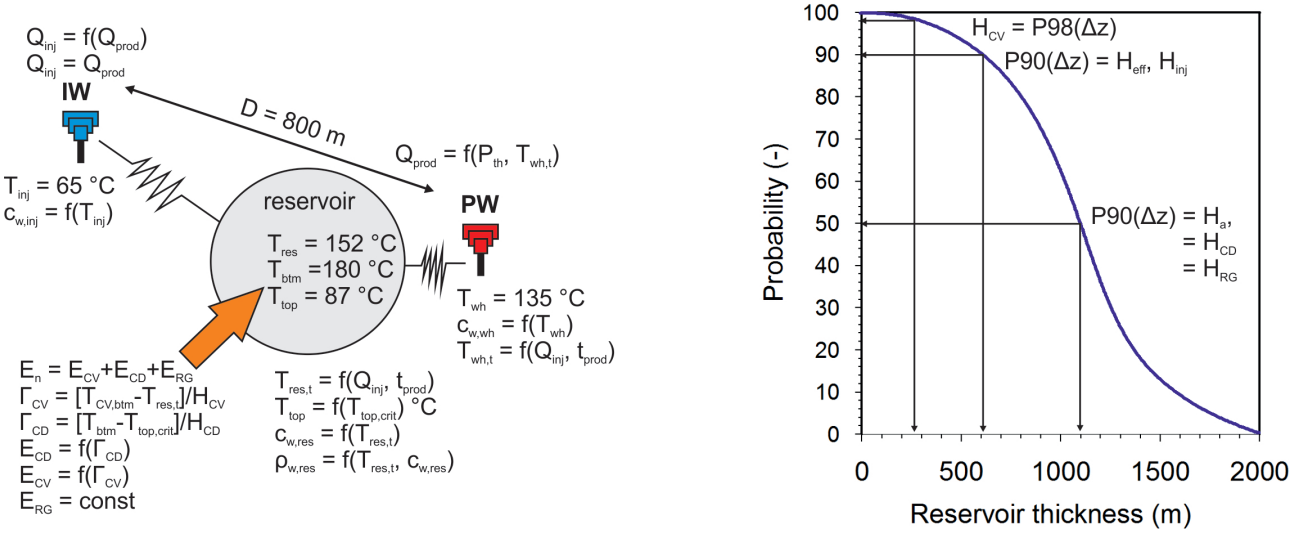

Fig. 3.5. *Basic visualization of lumped parameter model scenario (left) and CDF for reservoir thickness – Δz (right).*

et al., 2019) – see "Part II" paper for more detailed discussion. Because both models work as non-isothermal, i.e. $P_{th} = f(T_{wh,t})$ and $T_{wh,t} = f(T_{res,t})$, an objective demand on increase yield is solved through (45):

$$P_{th,t} = Q_{prod,t}.c_{w,wh}.\left(T_{wh,t} - T_{inj}\right) \quad (45)$$

Reservoir (w,res), wellhead (w,wh), and reinjection (w,inj) parameters such is the specific heat capacity (e.g. $c_{w,wh}$) and reservoir density (e.g. $\rho_{w,wh}$) are set as function of temperature to response for cooling or heating after the shut-in (46 to 47). All fluids invoke Bousinesq's approximations (e.g. Holzbecher, 1998; Rabinowitz et al., 1999; O'Sullivan, 2010; Pasquale et al., 2011; Lipsey et al., 2016):

$$\rho_{w,wh} = \rho_0.\left[1 - \beta_{vw}.\left(T_{wh,t} - 25\right)\right]$$
$$\text{where}: \beta_{vw} = 1.6.10^{-5} + \left(9.6.10^{-6}.T_{wh,t}\right) \quad (46)$$

$$c_{w,wh} = \frac{4245 - \left[1.841.\left(T_{wh,t} + 273.15\right)\right]}{\rho_{w,wh}}.10^{-3} \quad (47)$$

3.4.2 Boundary conditions: parameter "a" – reservoir production

The entire solution of reservoir prediction meets sparse exploration grid density, i.e. 3 geothermal wells per 33.6 km^2 of a total delineated area of the system. An obligatory objection is, thus, consideration of Mid Triassic carbonates as a solid (although fairly dissected) homogeneous body. Selection of effective *reservoir area for production* A_a is set to respect an energy balance in definition of parameter "a", providing desired energy exploitation to the total energy stored in a reservoir (see -24). So that A_a = 33.6 km^2.

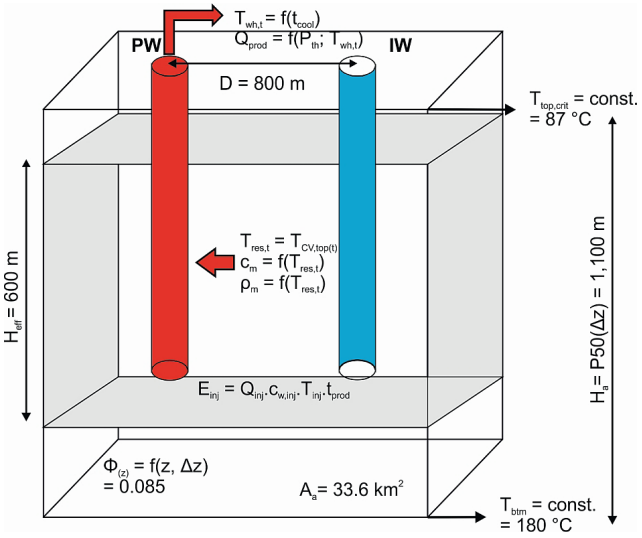

Fig. 3.6. *A simple conceptual model depict of ALPM production "parameter a" component.*

Definition of *effective reservoir thickness for production* H_a is based on Monte Carlo simulation of system's geometry used for sustainable thermal energy potential (Fričovský et al., 2019). At given CDF of total reservoir thickness, the H_a represents its 50th-percentile, i.e. $H_a = P50(\Delta z)$ = 1,100 m, as representative value at still tolerable level of confidence (Fig. 3.6).

The *effective reservoir volume available for production* V_a is function of A_a and H_a, so that $V_a = A_a.H_a$ of matrix associating saturated single phase reservoir fluid – geothermal brine. The fluid and the matrix contribute on total *specific heat capacity of the reservoir,* $\gamma_{a,a}$, generally described as (48):

$$\gamma_a = \left(1 - \phi_{(z)}\right).\rho_m.c_m + \phi_{(z)}.\rho_w.c_w \quad (48)$$

3.4.3 Boundary conditions: parameter "g" – reinjection

3.4.3.1 Geometry

According to a model (Fig. 3.4 and 3.5) the reinjection is set at the periphery of a single tank. Instead of considering the entire system, pressure drop in a reservoir defines a primary flow path towards the production zone. A cylindrical flow is assumed, turning cone-shaped towards producers (Fig. 3.7). As long as the distance is D = 800 m, the *effective distance of propagation* D_g equals the boundary distance, i.e. $D_g = D$ = 800 m. Unlike to previous case, *effective propagation thickness* H_g can not be described through a total reservoir thickness, as either effective porosity and permeability decreases with depth, i.e. $\Phi_{(z)} = f(z)$.

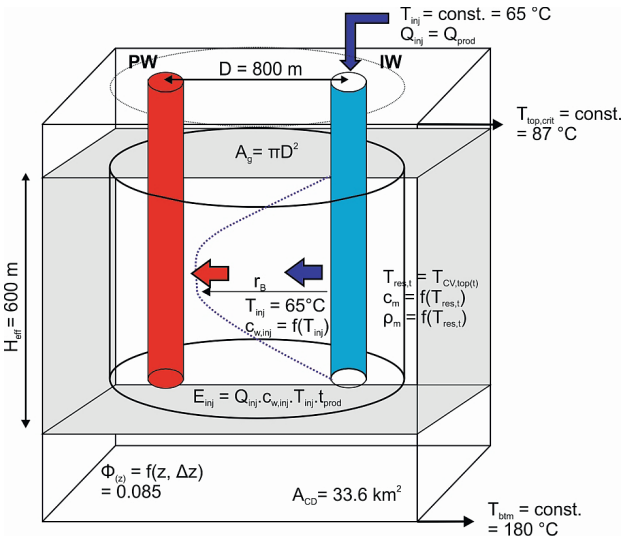

Fig. 3.7. *A simple conceptual model depict of ALPM reinjection "parameter g" component.*

Thus, a minimum thickness of Mid Triassic carbonates available to transmit the cold front is found at CDF (Fig. 3.7), at corresponding rate of probability, i.e. $H_a = P90(\Delta z)$ = 600 m. According to a flow geometry the *effective volume for reinjection* $V_g = \pi.D_g^2.H_g$ = 1.2 .10^9 m^3 of reservoir available for advective cooling or thermal exchange between stored and reinjected fluid that is of an impact on overall mean reservoir temperature $T_{res,t}$.

3.4.3.2 Reinjection rate

According to a fixed pressure conditions in reservoir under exploitation given by a tank model we consider the reinjection rate equal to that of production, i.e. $Q_{prod} = Q_{inj}$.

Then, both, the production and reinjection are given by energy balance under designed modeled scenario (45). Onset of cooling within production zone means, thus, increase in yieldrates ($Q_{prod,t}$) necessary to balance for loss of temperature to maintain desired thermal output (P_{th} = const.).

3.4.4 Boundary conditions: parameter "g'" – heat flux

The heat flux increment "g'" parameter stands for thermal gradient formation and destruction derived flow of energy available to correct for cooling during production or to enhance recovery after shut-in.

The DDHS is a conduction dominated CD2 play-type, i.e. conduction-dominated, orogenic belt type (Moeck, 2014). Indices do, however, exist on insulated convection cells formation restrained in extention to individual tectonic blocks (Fričovský et al., 2018a,b,c). Although of minor effect on a deep geothermal field distribution, consideration of their increment on heat flux due to cooling-induced gradient is, though, obligatory as long as all heat flow endmembers are invoked (40).

3.4.4.1 Conduction

Because of conductive environment, the stationary geothermal model has been constructed according to Fourier's equations (49) on heat conduction (Haenel et al., 1988) per individual stratigraphic layer, i.e. for Sarmatian, Badenian, Karpatian, and Mid Triassic carbonates. Because of insufficient spatial data available, grid refinement led to recalculation of a bulk thermal conductivity λ_B (50) based on temperature-related approximation for fluid λ_w (51) and depth-derived matrix λ_m conductivity (52) combining cubic mixing model (Sclater & Christie, 1980) with global porosity model for carbonates and siliciclastic lithofacies (Baldwin & Buttler, 1985). A reference thermal conductivity λ_{ref} for (52) is set as a mean of available data from GTD-1 and GTD-3 per each strata. A same procedure has been applied to yield distribution of radiogenic heat production Q_{RG} modifying (53) when using surface heat measurements ($Q_{RG(z=0)}$) in the Western Carpathians (Lizoň & Jančí, 1979).

$$T_{i+1} = T_i + \left(\frac{q_i.\Delta z_i}{\lambda_B}\right) - \left(\frac{Q_{RG,i}}{2\lambda_i}.\Delta z_i^{\,2}\right) \tag{49}$$

$$\lambda_B = \left\{\left[\left(1-\phi_{(z)}\right).\sqrt{\lambda_m}\right] + \left(\phi_{(z)}.\sqrt{\lambda_w}\right)\right\}^2 \tag{50}$$

$$\lambda_w = -922.47 + \left[2{,}839.8\left(\frac{T}{273.15}\right)\right] - \left[1{,}800.7\left(\frac{T}{273.15}\right)^2\right] + \left[527.77\left(\frac{T}{273.15}\right)^3\right] - \left[73.44\left(\frac{T}{273.15}\right)^4\right] \tag{51}$$

$$\lambda_m = \lambda_{ref} + 0.2.\left[\left(\frac{z_i}{1{,}000}\right) + \left(0.5\frac{\Delta z_i}{1{,}000}\right)\right] \tag{52}$$

$$Q_{RG,i} = Q_{RG(z)}.e^{-\frac{z_i}{D_{(RG)}}} \text{ where } D_{(RG)} = \frac{z - z_0}{\ln\left(\frac{Q_{RG(z=0)}}{Q_{RG(z=i)}}\right)} \tag{53}$$

At steady-state a stable conductive heat flux (54 – Haenel et al., 1988) within reservoir is a function of thermal gradient between reservoir base T_{btm} and reservoir top T_{top} temperature over a block thickness H_{CD} = P50(Δz) = 1,100 m (Fig. 3.8). In 1TIQ, the T_{btm} = const. = 180 °C, however, T_{top} modifies to $T_{top,crit}$ once production zone is subjected to cooling. Due to energy balance, thermal conductivity is assumed to realize across the entire system, so that A_{CD} = 33.6 km^2:

$$E_{CD} = A_{CD}.\lambda_B.\left(\frac{T_{btm} - T_{top}}{H_{CD}}\right) \tag{54}$$

Temperature at a top of a reservoir is function of time as borehole measurements already proven inflow from Karpatian basal clastics, so that effect of reinjection on recharge from a top can not be neglected. The reservoir top temperature is calculated using undisturbed environment (Axelsson et al., 1995) function (55). Hence $Q_{prod} = Q_{inj}$ = 1:1 according to fixed pressure boundary condition, a ratio of total over effective profile thickness is substituted (56):

$$T_{top} = T_{top,(t=0)} - \frac{Q_{inj}}{Q_{prod}}.\left(T_{res} - T_{res,t}\right) \tag{55}$$

$$T_{top} = T_{top,(t=0)} - \frac{\mathrm{P90}(\Delta z)}{\mathrm{P50}(\Delta z)}.\left(T_{res} - T_{res,t}\right) \Big| \begin{matrix} T_{top} = T_{top(t=0)} = 87°C \\ T_{top} = T_{top,crit} \end{matrix} \tag{56}$$

At a steady state, the T_{top} = 87 °C as a minimum reservoir top temperature according to a stationary geothermal model (Fričovský et al., 2018a). Solving for critical reservoir top temperature (57) means setting a boundary condition a temperature can not decay beyond at maximum rate of cooling, turning $T_{top} \in (T_{top(t=0)}; T_{top,crit})$. Further on, we assume conductive environment between reservoir top and top of the effective heat exchange profile. A vertical observation distance, i.e. a zone where cooling becomes negligible (Bjornsson et al., 1994; Axelsson, 2012b) is $L_{(z)}$ = 0.5ΔH where ΔH = P50(Δz) – P90(Δz) = (1,100-600)/2 = 250 m:

$$T_{top,crit} = T_{top,(t=0)} - \left(T_{top,(t=0)} - T_{inj}\right).\left\{1 - erf\left[\frac{\zeta_{CD} + L_{(z)}}{2.\sqrt{\frac{\lambda_m}{\rho_m.c_m}.t}}\right]\right\} \Big| \begin{matrix} T_{top,crit} = T_{top,(t=0)} = 87°C \\ T_{top,crit} = T_{inj} = 65°C \end{matrix}$$

$$\text{where}: \zeta_{CD} = \frac{2\lambda_B}{Q_{inj}.\rho_{w,inj}}.A_g \; ; \; A_g = \pi.D^2 \tag{57}$$

Provided setup allows conduction to increase in time as long as cooling realizes in profile of effective thermal exchange during production and reinjection, as well as to decay with progressive recovery. Hence thermal gradient is balanced to top of a reservoir, where temperatures can nod drop below reinjection temperature and neither they can recover above initial conditions, conduction appears fixed within reasonable interval.

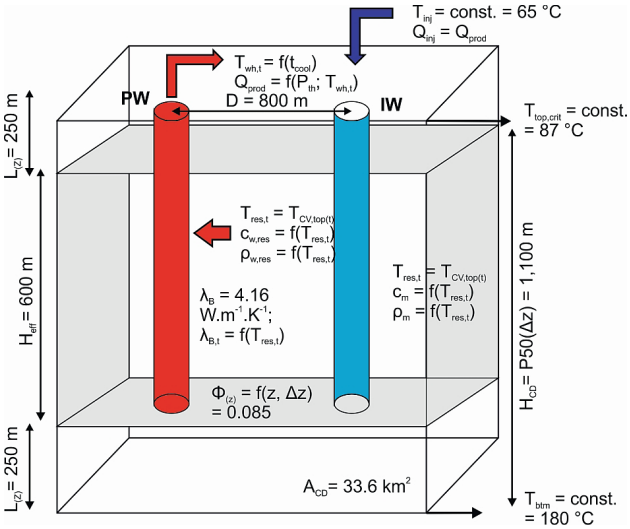

Fig. 3.8. *Depict of conceptual model for conductive heat flux increment to ALPM.*

3.4.4.2 Convection

Unlike conduction, convective heat increment into a profile of effective heat exchange due to reinjection remains questionable. Numerical indices calculated for horizontal (Fričovský et al., 2018b) and inclined (Fričovský et al., 2018c) homogeneous porous media did imply existence of 2 separate cells in deepest parts of produced block that can be of some contribution. Other studies, such as use of geochemical mixing models (e.g. Fournier et al., 1974; Fournier & Potter, 1982), solute (e.g. Fournier & Potter, 1978, 1979; Giggenbach, 1988) or multicomponent (e.g. Neupane et al., 2014; Spycher et al., 2014; Peiffer et al., 2014) geothermometry, able to track plausible convection through re- or un- equilibration of macrocomponents, solutes or mineral phases (e.g. Fričovský et al., 2016) haven't yer been conducted to prove or disprove the idea of vertical reservoir heat and mass flux through convection.

Disturbances to conductive environment (58) were studied for total reservoir area where actual Rayleigh number Ra exceeded that critical (Rac) corrected by a model unit cell inclination (φ = 2 – 52 ° increasing in SW-NE direction) and overheat ratio τ (Fričovský et al., 2018b). The (58) was solved for z = 0 at a top of the zone and z = H_{CV} towards the base, with boundary conditions given by magnitude of convective gradient $0 < \Gamma_{CV} < 2\Gamma_{CD}$ and zone thickness $H_{CV} > H_{CV,crit}$ calculated using (59) (Sheldon et al., 2011). Positive Rayleigh number anomaly in horizontal and vertical direction has been substituted as plausible convection zone width L_{CV}, oriented in W-E direction to follow general trend of thermal field distribution anisotropy (Fig. 3.9):

(58)

$$\frac{dT}{dz} = \frac{T_{i+1} - T_i}{H_{CV}} \cdot \left\{ \begin{array}{l} 4\pi 2\sqrt{\frac{Ra - Rac}{Ra} \cdot \left[\cos\left(\pi \frac{z}{H_{CV}}\right)\right]} \\ \cdot \left[\cos\left(\frac{L_{CV}}{H_{CV}}\right)\right] - 1 \end{array} \right\} \Bigg| \begin{array}{l} z = 0 \\ z = H_{CV} \end{array}$$

$$H_{CV,crit} = \frac{\frac{38.71 e^{-4.176\tau}}{\cos\varphi} \cdot \nu_D \cdot \lambda_m}{g_G \cdot K_m \cdot \rho_{w,CV} \cdot c_{w,CV} \cdot \beta_{vw} \cdot (T_{i+1} - T_i)} \qquad (59)$$

The linear stability analysis (e.g. Kassoy & Zebib, 1975; Garg & Kassoy, 1981) yields Ra = 42-117 within a block where Ra > Rac (Fričovský et al., 2018b,c). Solving for (59), temperature at a base of convective zone is given by $T_{CV,base}$ = 175 °C as a mean. Because towards the base the reservoir is expected undisturbed, $T_{CV,base}$ = const.

After (59), the representative convection zone height is H_{CV} = 270 m. As $H_{CV} > 0.5\Delta H$, where ΔH = P50(Δz) – P90(Δz) = (1,100-600)/2 = 250 m (distance between effective heat exchange profile and simulated reservoir base depth), temperature at a top of convection zone must vary in time (35), so that $T_{CV,top} = T_{res}$ and $T_{CV,top,t} = T_{res,t}$ (Fig. 3.10).

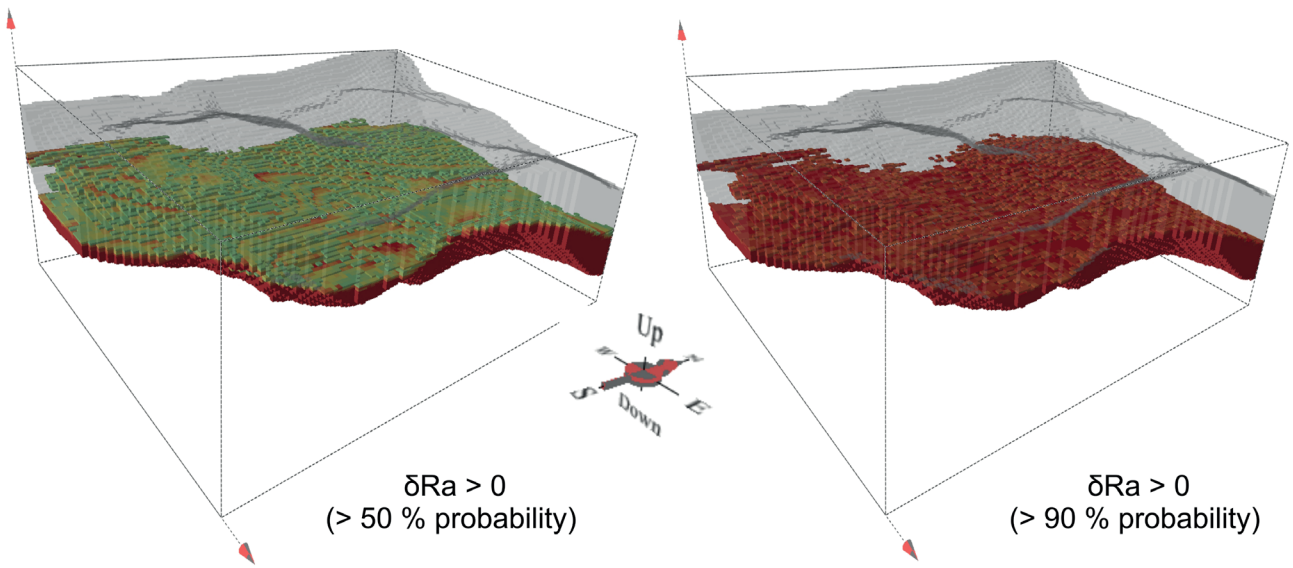

Fig. 3.9. *Conditioned Turning-bands simulation of δRa = Ra - Rac > 0 distribution in reservoir environment, indicating plausible zone for convection development.*

The whole model uses a constant permeability of $K_m = 9.912 .10^{-15}$ m^2 (Vranovská et al., 1999b) as fixed constant, because data from depths below those targeted by wells are not available yet. Obviously, new drillings may generate more inputs into the model. Again, most of parameters are set as function of temperature at a base of convection cell. Dynamic fluid viscosity ν_D (60) has been approached using model by Lipsey et al. (2016):

$$\nu_D = 2.4141.10^{-5}.10^{\frac{247.8}{\left[\left(T_{CV,btm}+273.15\right)-140\right]}} \quad (60)$$

Finally, the convective heat increment (Haenel et al., 1988) to the effective profile is governed by (61) for which influenced area is $A_{CV} = 8.1$ km^2 equal to extension of the block, geothermal parameters are set function of reservoir temperature $T_{res,t}$ and vertical fluid filtration velocity ν_z is given by a difference between viscous and buoyant forces along a convective profile (62 – Lippsey et al., 2016):

$$E_{CV} = A_{CV}.\phi_{(z)}.\rho_{w,res}.c_{w,res}.\nu_z.\left(T_{CV,btm} - T_{res,t}\right) \quad (61)$$

$$\nu_z = \frac{\nu_D.H_{CV}.\lambda_m}{\phi_{(z)}.\rho_{w,res}.c_{w,res}.H} \quad (62)$$

Fixing E_{CV} controls a rate of heat increment according to change in initial conditions, as the gradient forms between fixed convection zone bottom and dynamic convection zone top temperature. Thus, heat increment can not exceed a rate given by predicted change in reservoir environment, either considering cooling or recovery.

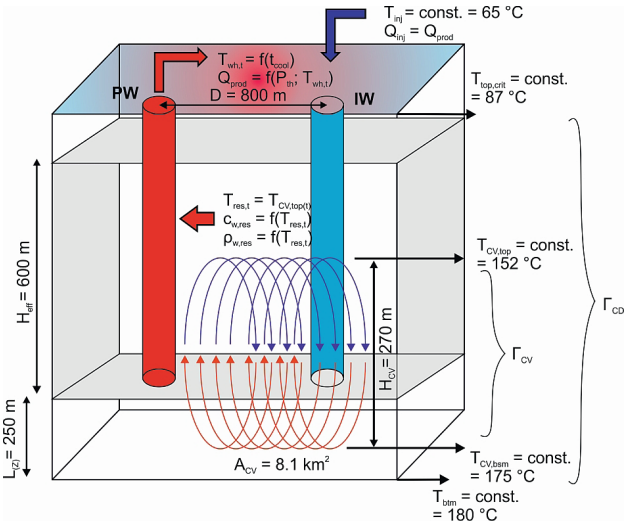

Fig. 3.10. *Simplified conceptual model of convective heat flux increment in ALPM parameter g'.*

3.4.4.3 Radiogenic heat generation

Both, the convection and conduction are controlled by thermal gradient (54 and 62). The radiogenic heat generation is, however, of a minor heat contribution, but kept constant in time, as at low temperatures, the rate of heat generated is independent on temperature (Čermák et al., 1991). Another difference to the convection and conduction is a fact that the radiation generates, not only transfers a heat. As such, the heat generated is later on transported conductively.

Equation (53) defines unit heat generated in steady environment. The $Q_{RG(z)}$ that stands for energy produced through radioactive isotope decay at representative depth can, however, be approximated as long as concentration of isotopes is known (63 – Čermák et al., 1991):

$$Q_{RG(z)} = \rho_{m(z)}.\left[\left(9.7.10^{-5}C_U\right)+\left(2.63.10-9C_{Th}\right)+\left(3.57.10-9C_K\right)\right] \quad (63)$$

(Unless concentrations can be found in literature (e.g. Lizoň & Jančí, 1979), the formulation reflects distribution of heat generation with depth. Area of interest where generation applies is limited to $A_{RG} = 16.3$ km^2 that corresponds to thermal field anomaly at a site, because of consequent heat diffusivity. For thickness H_{RG} we select the entire modeled thickness at corresponding probability for the block, i.e. $H_{RG} = P50(\Delta z) = 1{,}100$ m. Straight forward is then calculation of constant heat increment E_{RG} (64) into the profile of effective heat exchange during production and recovery (Haenel et al., 1988):

$$E_{RG} = Q_{RG,i}.H_{RG}.A_{RG} \quad (64)$$

3.4.5 Reservoir state conditions

3.4.5.1 Steady state and pseudo-steady state

Distinguishing the steady- and pseudo-steady- state in 1TIQ/1TER ALPM algorithm is secured through a cold-front diameter r_B spatial extension (Fig. 3.11), that is practically a function of Q_{inj} ($Q_{inj} = Q_{prod}$) and t_{prod}, as long as T_{inj} = const. = 65 °C, so that $c_{w,inj}$ = const. (43).

The *steady state* is given at $t_{prod} = 0$, i.e. where $Q_{prod} = Q_{inj} = 0$ kg.s^{-1}, representing a time prior launching reservoir production and reinjection, assuming in ALMP equal time of turn-on. The *pseudo-steady state* (PSS) represents a reservoir state off any cooling at any distance from reinjection site ($t_{cool} = 0$). Essentially, $t_{prod} < t_B$ is a general description. For an instance, the pseudo-steady state for production zone (D = 800 m) can be rewritten as $r_B < D$ or $r_B < 800$ m. Although there is no breakthrough towards production zone, $t_{cool} = 0$ for D = 800, it is not a case for parts of the system closer to the reinjectors, where cooling ($t_{cool} \neq 0$) is controlled by $r_B \geq D$ according to (43).

Reservoir temperatures prior breakthrough equal initial conditions, thus for $t_{cool} = 0$ $T_{wh,t} = T_{wh} = 135$ °C, $T_{res,t} = T_{res} = 152$ °C (Fig. 3) and $T_{top,crit} = T_{top} = 87$ °C (Fig. 8). Then, each parameter X that is a function of temperature (see the section with critical input data tables) is defined through $X = f(T_{(t=0)})$. If there is no thermal breakthrough yielded in 1TIQ, the 1TER model is set off, as no recovery is needed.

Distribution of conductive and convective heat increment and distribution in a reservoir equals the initial state during PSS as at distance D that meets $D > r_B$ there is no thermal gradient induction. Considering a system as CD2 play-type (Moeck, 2014; Fričovský et al., 2018a, 2019), a ratio of convective Γ_{CV} to conductive gradient Γ_{CD} (65)

yields $\Delta\Gamma_{CV}/\Gamma_{CD} = 0.4$, that characterizes a stable, diffuse reservoir conditions where (if any) convection occurs at natural conditions according to linear stability analysis. As long as radiogenic heat production is independent on temperature variation, it remains constant, not related to any changes in a reservoir state:

$$\Gamma_{CV} / \Gamma_{CD} = \frac{\left[\frac{\left(T_{CV,btm} - T_{CV,top}\right)}{H_{CV}}\right]}{\left[\frac{\left(T_{CD,btm} - T_{CD,top}\right)}{H_{CD}}\right]} = \frac{\left[\frac{\left(T_{CV,btm} - T_{res}\right)}{H_{CV}}\right]}{\left[\frac{\left(T_{btm} - T_{top}\right)}{P50(\Delta z)}\right]} \quad (65)$$

3.4.5.2 Transient state

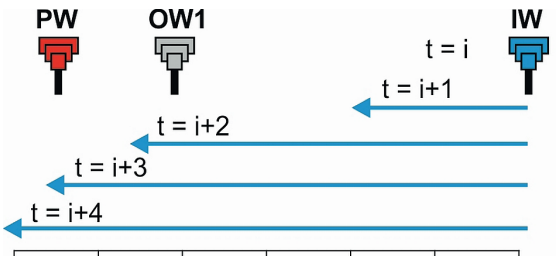

point	t= i	t= i+1	t= i+2	t=i+3	t=i+4
IW	SS	TRS	TRS	TRS	TRS
OW	SS	PSS	TRS	TRS	TRS
PW	SS	PSS	PSS	TRS	TRS

Explanations: ***IW*** - injector, ***OW*** - observation well, ***PW*** - production well, ***SS*** - steady state, ***PSS*** - pseudo-steady state, ***TRS*** - transient state

Fig. 3.11. *Schematic time-domain visualization on variation in reservoir states during pre-production and field exploitation related to a distance D.*

The transient state replaces the pseudo-steady state as long as a cold front propagates at a distance D from a reinjector described as $D \leq r_B$ and $t_B < t_{prod}$ (Fig. 3.11). A breakthrough initiates instant cooling, so that $t_{cool} \neq 0$, turning PSS conditions invalid. For 1TIQ model, decay of a mean reservoir temperature Tres starts immediately according to (35), i.e. $T_{res,t} \neq T_{res}$. Hence wellhead temperature $T_{wh,t}$ is function of $T_{res,t}$, the $T_{wh,t} \neq T_{wh}$. Securing energy and mass balance according to (35) requires a progressive increase in withdrawals Q_{prod}, i.e. $Q_{prod} = f(P_{th})$, so that $Q_{prod} = f(T_{res,t})$ to maintain constant thermal output. Because $Q_{prod} = Q_{inj}$, the rate of injection increases simultaneously, i.e. $Q_{inj,t} > Q_{inj}$.

A period of cooling is easily determined as $t_{cool} \epsilon < t_B$; $t_{si} >$, i.e. $t_{cool} = t_{si} - t_B$, i.e. for $t_{prod} = 100$ yrs a cooling stage is $t_{cool} = 100 - t_B$. When a critical cooling rate is introduced (some discussion is below), set in 1TIQ model as a shut-in according to $t_{si} = t_{Twh,t(crit)}$ where $T_{wh,t(crit)} = 0.9T_{wh} = 122$ °C, the $t_{cool} = 100 - t_B$ as long as $T_{wh,t} > T_{wh,t(crit)}$, otherwise $t_{cool} = t_{si} - t_B$ as a shut is expected prior end of desired period of production if wellhead temperature intercepts the set boundary condition. Unlike an instant decrease in mean reservoir and wellhead temperature, temperature at a top of the reservoir transits from T_{top} to $T_{top,crit}$ considerably slower, following (56 to 57). A lag in the transition is given by $L_{(Z)}$, as there is some thermal diffusion of cooling accounted between reservoir top and an upper boundary of effective thermal exchange profile, i.e. $L_{(z)} = 250$ m. Temperature at a base of the reservoir T_{btm} is not submitted to any change in a model, expecting a rapid decay of cooling effect from the effective heat-exchange profile.

Both, 1TIQ and 1TER ALPMs are constructed and upscaled as unisothermal. Thus, reservoir (res) and wellhead (wh) geothermal properties become a function of decay in temperature, so that for each parameter X that relates to a dynamic change in temperature, the general formula to describe such a link becomes $X = f(T_{(t\neq0)})$, following e.g. (46) or (47). Yet reinjection properties (inj) do not change during transition between PSS and transient state as $T_{inj} = \text{const.} = 65$ °C.

As long as $T_{res,t} = T_{CV,top(t)}$ causes a convective gradient to increase (65) proportionally to a cooling rate. The 1TIQ solution expects, thus, initiation of induced convection extending in a height H_{CV} (59) and a relative heat increment (66), so that $\Gamma_{CV}/\Gamma_{CD} \neq 0.4$:

$$Q_{CV} = A_{CV}.H_{CV}.\phi.\rho_{w,res(t)}.c_{w,res(t)}.\nu_{(z)}.\left(T_{CV,btm} - T_{res,t}\right) \quad (66)$$

Unlike $T_{res,t}$, trend in $T_{top,crit}$ is of much lower magnitude, i.e. conductive heat flux Q_{CD} (67) increases inproportionally (65) to the Q_{CV}, because of a lag in expected time of cooling temperature at a top of a reservoir ($T_{top,crit} = T_{top,CD}$):

$$Q_{CD} = A_{CD}.\lambda_B.\left(\frac{T_{btm} - T_{top,crit(t)}}{H_{CD}}\right) \quad (67)$$

The Γ_{CV}/Γ_{CD} allows to assess a relative rate of a change in reservoir geothermal field unstationarity due to cooling. After Sheldon et a. (2011) the convection occurs at $0 < 2\Gamma_{CD}$ that is an exact case of situation at DDHS. Yet considering stability of convective energy and mass flux, we consider a ratio $\Gamma_{CV}/\Gamma_{CD} \leq 0.5$ an indice on quiet, normal-gradient driven convection, not compromising conduction-dominated environment. Then, for $\Gamma_{CV}/\Gamma_{CD} = 0.5 - 1$ the induced convection gains proportion, yet a field may still be considered conduction dominated. Increase in the gradient ratio to $\Gamma_{CV}/\Gamma_{CD} = 1 - 1.5$ is considered a sign of convective reservoir conditions prevailing over conduction, where convection cells conserve their phase and symmetry stability. However, for $\Gamma_{CV}/\Gamma_{CD} = 1.5 - 2.0$ the ALPM classifies a reservoir environment as convective, yet with destruction of cells' symmetry, while we assume that at $\Gamma_{CV}/\Gamma_{CD} > 2$ a convection is self-destroyed through massive cooling of the cell. Provided stability analysis give accent to assess impact of production not only geothermal field, but stationarity of a system that controls consequent reservoir heat and mass processes, such is modification of brine chemistry or equilibration, playing a role in evaluation of corrosion or scaling.

3.4.5.3 Critical cooling rate

The 1TIQ ALPM starts at $t_{prod} = 0$ (steady state). At any time between $t_{prod} = 0$ and $t_{prod} = t_{si}$, the PSS controls reservoir response as described above. For theoretical considerations

it is possible to fix the 1TIQ solution for $T_{wh,t} \rightarrow \lim T_{inj}$, $T_{top,crit} \rightarrow \lim T_{inj}$ and $T_{res,t} \rightarrow \lim T_{inj}$. However, as long as difference in wellhead ($T_{wh,t} - T_{inj}$) or mean reservoir ($T_{res,t} - T_{inj}$) is zero, there is no gradient accessible, turning $Q_{prod,t} \rightarrow \lim\infty$ to balance production capacity demands (45), that makes such fixation unrealistic. Moreover, intense cooling often leads to more or (rather) less reversible changes in reservoir conditions and environment, taking excessive time to recover just after production stops. It is, obviously, because of multiple technical and reservoir engineering issues.

Instead, we accredit a compromise between reservoir sustainability, renewability of a resource and economical feasibility for a theoretical field operator, following a tolerable (critical) cooling rate in 1TIQ model. This has already been in multiple guidebooks and "best practices" (Tester et al., 2006; Sutter et al., 2011; Fox et al., 2013; Williams, 2007, 2014). A tolerated cooling rate is set for $T_{wh,t(crit)} = 0.9T_{wh}$, i.e. a production stops at $t_{si} = t_{Twh,t(crit)}$. Because $T_{wh} = 135$ °C, the $T_{wh,t(crit)} = 122$ °C, so each scenario in 1TIQ model is ran until $T_{wh,t} \geq T_{wh,t(crit)} = 122$ °C. Thus, if $T_{wh,t} < 122$ °C at $t_{prod} < 100$ yrs, production is shut-in ahead of desired period ($t_{si} = t_{Twh,t(crit)}$) of production, not considering such a scenario sustainable. Otherwise $t_{si} = t_{prod}$ for scenarios of $T_{wh,t} \geq 122$ °C at $t_{prod} = 100$ yrs. For both cases, reaching the t_{si} gives $Q_{prod} = Q_{inj} = 0$ kg.s^{-1} and the 1TER model for temperature and energy recovery starts instantly.

3.4.5.4 Thermal recovery

The 1tank energy-recovery model starts at t_{si}, turning Q_{prod} and Q_{inj} instantly to zero, because of no natural recharge to the reservoir system. While for 1TIQ the steady-state is described through reservoir parameters at initial-state, initial conditions for 1TER model correspond to a situation of a transient-state at t_{si}. For each parameter X that is a function of temperature there is, thus, a clear definition $X = f(T_{t(si)})$, no matter on whether the $T_{t(si)}$ stands for a state at $t_{si} = t_{prod} = 100$ yrs or $t_{si} \leq 100$ yrs.

The time of shut-in is, however, crucial in setting a period a system is evaluated for reclamation. As renewability of a resource is defined as ability of a system to gain or approach initial conditions at time of comparable to that it was utilized (e.g. Rybach & Mongillo, 2006), a time the 1TER runs reclamation predicting equals the time of production, i.e. $t_{reco} = t_{si}$. This allows then evaluation of its renewability, i.e. to mark a scenario as of renewable approach to the resource as long as $t_{reco} \leq t_{si}$ with positive renewable capacity ($\Delta t_{reco} = t_{prod} - t_{si} \geq 0$) or non-renewable for $t_{reco} > t_{si}$ with negative renewable capacity ($\Delta t_{reco} < 0$). Obviously, the longer is the production, the longer is a time accessible for recovery, yet maximum time corresponds to a desired period of production, i.e. $t_{prod} = 100$ yrs according to a sustainable reservoir management concept.

With no natural hot-water recharge into system ($Q_{rech} = 0$ kg.s^{-1}) the 1TER model accounts natural heat increment from a basis of the system. During the reclamation, temperature recovers according to $T_{wh,r} \epsilon < T_{wh,t} = T_{wh,t(si)}$; $T_{wh} = T_{wh(t=0)} >$ and $T_{res,r} \epsilon < T_{res,t} = T_{res,t(si)}$; $T_{res} = T_{res(t=0)} >$ and $T_{top,r} \epsilon < T_{top,crit}$; $T_{top} = T_{top(t=0)} >$. Fixing $T_{wh,r} \leq T_{wh}$, $T_{res,r} \leq T_{res}$ and $T_{top,r} \leq T_{top}$ restrains disruptions in energy and mass balance in the system, not exceeding initial settings. During reclamation, every parameter that is a function of temperature follows $X = f(T_{reco})$.

A progressive recovery erases, however, an induced convective or conductive gradient generated previously through cooling in 1TIQ model. Keeping $T_{CV,btm}$ and T_{btm} constant, increase in $T_{CV,top} = T_{res,r}$ and $T_{CD,top} = T_{top,r}$ reduces temperature difference (65), causing a heat increment to fall towards initial conditions. Simultaneously, $\Gamma_{CV}/\Gamma_{CD} \rightarrow \lim 0.4$ with t_{reco}. Obviously, for scenarios where $T_{top,r} = T_{top}$ and $T_{res,r} = T_{res}$ at $t_{reco} = t_{si}$, restoration of initial conduction-dominated environment with natural (plausible) convection may occur, depending on a rate of convection / conduction ratio.

3.5 Scenario selection approach

3.5.1 Review on geothermal reserves booking and constant production strategies selection

3.5.1.1 USGS volume method

The USGS volume (or stored-heat) method (Muffler & Cataldi, 1978) became one of most utilized in geothermal resource assessment as not requiring field production data and history matching (Sanyal, 2007), at least in early stages of evaluation process. The method counts the total thermal energy stored in the reservoir H_T (68) be it a sum of heat stored in the rock H_R and reservoir fluid H_W (Grant, 2014; Garg & Combs, 2015) as a function of reservoir heat capacity γ_a; herein a single-phase saturated geothermal water in Mid Triassic carbonates in hydraulic connection to the Karpatian basal conglomerates (Vranovská et al., 1999, 2002):

$$H_T = H_M + H_W = \gamma_a . V . \left(T_{res} - T_{inj} \right)$$

where (68)

$$\gamma_a = \rho \bar{c}_w + \rho \bar{c}_m = \phi . \rho_w . c_w + \left(1 - \phi\right) . \rho_m . c_m$$

The H_T acknowledges not only to a heat that is stored, but to the heat that is in a flow through the reservoir as well (Axelsson et al., 2005), i.e. the heat flux driven by a gradient between reservoir base and a top. A risk of misestimates on a scale of multiples to folds arises, if only "known" values are being substituted to Monte Carlo simulations (Grant, 2000, 2014) addressing booking the geothermal reserves (Sanyal & Sarmiento, 2005; Garg & Combs, 2015). Critical moment of a method is, however, definition of recoverable heat in place H_0 (69), i.e. a part of a heat reasonably exploitable (Doveri et al., 2010; Grant, 2014):

$$H_0 = R_0 . H_T \tag{69}$$

Obviously, the recovery factor R_0 is of essential impact on H_0 assessment. Instead of a standard method on R_0 estimate comparing energy produced at the wellhead over that accumulated in a reservoir (Garg & Combs, 2010, 2015; Williams, 2014; Takahashi & Yoshida, 2016) working with

fluid enthalpies (well applicable in assessment of potential for power production) a concept of production-based recovery efficiency has been used (Ungemach et al. 2005, 2007, 2009). This is exactly designed for doublet field operation. The production efficiency (η_{prod}) measures (70) energy produced ($Q_{prod}.\rho_{w,wh}.c_{w,wh}$) during a given period of time (t_{prod}) over energy stored in reservoir ($\gamma_a.A.\Delta z$). Then, accessible recovery R0 is derived through a gradient to production (T_{inj}) and reservoir (T_s) conditions (71):

$$\eta_{prod} = \frac{Q_{prod}}{A.\Delta z}.\frac{\rho_{w,wh}.c_{w,wh}}{\gamma_a}.t_{prod} \tag{70}$$

$$R_0 = \eta_{prod}.\frac{T_{res} - T_{inj}}{T_{res} - T_s} \tag{71}$$

3.5.1.2 Geothermal reserves booking

A concept of geothermal reserves booking – GRB (Sanyal & Sarmiento, 2005) is based on probabilistic Monte Carlo simulation – MCS (Rubinstein & Kroese, 1991), involving 5,000 iterations prior obtaining inverse distribution function (IDF) for H_0 (69) through 10,000 iterations of H_T. For R_0, the MCS yields $R_0 = 0.053$ from IDF curve, representing a median of $P90(R_0)$ to $P50(R_0)$ interval, obviously being more conservative estimate than using arbitrary set constants, i.e. $R_0 = 0.1$ (Fendek et al., 2005) or $R_0 = 0.075$ (Vranovská et al., 1999a). MCS simulation of H_T (68) yielded an IDF function converted to H_0 using (69). Booking (Fig. 3.12) is then based on following determinations (Sanyal & Sarmiento, 2005; Garg & Combs, 2015):

- geothermal resources: $RS_T = [P10(H_T) – P10(H_0) / t_{prod}]$
- inferred reserves: $R_{inf} = [P10(H_0) – M(H_0) / t_{prod}]$ if $M(H_0) < P50(H_0)$
- inferred reserves: $R_{inf} = [P10(H_0) – P50(H_0) / t_{prod}]$ if $M(H_0) > P50(H_0)$
- probable reserves: $R_{pb} = [M(H_0) – P90(H_0) / t_{prod}]$ if $M(H_0) < P50(H_0)$
- probable reserves: $R_{pb} = [P50(H_0) – P90(H_0) / t_{prod}]$ if $M(H_0) > P50(H_0)$
- proven reserves: $R_{pv} = (P90(H_0) / t_{prod})$

Note the booking based on probabilistic simulation using IDF through percentiles and mode well reflects certainty levels in definition of McKelvey's scheme (for reading we refer to: Muffler – Cataldi, 1978; Clotworthy et al., 2006; Williams et al., 2011; Falcone et al., 2013; Falcone & Beardsmore, 2015; Sarmiento et al., 2013). Introduction of a period for balancing the reservoir available energy content, i.e. $t_{prod} = 100$ yrs, the booking counts:

- geothermal resources: $RS_T = 3{,}015$ MWth
- geothermal reserves: $RE_T = 180$ MWth
- inferred reserves: $R_{inf} = 83$ MWth
- probable reserves: $R_{pb} = 60$ MWth
- proven reserves: $R_{pv} = 37$ MWth

3.5.1.3 Reserve capacity ratio

The reserve capacity ratio approach is based on a balance evaluation between accessible energy stored in the reservoir and energy removed through desired or installed capacity, be it thermal output in conditions of the DDHS. In its origin (Bjarnadottir, 2010), the method accounts on a reserve capacity (R_{cap}) defining differences between a part of energy expected and the one that has already been proven. Then, the reserve capacity ratio (72) assesses a proportion between energy left in the reservoir and that assumed to be accumulated:

$$r_{cap} = \frac{R_{cap}}{R_{pb}} = \frac{R_{pb} - R_{pv}}{R_{pb}} \tag{72}$$

In her work Bjarnadottir (2010) developed 5-level scheme to evaluate sustainability of Icelandic geothermal fields operation as given by an energy balance. The scheme

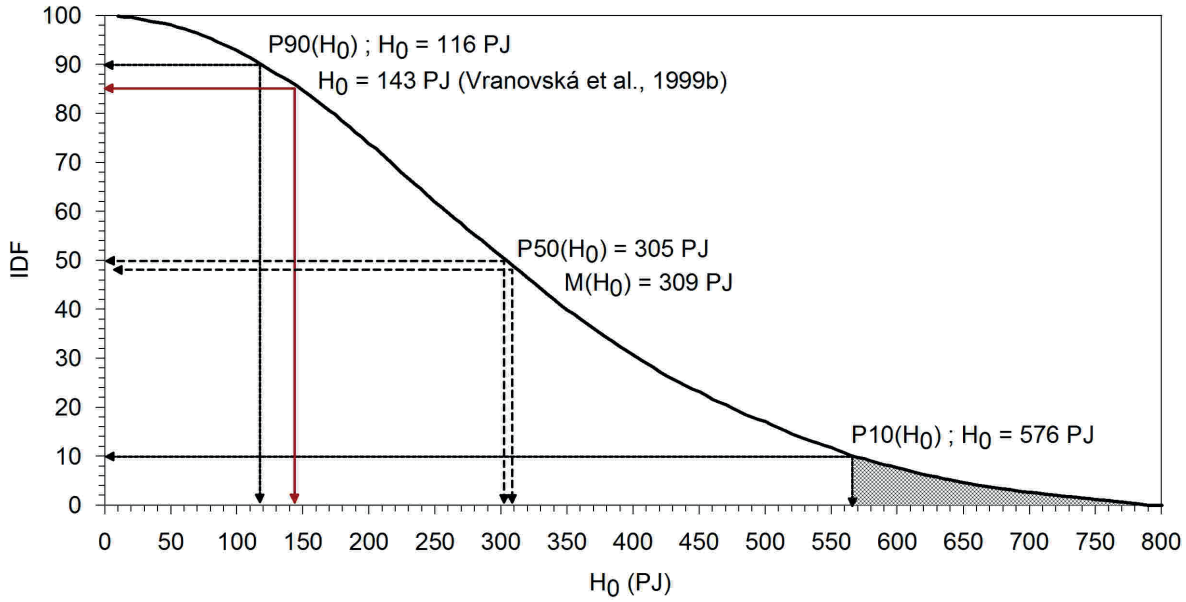

Fig. 3.12. *Review on geothermal reserves booking scheme for the DDHS.*

has been modified (Fričovský et al., 2019) to delineate 4-levels only. The $r_{cap} > 0.5$ describes a field which at least same portion of energy that is removed is still stored in the reservoir, moreover, for $r_{cap} > 0.75$, production capacity or longevity may be extended up to doubling.

3.5.1.4 Definition of sustainable levels of production

A detailed study on reserve capacity ratio analysis is provided in paper of Fričovský et al. (2019). Note this is an energy-balanced approach suitable for tentative reservoir analysis, where insufficient production and monitoring data restrain more precise estimates. However, a strong advantage of the method is its applicability at a scale (e.g. Fričovský et al., 2020b).

The results obtained combining reserve capacity ratio analysis with the USGS method give (Fig. 3.13):

- a maximum thermal output that correspondents to a sustainable level when balanced for $t_{prod} = 100$ yrs is $P_{th(0.5)} = 49$ MWth corresponding to $r_{cap} = 0.5$, equal to $H_0 = 154$ PJ at P85(H_0) confidence level (Fig. 3.12)
- a thermal output opting for doubling the production or prolonging a period of production up to by two when balanced for $t_{prod} = 100$ yrs is $P_{th(0.75)}$ at $r_{cap} = 0.75$ level
- each production higher than $P_{th} = 49$ MWth compromises, thus, an energy balance in within a system and so with longevity of a production

cases where $t_{si} \geq t_{prod} = 100$ yrs because of $t_B \geq t_{prod}$ ($t_{cool} = 0$), the 1TER model does not apply, as there is no cooling. If scenarios are described according to $t_B < t_{prod}$ ($t_{cool} \neq 0$) but $T_{wh,t} \geq T_{wh,t(crit)} = 122$ °C, recovery starts at $t_{si} = 100$ yrs, as the critical cooling rate boundary condition has not been reached in 1TIQ model. Otherwise, the module simulates shut-in at production zone at $t_{prod} = t_{si} < 100$ yrs.

3.5.2 Review on potential-based resource classification and stepwise scenario selection

Unlike the USGS volume method, evaluation of reservoir according to a thermal potential stored in rock, exploitable at certain technical limits is less presented, with some studies already conducted in Australia (Williams et al., 2010; Beardsmore et al., 2010) or Canada (Deibert et al., 2010). The scheme has been proposed as being more familiar to field operators and investors through identified categories rather than referring to a geological probability (Beardsmore et al., 2010, Falcone & Beardsmore, 2015).

A worldwide praxis has shown that stepwise field operation has many advantages if compared to produce at constant withdrawal or output. The essential amongst is minimizing a risk of an unexpected resource deterioration as stepwise development provides the operator with time to conduct a long-term monitoring during early stages of production and assess possibilities of reservoir response when opting to increase the rate (Stefansson & Axelsson, 2005; Bromley et al., 2006). It may, thus, contribute slightly

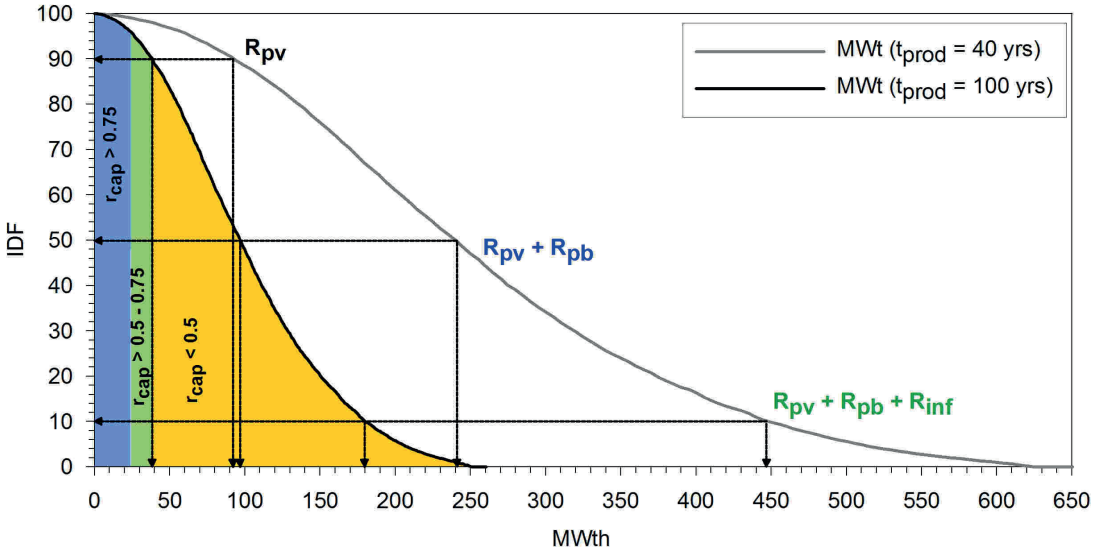

Fig. 3.13. *Review on geothermal reserves booking scheme for the DDHS.*

3.5.1.5 Constant production scenarios considerations

ALPMs application aims to analyze reservoir response on production through breakthrough and induced cooling after cold-front propagation to the production zone. A wide range of scenarios, i.e. $P_{th} = 1 – 240$ is selected to cover plausible changes in reservoir thermal conditions and heat flow dynamics, explaining importance of sustainable production. Constant thermal output strategies (P_{th} = const.) are expected to maintain desired P_{th} during $t_{prod} = 100$ yrs, and to switch between 1TIQ and 1TER model at t_{si}. For more to what stands beyond a principle of sustainable geothermal energy production.

To compare effects of stepwise and constant production on reservoir, a model of sustainable P_S and developable P_D potential assessment has been applied in following.

3.5.2.1 Sustainable and developable potential assessment

A *theoretical potential* P_M (73) accounts energy stored in a reservoir up to a 10 km depth and available for given longevity of extraction under certain geothermal

settings, considering thermal efficiency η_{th} when used either for power production or heat exchange (Falcone & Beardsmore, 2015):

$$P_M = \frac{A.\Delta z.\gamma_a.\Delta T_{res}.\eta_{th}}{t_{prod}} \quad (73)$$
$$\text{where}: \Delta T_{res} = T_{res} - T_{ref} \text{ and } T_{ref} = T_s + T_{inj}$$

As long as thermal efficiency of heat conversion or exchange is not known, the cycle efficiency η_{th} (74) is approached as function of a critical temperature T_c between a reference and definition point (DiPippo, 2007):

$$\eta_{th} = 5.2.10^{-4} T_c + 0.032$$
$$\text{where } T_c = \frac{T_{res} + T_{ref}}{2} = \frac{T_{res} + (T_{inj} + T_s)}{2} \quad (74)$$

A *technical potential* P_T (75) gives energy up to 6.5 km available for extraction with current or predictable technology in no far than 30 years (Beardsmore et al., 2010). To yield, a theoretical potential is corrected according to tolerable reservoir cooling rate (R_{TD}; set to 10 % to initial conditions), recoverability ($R_0 = 0.053$) and resource accessibility R_a; the latter defined as a ratio of area with no limits on development to the entire area of a system, including any urban or natural restrains (Agemar et al., 2012):

$$P_T = P_M.R_0.R_a.R_{TD} \quad (75)$$

There is, however, no general guide on sustainable and developable thermal potential assessment and methods differ between national codes. Hereafter, analogue to a booking scheme (Sanyal & Sarmiento, 2005) has been adopted, with baseline provided by MCS obtained IDF of technical potential P_T.

The *sustainable potential* P_S represents part of P_T that can be produced and maintained during desired t_{prod} with minimizing risk of reservoir and energy production collapse (Rybach, 2015). Obviously, such category calls a high confidence level. As such, we approached the P_S to proven reserves determination in booking, i.e. $P_S = P90(P_T)$, obtaining robust certainty in an estimate. The *developable potential* P_D sums energy available for increase in production at sustainable conditions, i.e. available to develop the P_S more at a minimum risk on production longevity (Rybach, 2015).

Now let us assume the $P_S + P_D$ must not compromise the longevity (sustainability) of production. While probabilistic aspect of P_D definition can be solved through IDF construction for P_T (Fig. 3), the aspect of sustainability is somewhat approached through an entire concept beyond the reserve capacity ratio. Thus, $P_S + P_D \leq M(P_T)$, so that $P_S + P_D > P50(P_T)$. This secures a minimum acceptable risk of failure. Substitution of reserve capacity ratio concept gives the potential difference (analogue to R_{cap}) as $\Delta P_D = M(P_T) - P90(P_T)$ or $\Delta P_D = M(P_T) - P_S$. Now knowing that at least an equal part of potential is supposed to remain left in a reservoir to provide safe reserves for a future, the P_D is accessed through (76):

$$P_D = \frac{M(P_T) - P90(P_T)}{2} = \frac{\Delta P_D}{2} \quad (76)$$

Note that P_D is in its principle analogous to $P_{th(0.5)}$, i.e. to the maximum thermal output available in a reservoir at $r_{cap} = 0.5$ representing a critical capacity for sustainable production.

3.5.2.2 Stepwise production scenarios considerations

Inverse distribution function of P_T (Fig. 3.14) yields: $P90(P_T) = 43$ MWth that corresponds to definition of sustainable potential P_S. Although $M(P_T) > P50(P_T)$, striking IDF curve's skewness to the left conditions use of median $M(P_T)$ instead of $P50(P_T)$ not to underestimate further computations. The $M(P_T) = 101$ MWth. The potential difference is then $\Delta P_D = 101 - 43$ MWth and thus $\Delta P_D = 58$ MWth. As long as the same amount of potential must remain in a reservoir available as the one that can be

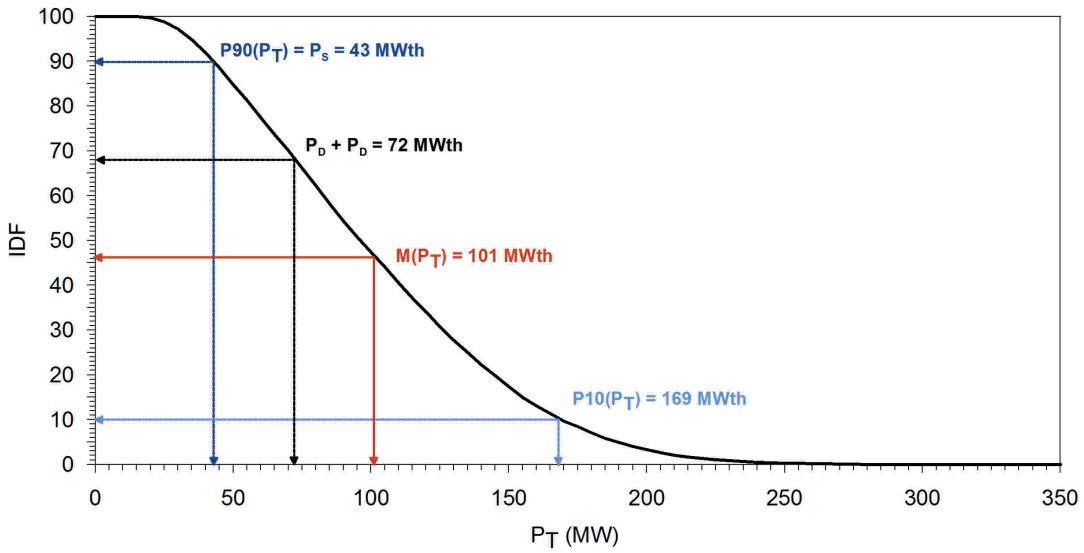

Fig. 3.14. *Technical potential IDF distribution with interpretation of PT, PS and PD.*

extracted more, the $P_D = 0.5\Delta P_D$, so that the developable potential is assessed for $P_D = 29$ MWth.

Definition of P_S and P_D expects a stepwise field development in its principle, opening a production at the P_S first. To demonstrate an interaction of such field development, we set:

- increase in production from P_S to $P_S + P_D$ at steps of $t_{prod,1}/t_{prod,2}$ = 70/30, 80/20 years
- decrease in production from $P_S + P_D$ to P_S at steps of $t_{prod,1}/t_{prod,2}$ = 20/80, 30/70 years

AS $P_S + P_D$ = 72 MWth, a comparison is run for case-studies to option operating a field at P_{th} = 72 MWth constantly.

3.6 Symbols and indexes for heads 3.3 to 3.5

3.6.1 Symbols

Symbol	Unit	Explanation
a	-	production parameter in 1TIQ / 1TER model
A	m^2	area
c	$J.kg^{-1}.K^{-1}$	specific thermal capacity
C	$J.kg^{-1}.K^{-1}$	thermal capacity
C_U, C_{TH}, C_K	$kg.kg^{-1}$	radioactive isotopes concentration
D	m	Horizontal distance between producer / reinjector
$D_{(RG)}$	-	radiogenic heat capacity depth distribution function
E	J, W	energy
$E_{TH(122)}$	TWh,th	cumulative production of GTE at $T_{wh,t}$ = 122 °C
g	-	reinjection parameter in 1TIQ / 1TER model
g’	-	heat influx parameter in 1TIQ / 1TER model
g_G	$m.s^{-2}$	gravity acceleration
H	m	height, thickness
H	J	heat
K_m	m^2	critical permeability for conductive flow onset
$L_{(Z)}$	m	observation vertical distance
m^*	$kg.s^{-1}$, $m^3.s^{-1}$	mass flow rate
M	kg, m^3	total (reservoir fluid) mass
p	Pa	pressure
P_D	MWth	developable potential
P_M	MWth	theoretical potential
P_S	MWth	sustainable potential
P_T	MWth	technical potential
P(X)	-	percentile
q	$W.m^{-2}$	heat flow density
Q	$kg.s^{-1}$	yieldrate, withdrawal, reinjection
r_B	m	cold-front appron, cold-front diameter
r_{cap}	-	reserve capacity ratio
R_0	-	coefficient of reduction (coefficient of recovery)
R_a	-	resource accessibility coefficient
R_{cap}	MWth	reserve capacity
R_{pb}	MWth	probable reserves
R_{pv}	MWth	proven reserves
R_{TD}	-	tolerated cooling rate coefficient
Ra	-	actual Rayleigh number
Rac	-	critical Rayleigh number
t	s, yrs	time
t_B	yrs	thermal breakthrough
T	°C	temperature

Symbol	Unit	Explanation
V	m^3	volume
x	-	net heat increment in 1TIQ / 1TER model
z	m	depth
Symbol	Unit	Explanation
z	m	depth
βvw	K^{-1}	coefficient of volumetric heat expansion
γ	$J.m^3.K^{-1}$	total heat capacity
Γ	-	gradient
Δz	m	thickness
ζ	-	conductive diffusion ratio
η	-	production efficiency
η_{th}	-	thermal (triangle) efficiency
κ	$kg.MPa^{-1}$	storage capacity
λ	$W.m^{-1}.K^{-1}$	thermal conductivity
Λ	-	coefficient of diffuse cooling retardation (heat exchange)
ν_D	$Pa.s^{-1}$	thermal viscosity
ν_z	$m.s^{-1}$	vertical filtration velocity
ρ	$kg.m^{-3}$	specific density
τ	-	overheat ratio
φ	°	angle of inclination
Φ	-	porosity
ψ	$kg.MPa^{-1}.s^{-1}$	productivity index

3.6.2 Indexes

Index	Explanation
0	reference conditions
a	aquifer, reservoir
B	bulk
c	current (energy and/or mass in reservoir)
cool	cooling
crit	critical
CD	(related to) conduction
CV	(related to) convection
eff	effective
i	i-th (observed) layer
i+1	top-wall layer
ini	initial
inj	reinjection
IN	(energy) influx
m	matrix, rock
M	reservoir matrix
n	renewable
net	net mass and/or volume
OUT	(energy, mass) losses
prod	production
PROD	energy produced, withdrawn
rech	natural recharge
ref	reference

Index	Explanation
reco	recovery
res	reservoir
RG	(related to) radiogenic heat production
si	shut-in
S	surface, ambient
t	(with) time
T	total
th	thermal
top	reservoir top, convection cell top
w	water (reservoir fluid)
wh	wellhead
W	geothermal fluid
(z)	(related to) depth

3.7 Results – production scenarios

3.7.1 Thermal breakthrough

The thermal breakthrough (t_B) accounts for a time the reinjected fluid at considerably lower temperature as is that of the reservoir environment arrives to the producer, instantly launching cooling of the effective zone; theoretically up to a moment at which the fluid and geothermal reservoir reach thermal equilibrium.

We used an advective model with a diffuse retardation to assess velocity of breakthrough propagation, as this yields a time at which 1TIQ applies. Setting $Q_{prod} = Q_{inj}$ = 1:1, for a given reservoir geometry (H_{eff} = 600 m, D = 800 m), production parameters ($Q_{prod} = f(P_{th})$; $\rho_{w,inj}$ $c_{w,inj} = f(T_{inj})$; $\gamma_a = f(T_{res}, \Phi)$ and designed period of a fluid withdrawal / reinjection (t_{prod} = 100 years), the model assumes yieldrates at $Q_{prod} \leq 158$ kg.s^{-1} safe of breakthrough (Fig. 3.15). Assuming mean annual wellhead temperature T_{wh} = 135 °C and T_{inj} = 65 °C, the rate corresponds to P_{th} = 38 MWth. Introducing conservative error of estimation at a scale of +/- 1/10t_{prod} = 100 +/- 10 years, the recommended opening production rate would rather not exceed Q_{prod} = 140 – 158 kg.s^{-1} (P_{th} = 36 – 38 MWth) to mitigate breakthrough. Then, the plot demonstrates some cooling even for P_{th} = 49 MWth (critical sustainable production capacity according to r_{cap} analysis), hence t_{cool} = 100 – 79 = 21 years. Obviously, cooling rate controlled through $Q_{inj}.c_{w,inj}.t_{prod}$ (where $c_{w,inj} = f(T_{inj})$ = const.) increases with demand on production ($Q_{prod} = Q_{inj}$), progressively taking over an effect of diffuse retardation along effective heat exchange profile within reservoir. Some caution must, however, be paid for $P_{th} = R_{pv}$ = 37 MWth ($Q_{prod} = Q_{inj}$ = 147 kg.s^{-1}) too, as t_B = 103 years in the model. Although $t_B > t_{prod}$, i.e. cooling is expected after production terminates, the calculated t_B is still within a set error of estimate, thus, left to account on uncertainties.

Reinjection temperature reduction to T_{inj} = 25 °C results in less withdrawal demand on wellhead due to building up a thermal gradient, so that critical production for cold-front propagation increases for Q_{prod} = 154 kg.s^{-1} or P_{th} = 61 MWth. A same effect in increasing production capacity ahead of breakthrough is obtained shortening a desired period of production. For t_{prod} = 40 years the P_{th} = 90 MWth, Q_{prod} = 382 kg.s^{-1} even with T_{inj} = 65 °C. This is in somewhat match to TOUGH2 based model presented by e.g. Giese (1998, 1999), estimating accessible potential of P_{th} = 92 MWth at comparable time scale. Although probability of cooling prior shut-in may be considered low in absolute values, position of cold-front apron moves dramatically towards producers, calling to account on uncertainties too.

The breakthrough model is sensitive to variation in effective thickness of heat exchange profile (HEP), as long as D = const., $Q_{inj} = Q_{prod}$, $c_{w,inj}$, $\rho_{w,inj}$ are constant functions of return temperature, and γ_a is derived through T_{res} according to a mean reservoir temperature model. For H_{eff} = 800 m at P73(Δz), production of P_{th} = 51 MWth ($Q_{prod} = Q_{inj}$ = 205 kg.s^{-1}) would be still capable to restrain a breakthrough, with the potential increased to P_{th} = 64 MWth ($Q_{prod} = Q_{inj}$ = 205 kg.s^{-1}) if H_{eff} = 1000 m estimated as P54(Δz). Otherwise, for reduced thickness of H_{eff} = 400 m corresponding to P96(Δz) the capacity is assumed to drop to P_{th} = 26 MWth or $Q_{prod} = Q_{inj}$ = 105 kg.s^{-1}).

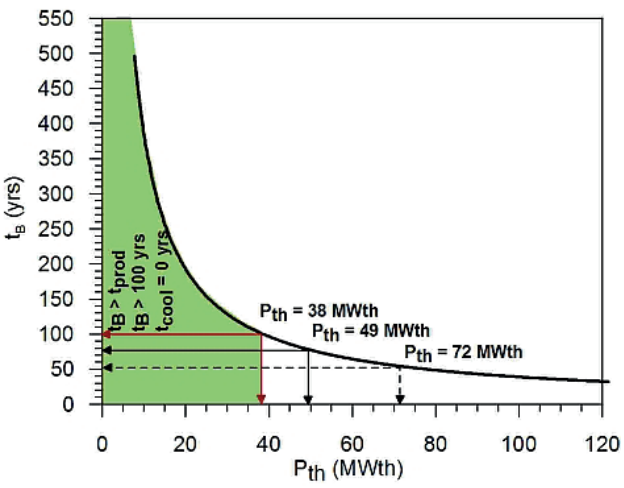

Fig.3.15. *Thermal breakthrough model: constant production summation curve.*

To demonstrate impact of production on breakthrough, we compared constant production of P_{th} = 72 MWth and a stepwise production development given by potential analysis, i.e. from P_S = 43 MWth to $P_S + P_D$ = 43 + 29 = 72 MWth (Fig. 3.14). The constant strategy yields t_B = 53 years (t_{cool} = 47 years). To reach $t_B \geq t_{prod}$ or $t_B \geq 100$ years, a model setup would require $H_{eff} > 1100$ m (P43(Δz)), or extension of a distance between producer and injector to D ≥ 1000 m.

Step-wise development as considered ($t_{prod,1}/t_{prod,2}$ = 70/30 and 80/20 years) from P_S to $P_S + P_D$ instantly prolongs a time of breakthrough, reducing, thus, time of production zone cooling. Although cold front arrives to producers at t_B < 100 yrs, the delay is long enough to perform relevant field monitoring and field developments to reduce risk of cooling (Fig. 3.16). Shortening t_{cool} limits, then, drop in mean reservoir and wellhead temperature in 1TIQ model, so that the scenario can be maintained in production for t_{prod} = 100 years, introducing the critical cooling rate as boundary condition for shut-in (see case study below).

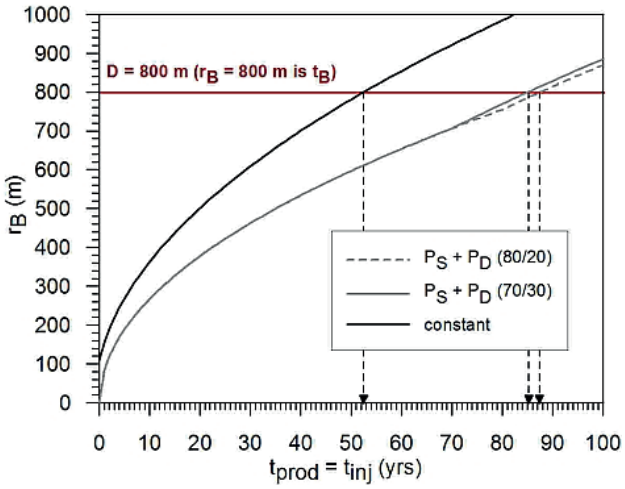

Fig. 3.16. Thermal breakthrough: comparison between constant and step-wise production strategies – visualization of cold-front apron propagation.

3.7.2 Reservoir response

At a time of cold-front arrival to producer(s), the cooling realizes during the t_{cool} period, changing reservoir and wellhead attributes instantly. This is when 1TIQ model of the entire ALPM module estimator applies, transiting from pseudo-steady state to transition state. Use of 1TIQ gives a hint on what production scale can be considered to at least open a production, keeping longevity of resource utilization in scope through mitigation of negative impacts on reservoir fluid and its energy balance.

3.7.2.1 Reservoir cooling

Reservoir cooling prediction is carried through application of 1-tank closed analytical pseudo lumped-parameter model with dynamic heat flux and reinjection (1TIQ). Although no history matching was applied, future upscaling for monitoring data is available as soon as their quality becomes sound, avoiding errors plausible at a recent state of their completion.

For each production option, the model starts at $t = t_{prod} = 0$. As long as $t_B > t_{prod}$, there is no cooling induced, so that $T_{res,t} = T_{res}$ and so it is for $T_{wh,t} = T_{wh}$ ($t_{cool} = 0$). After a cold-front arrival ($t_B < t_{prod}$), the cooling of production zone starts, so that $t_{cool} \neq 0$. Consequent change in $T_{res,t} \neq T_{res}$ and $T_{wh,t} \neq T_{wh}$ modifies reservoir parameters set as analytical functions of temperature, yielding non-isothermal reservoir response forecasting in a model. Drop in reservoir temperature inducing decay of temperature at a wellhead recalls consideration of constant production (P_{th} = const.) or withdrawal (Q_{prod} = const.) maintaining. The first management requires increase in Q_{prod} due to decline of thermal gradient at a wellhead, increasing the Q_{inj} at a same time ($Q_{prod} = Q_{inj}$), however, it also allows to maintain optimized thermal output up to a point where tolerable cooling boundary condition is reached, or the system is produced due to desired period of production. Hence reinjection equals the withdrawal, the cooling of production zone is expected intense and progressive. The latter management considers maintaining set Q_{prod} and thus the Q_{inj}, however, thermal output at the wellhead is reduced with drop in thermal output due to cooling, so field management and project strategies must opt for optimized output at terminal stages of production. Although this management usually leads to less intense cooling, it is rarely applied in praxis, and so is skipped in this paper.

The boundary condition of maximum allowed cooling at a wellhead by 10 % has been applied to all cases, i.e. for T_{wh} = 135 °C at $t = t_{prod} = 0$, the critical temperature was set to $T_{wh,t(crit)}$ = 122 °C. Then, for $T_{wh,t} < T_{wh,t(crit)}$ the production is supposed to shut-in (t_{si}), i.e. $t_{si} < t_{prod}$ and $t_{si} < 100$ yrs respectively. For scenarios of $T_{wh,t} \geq T_{wh,t(crit)}$ at $t_{prod} = 100$ yrs, the $t_{si} = t_{prod} = 100$ yrs, defining it sustainable.

Running the algorithm on a t_{prod} = 100 yrs scale, the critical capacity a system is capable to hold for a desired period of production is P_{th} = 51 MWth (t_{si} = 100 years), increasing the production / reinjection

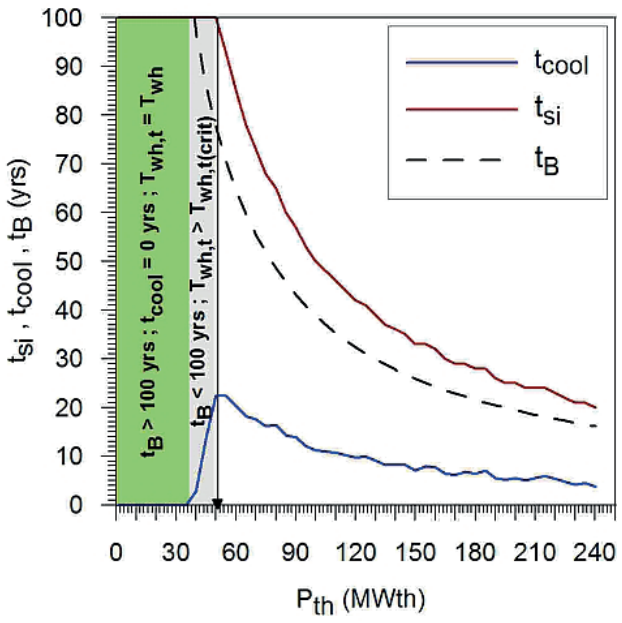

Fig. 3.17. Reservoir cooling prediction: shut-in (tsi) and cooling (tcool) variation.

rate from Q_{prod} = 214 kg.s^{-1} to Q_{prod} = 262 kg.s^{-1} at the end of production. However, because of an analytical character of a model in use, we rather recommend not to exceed the initial production of P_{th} = 49 MWth, i.e. Q_{prod} = 194 kg.s^{-1} (t_{prod} = 0) and Q_{prod} = 230 kg.s^{-1} at $t_{prod} = t_{si}$ = 100 yrs, prior gaining detailed monitoring data for model calibration (Fig. 3.17). This matches well to a sustainable capacity given by r_{cap} analysis, implying such production safe for opening (for further scenario analysis see case studies section in following). Figure 3.17 explains that with invoking the critical cooling boundary condition, the $t_{si} = t_{prod}$ = 100 yrs for P_{th} = 38 – 51 MWth ($T_{wh,t}$ at t_{prod} = 100 years is above 122 °C), increasing t_{cool} with shortening the t_B, hence $t_{cool} = t_{si} - t_B$. At higher production rates, the t_{si} falls along with t_{cool}, due to rapid cooling in production zone as thermal breakthrough shortens. The model expects, thus, that all production exceeding P_{th} = 51 MWth would cause drop in $T_{wh,t}$ far below 122 °C at t_{prod} = 100 yrs, turning such scenarios unsustainable.

Cooling of HEP changes not only T_{res}, but dispersively decays temperature at a top of the reservoir (Fig. 3.18), though the deviation is apparently less intense. Where t_B > 0 yrs and $t_{si} \geq$ 100 yrs, the $T_{top,crit}$ = 75 – 87 °C for constant production, as an effect of long-term, whatever weak in an impact, cooling. Unlike, for scenarios short in shut-in period, i.e. defined at $t_B < t_{prod}$ and t_{si} < 100 yrs, the $T_{top,crit}$ = 75 – 82 °C respectively, due to considerable shorter t_{cool}. Yet some heat flux from overburden to balance a loss in temperature can not be excluded in considerations.

Any drop in $T_{top,crit}$ generates conductive heat flux increment from a base of the reservoir, while decrease in $T_{res,t}$ triggers convection expected to occur between a reservoir base and effective heat exchange profile. According to (40), combination of both, along with radiogenic heat production (constant at given temperature conditions) poses effect of induced cooling retardation. Hence dispersed, it is not intense enough to mitigate and stop cooling itself at high production rates. Such non-linearity in thermal field explains, however, why modeled drop in t_{si} is not strictly proportional to increase in P_{th}.

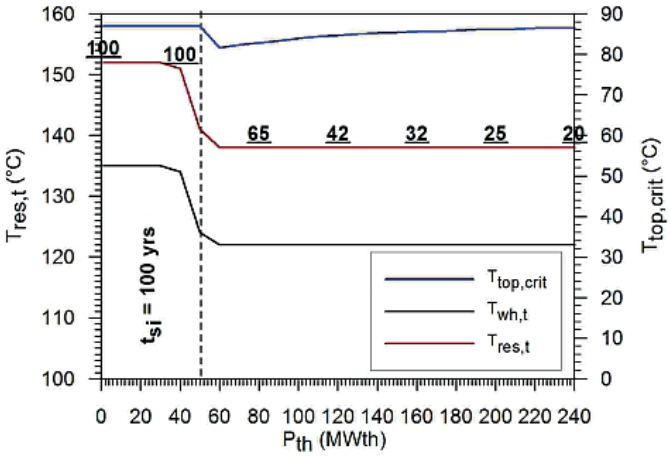

Fig. 3.18. *Thermal field ($T_{res,t}$; $T_{top,crit}$) and wellhead conditions ($T_{wh,t}$) at a shut-in (tsi; in underlined numbers)*

3.7.2.2 1TER lumped/analytical model: reservoir thermal recovery

For cases where t_B < 100 yrs, so that $t_{cool} \neq$ 0 yrs, the 1TER, i.e. one-tank closed energy recovery model) has been applied. The model accounts on reservoir dynamics, including variation in mean reservoir and reservoir top temperature in time that are of an effect on conductive and convective heat increment distribution as the system recovers from production. Unlike 1TIQ, the $Q_{prod} = Q_{inj}$ = 0 kg.s^{-1}, leaving a reservoir to recover due to a natural heat increment only. Distribution of conduction and convection in a reservoir ("tank") is not equal. While conduction is expected to cover entire reservoir body (see 3.4.4.1), convection controls thermal field in deepest parts of the system, limited to a profile between HEP and reservoir base (see 3.4.4.2). Then, while $T_{top,r}$ recovers due to conduction only, the $T_{res,r}$ recovery is accelerated through convection and conduction, involving constant heat increment from radiogenic heat production.

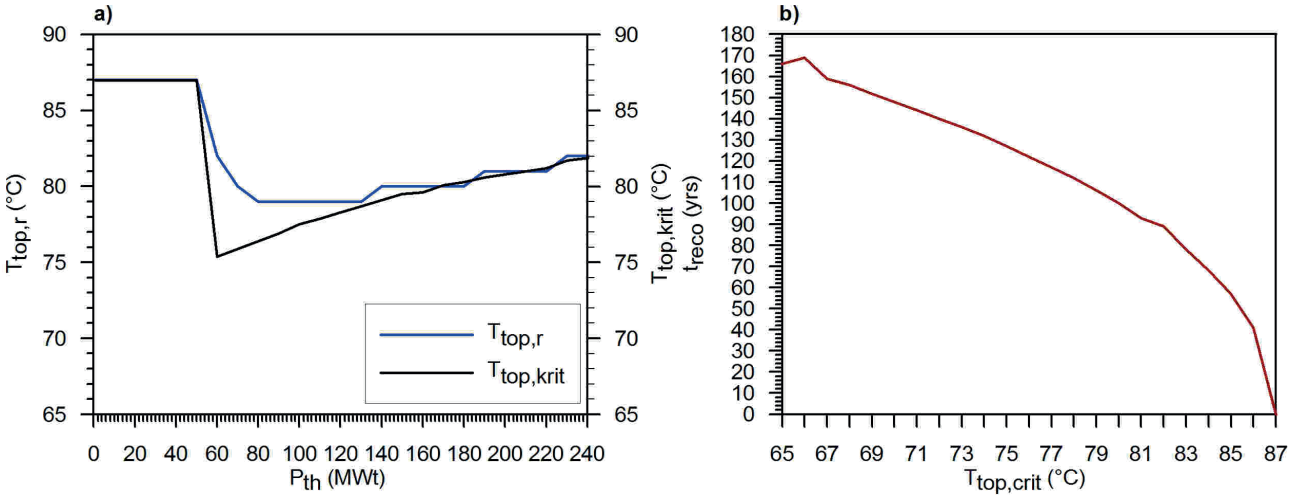

Fig. 3.19. *Reservoir top temperature ($T_{top,r}$) and recovery period (t_{reco}) for critical reservoir top temperature at variable rates (a) and $T_{top,crit}$ at t_{si} (b).*

We let the recovery to start at a time of shut-in, so that $t_{reco} = 0 = t_{si}$. Again, for scenarios where $t_B > 100$ yrs, the $t_{cool} = 0$, and so that $t_{reco} = 0$. For scenarios of $P_{th} < 51$ MWth, the breakthrough-caused cooling ($t_{cool} \neq 0$) generates a reclamation period of reservoir top temperature at $t_{reco} < 30$ yrs (Fig. 3.19). Obviously, 1TER implies a system is capable to recover initial (pseudo-initial) conditions, i.e. $t_{reco} \leq 100$ yrs as long as $T_{top,crit} \geq 80$ °C at t_{si}.

While recovery of temperature at a top of the reservoir is in control of diffuse heat transfer in the reservoir body, response of mean reservoir temperature gives an impact to both, convective heat increment and wellhead temperature. It is, thus, the reservoir temperature recovery that is used to trace renewability of a resource and somewhat renewability of a production prior a time of reclamation.

The 1TIQ model yields $T_{res,t} = T_{res} = 152$ °C for $P_{th} \leq 38$ MWth ($t_B \geq 100$ yrs, $t_{si} = 100$ yrs and $t_{cool} = 0$ yrs), so that no recovery is required ($t_{reco} = 0$). This is, however, related to production zone only. At reinjection site, the cooling starts at time of production / reinjection opening – analysis of reinjection zone is not included in this paper.

As long as production is between $P_{th} = 38 – 51$ MWth, the $t_B \leq 100$ yrs and $t_{cool} \neq 0$ yrs. Due to expected cooling, mean reservoir temperature declines, assumed $T_{res,t} = 138 – 152$ °C at t_{si}. Then, the 1TER model estimates a system as able to recover between $t_{reco} = 0 – 60$ yrs, depending on $T_{res,t}$. In turn, the $T_{res,r} = T_{res}$ at $t_{reco} \leq t_{si}$. With time required for mean reservoir temperature recovery assumed shorter than that of production, a renewable capacity ($\Delta t_{reco} = t_{si} – t_{reco}$) is positive (Fig. 3.20). A model predicts the $P_{th} = 51$ MWth as maximum capacity considered sustainable ($t_{si} \geq 100$ yrs) and renewable ($\Delta t_{reco} > 0$). This matches well to the 1TIQ model, increasing reliability of carried upscaling.

At production rates greater than $P_{th} = 51$ MWth, the recovery starts at $t_{si} \leq 100$ yrs. It does, however, shorten the time available for reclamation due to $t_{reco} \leq t_{si}$ criterion on a resource renewability. Hence $T_{res,t} = 138$ °C at a time of shut-in, the 1TER expects temperature to recover at $t_{reco} = 30 – 65$ yrs depending on rate of variation in $T_{top,crit}$. Setting $t_{reco} = t_{si}$ as a condition, the 1TER yields $T_{res,r} < T_{res}$, so estimating $\Delta t_{reco} < 0$ for production rates over 90 MWth. Thus, production at higher capacity than the critical can neither be considered sustainable ($t_{si} < 100$ yrs), nor of renewable impact on reservoir and a resource.

A relation between mean reservoir temperature recovery and a diffuse heat flux is depicted on Figure 3.21. The greater is a thermal gradient between reservoir base (constant $T_{btm} = 180$ °C) and reservoir top at production termination, the shorter is a period required for recovery. Obviously, the lower is $T_{top,crit}$, the longer it takes to recover, maintaining increased conductive gradient when compared to initial (steady-state) conditions. Now

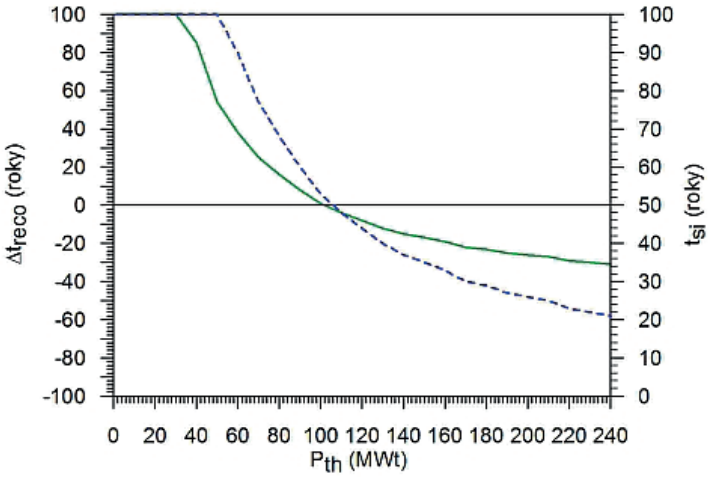

Fig. 3.20. Model solution on reservoir recovery and renewable capacity for $t_{reco} = t_{si}$. Green line: Δt_{reco}, blue line: t_{si}.

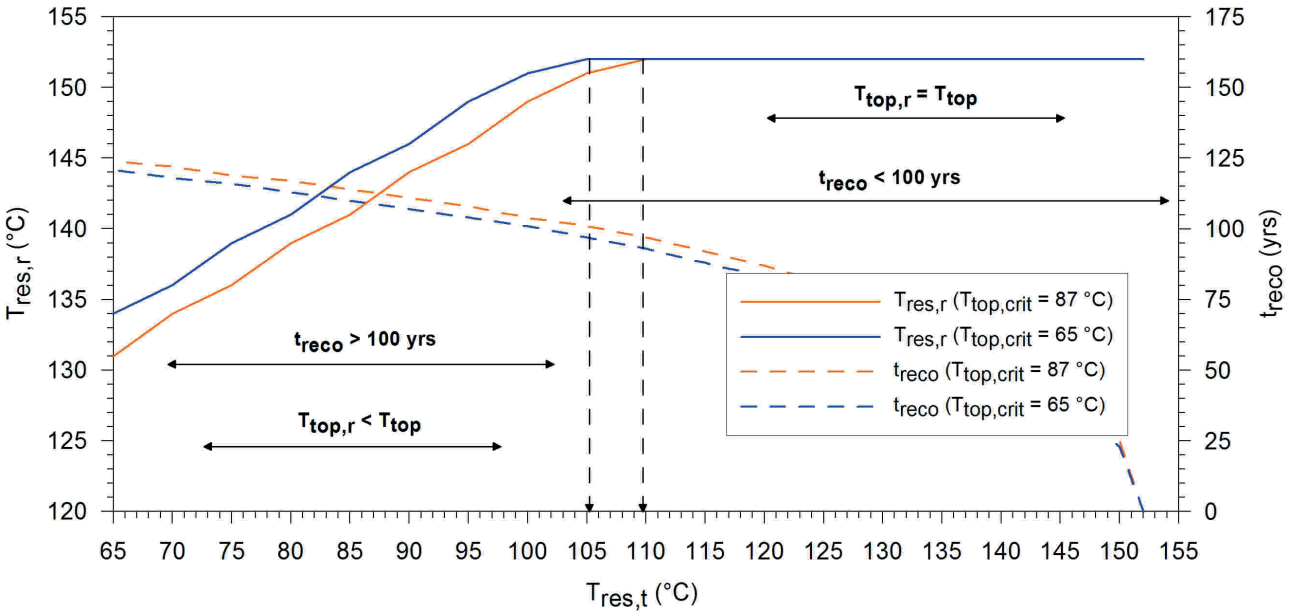

Fig. 3.21. Relation between mean reservoir temperature at t_{si} ($T_{res,t}$), at $t_{reco} = t_{si}$ ($T_{res,r}$) and critical reservoir top temperature ($T_{top,crit}$) at t_{si}.

consider a situation the production is maintained constant for t_{prod} = 100 yrs, though a critical cooling rate boundary condition is omitted in the model. This allows to extend available reclamation time for $t_{prod} = t_{si} = t_{reco}$ = 100 years. According to 1TER estimate, a system will not be able to recover to steady-state conditions ($T_{res,r} < T_{res}$) at t_{reco} = 100 years if $T_{res,t}$ < 105 °C at t_{si}, scoring negative renewable capacity for such a case.

3.7.3 Reservoir dynamics

An accent towards conductive play-type (Moeck, 2014; Fričovský et al., 2018a) is given in upscaling of the model for DDHS. Both, the 1TIQ and 1TER model assume dominant diffuse heat transfer between reservoir base and its top, driven by conductive gradient. So far, numerical indices analysis (Fričovský et al., 2018b, Vizi et al., 2020) propose creation of separate convection cells in deepest parts of reservoir, limited to tectonic blocks, owing to plausible upwelling and sink vectors along faults that dissect the Mid Triassic profile.

To account on different proportion of a diffuse and convective heat flux in a model, we introduced the relative conductive ($\Gamma_{CD} = (T_{btm}-T_{top,crit}) / H_{CD}$) and convective ($\Gamma_{CV} = (T_{btm}-T_{top,crit}) / H_{CV}$) gradients, equal to Γ_{CD} = 42.3 °C.km^{-1} and Γ_{CV} = 17 °C.km^{-1} respectively, i.e. Γ_{CV}/Γ_{CD} = 0.4 at initial conditions. Thus, while any change in mean reservoir temperature due to cooling gives an increment to convection ($T_{res} > T_{res,t}$) as $\Gamma_{CV,t} > \Gamma_{CV}$, drop in critical reservoir top temperature triggers conductive heat flux through a model, i.e. $T_{top,crit} < T_{top}$, so that $\Gamma_{CD,t} > \Gamma_{CD}$. However, results yielded by 1TIQ show clearly the $T_{res,t}$ is predicted to decline more rapidly than that at a top of a reservoir, driving a robust increase in Γ_{CV} when compared to Γ_{CD}.

In case $t_B > t_{prod}$, there is no cooling induced in production zone (D = 800 m) and the system remains in pseudo-steady state. This describes conduction-dominates system with quiet, stable convection due to a gradient within a cell, thermally equilibrated with a reservoir – in its deepest parts. Breakthrough expects induced convection to take part in response to reservoir cooling (Fig. 3.22) for P_{th} > 38 MWth. Generated convection is unlikely to extend vertically to cover entire reservoir profile, rather we assume a cell growth rate of a few to tens of meters. At this amplitude, convection phase and stability of geometry is likely maintained, not placing a rapid impact on reservoir geothermal fluid chemistry. Besides, there are dramatic changes expected in 1TIQ model close to reinjection zone – note presented in this paper. At D = 200 m ($T_{res,t}$ << 138 °C), the return may cool down a reservoir to a state at which convection prevails over conduction, stability of cells' geometry and its phase changes, gaining potential to cause major changes in reservoir fluid mobile phase and chemistry.

Reservoir recovery, including building up $T_{res,r}$ and $T_{top,r}$ after shut-in is definitely a progressive process lacking any linearity as long as heat fluxes are accounted in 1TER algorithm. Instead, when a $T_{res,r}$ and $T_{top,r}$ temperature rise, the gradient slowly ceases and so does recovery. However, the model for D = 800 m shows that a system is able to gain initial, diffusion-dominated conditions as long as a production is not greater than 90 MWth, consequent to combination of a reservoir state at time of shut-in, including $t_{si} = t_{prod}$ = 60 yrs. Though, scenarios considered sustainable and renewable ($P_{th} \leq$ 51 MWth) may recover initial state of heat flux endmembers. To compare, for D = 200 m simulating proximity to reinjector, the system will not recover initial conduction-dominated state for $P_{th} \geq$ 60 MWth, instead, convection at variable stability rate should be still expected. For production rates between at a range of P_{th} = 37 – 60 MWth, combination of diffuse environment with still induced convection should be taken into account while performing further reservoir analysis, especially reservoir chemistry.

3.8 Results – case studies

One reason of 1TIQ and 1TER model application was to study a maximum constant capacity a reservoir can hold for a desired t_{prod}, to meet criteria of sustainable production ($t_{si} = t_{Twh,t(crit)} \geq t_{prod}$ = 100 yrs), and renewable approach

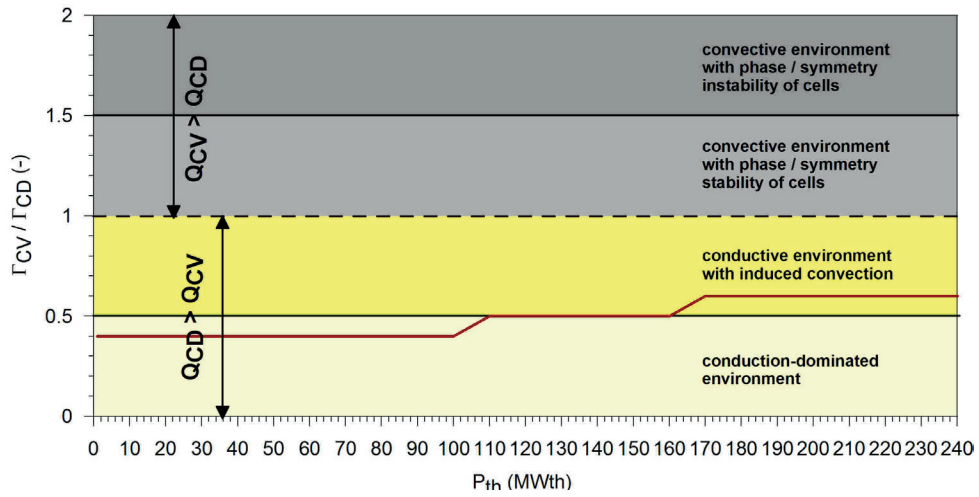

Fig. 3.22. *Reservoir state dynamics depiction as based on relative convective / conductive gradient at $t_{prod} = t_{si}$ and $t_{reco} = t_{si}$.*

($t_{reco} \leq t_{si}$ = 100 yrs) to the system. However, we used both models to test strategies obtained from reservoir energy balance studies, such is:

- derivation of maximum sustainable rate (P_{th} = 49 MWth) through reserve capacity ratio application (Bjarnadottir, 2010) to geothermal reserves booking scheme of the DDHS (Fričovský et al., 2019a)
- definition of sustainable (P_S) and developable (P_D) potential, i.e. P_S = 43 MWth, P_D = 29 MWth as based on potential-balance classification (e.g. Rybach, 2015).

The latter case has then been used to demonstrate a difference of reservoir response on stepwise and constant production.

3.8.1 Constant production scenario: P_{th} = 49 MWth

A given constant production rate represents a critical capacity a system is supposed to hold for desired production period (t_{prod} = 100 years) posing any compromise on reservoir sustainability (r_{cap} = 0.5). At such, it has also been proposed as an output recommended for production given by a reservoir response analysis (Fig. 3.17), accenting rather conservative approach due to unability to carry on a history matching for the model.

According to a thermal breakthrough model (Fig. 3.15), a cold front is assumed to propagate towards production zone at t_B = 79 yrs. For a t_{prod} = 100 yrs baseline, 1TIQ model applied a cooling period of t_{cool} = 21 yrs (by $t_{cool} = t_{prod} - t_B$) to predict changes in reservoir thermal settings because of a response to production.

After breakthrough at D = 800 m, the reservoir cools progressively in a model (Fig. 3.23). Expected drop of reservoir $T_{res,t}$ = 141 °C and wellhead $T_{wh,t}$ = 124 °C temperature implies, though, the capacity can constantly be maintained through the desired t_{prod}, as $T_{wh,t} > T_{wh,t(crit)}$, i.e. $t_{prod} = t_{si}$ = 100 yrs. Because of cooling, withdrawals are supposed to increase, i.e. Q_{prod} = 194 kg.s^{-1} at t_{prod} = 0 and Q_{prod} = 230 kg.s^{-1} at t_{si}. Drop in $T_{res,t}$ and $T_{top,crit}$ ($T_{top,crit}$ = 79 °C) stimulates Γ_{CV}/Γ_{CD} = 0.55 at t_{si}, changing a diffusion-dominant environment to a reservoir with induced convection. However, at D < 600 m, a system may experience rapid cooling ($T_{res,t} = T_{inj}$ = 65 °C), and consequent intense change in reservoir heat flow dynamics.

A 1TER model of thermal recovery after shut-in yields optimistic assumptions. Fixing $T_{res,t}$ = 141 °C at t_{si}, a system may be able to recover a mean reservoir temperature at t_{reco} = 53 yrs. As $t_{reco} < t_{si}$, the model yields positive renewable capacity ($\Delta t_{reco} = t_{si} - t_{reco} > 0$). Because both, the $T_{res,t}$ and $T_{top,r}$ approach initial conditions at D = 800 m, a system is expected to return into a conduction-dominated environment, with quiet, steady ("steady state" thermal gradient driven) convection.

3.8.2 Constant production scenario: P_{th} = 72 MWth

Although a total capacity of P_{th} = 72 MWth has been calculated as combining the sustainable and developable potential, i.e. P_S and P_D, expecting a stepwise approach in a principle, we add a constant output scenario model as comparative in presenting on how both strategies may differ on reservoir response.

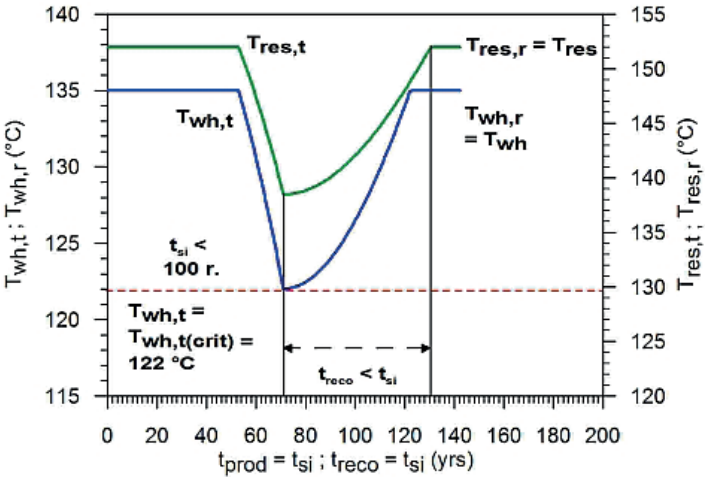

Fig. 3.24. Preview on 1TIQ / 1TER reservoir response model estimation for constant P_{th} = 72 MWth production strategy.

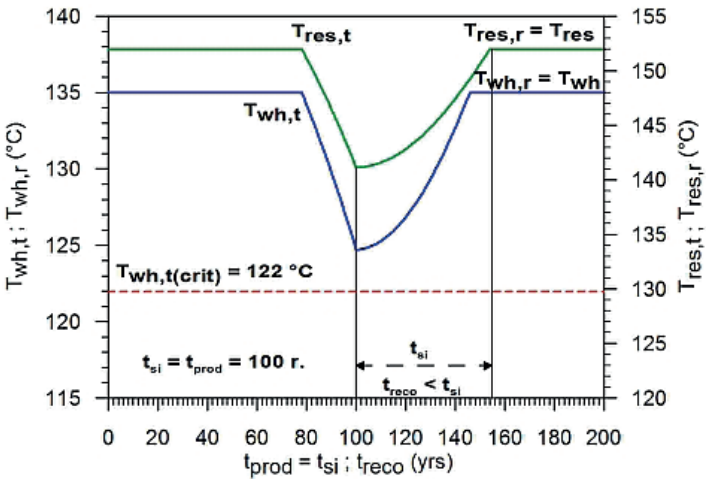

Fig. 3.23. Preview on 1TIQ / 1TER reservoir response model estimation for constant P_{th} = 49 MWth production strategy.

If the capacity is held constant since t_{prod} = 0, a breakthrough is expected to happen at around t_B = 53 yrs (Fig. 3.15). For t_{prod} = 100 yrs, a 1TIQ model cools, thus, a reservoir for t_{cool} = 47 yrs. However, the model predicts interception of $t_{si} = t_{Twh,t(crit)}$ at t_{si} = 71 yrs, where $T_{wh,t}$ = 122 °C and $T_{res,t}$ = 138 °C for D = 800 m (Fig. 3.24). Due to cooling, an initial yield of Q_{prod} = 285 kg.s^{-1} increases to Q_{prod} = 350 kg.s^{-1} at t_{si}, prompting a question on how recent 3-wells scheme can hold such deliverability.

An instant recovery is calculated for t_{reco} = 60 yrs for $T_{res,r}$, so that $t_{reco} < t_{si}$, and an approach can be considered renewable in interaction with reservoir. Yet a fact that t_{si} < 100 yrs means a strategy compromises principle of sustainable reservoir operation.

3.8.3. Stepwise field development: P_{th} = 43 → 72 MWth

Energy potential classification (Rybach, 2015) is rather a producer- or field operator- oriented scheme, working with more understandable classes then is a certainty-based McKelvey's diagram. In principle, a sustainable potential P_S = 43 MWth represents a part of total potential a system is supposed to maintain for a desired period of production, not compromising energy balance in a reservoir. The developable potential P_D = 29 MWth gives amount of energy recoverable under sustainable potential to supply a sustainable potential for some part of desired period of production. A stepwise approach in field management is, thus, in essential principles of both.

We tested stepwise field development first, considering $t_{prod,1}/t_{prod,2}$ schemes as 70/30 and 80/20 yrs. Unlike a constant production variant, both schemes appear as sustainable (Fig. 3.25), as for $t_{prod} = t_{si}$ = 100 yrs the $T_{wh,t}$ = 125 °C and $T_{wh,t}$ = 128 °C respectively, i.e. the critical boundary condition $T_{wh,t} \leq T_{wh,t(crit)}$ has not been reached through t_{prod} = 100 yrs, consequent to a calculated breakthrough at t_B = 85 and 87 yrs. Initial yield of $Q_{prod} = Q_{inj}$ = 285 kg.s^{-1} at t_{prod} = 0 yrs is forecasted to increase to Q_{prod} = 333 kg.s^{-1} and Q_{prod} = 320 kg.s^{-1}, balancing loss of thermal gradient at the wellhead. Immediate recovery after shut-in is supposed as capable to generate return of initial conditions at t_{reco} = 62 yrs and t_{reco} = 59 yrs, turning renewable capacity positive, i.e. $t_{reco} < t_{si}$. Both stepwise field development variants can, thus, be classified as sustainable and renewable approaches.

3.8.4. Stepwise field reduction: P_{th} = 72 → 43 MWth

In following, we tested mirroring of field development strategies, i.e. proceeding from a full development at $P_S + P_D$ = 72 MWth to P_S = 43 MWth, simulating field is operated at all pace first to shorten a payback, and then left easing impact of production on reservoir. A time-step scheme is given by $t_{prod,1}/t_{prod,2}$ = 20/80 and 30/70. Higher initial production (P_{th} = 72 MWth ; Q_{prod} = 285 kg.s^{-1}) accelerates cold front arrival in 1TIQ at t_B = 71 and 64 yrs respectively, resulting in a cooling period prolongation. Then, model estimates reaching $T_{wh,t}$ = 122 °C at t_{si} = 100 yrs and $T_{wh,t}$ = 121 °C at t_{si} = 99 yrs respectively, questioning both options in their sustainability ($T_{wh,t} \approx T_{wh,t(crit)}$). These absolute values do not account on uncertainties, yet compromising sustainability of this strategy even more. Use of 1TER algorithm predicts recovery of initial conditions for both scenarios at t_{reco} = 61 yrs, so that $t_{si} \geq t_{reco}$, classifying the approach renewable (Fig. 3.26).

Obviously, when opting for a safe strategy for initial field operation, a stepwise development is highly recommended. This provides time enough to study field response under detailed production monitoring, including multiple recalibrations of model. Unlike, a straight-forward peaking production, maximizing reservoir economics, is easy to compromise production longevity, and, thus, sustainability of a resource production and use.

3.9 Discussion

3.9.1. ALPM model limitations

Obvious importance of the DDHS requires application of multiple approaches to study conditions securing longevity and renewability of resource production. Analytical and lumped parameter models are capable to carry simulations on reservoir response and reclamation, yielding tentative guide for opening a field production. This may, however, be enough at early stages of reservoir opening, providing field operator sufficient time for further field and production monitoring, consequently leading to reliable data collection allowing use of more sophisticated, numerical models. Otherwise, with a few and unsound data, numerical models yield robust errors of estimates. In use of ALPMs, it is, however, necessary to respect and understand its limits.

3.9.1.1 Model calibration and history matching

A fact that model has not been calibrated using history matching has repeatedly been commented in the paper. Authors are not convinced that available data from uncomplete pumping tests, including multiple drawdown stages, are representative enough. This is instantly a case of temperature response and deliverability. To mitigate effects

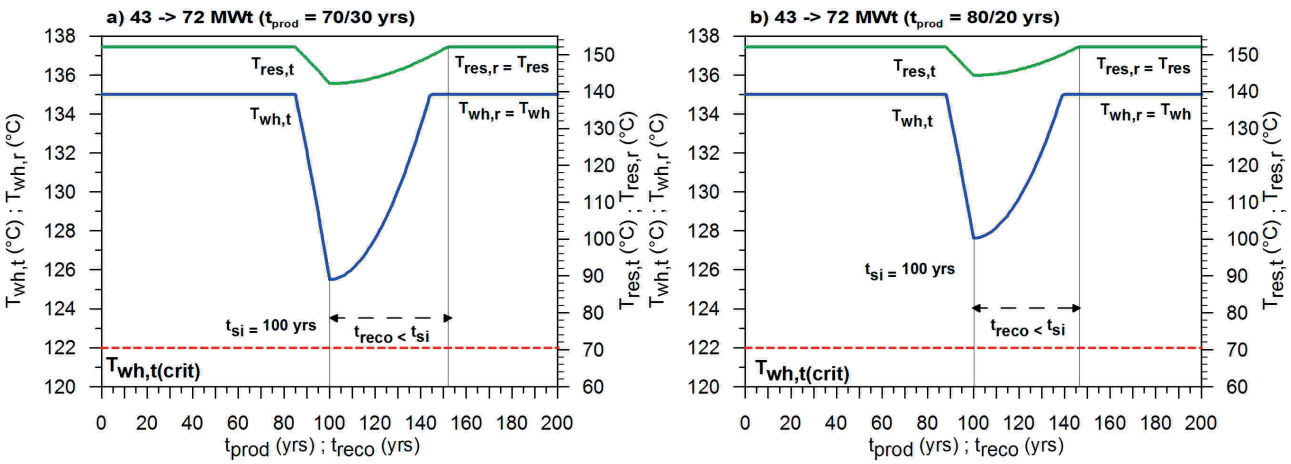

Fig. 3.25. Preview on 1TIQ / 1TER reservoir response model estimation for stepwise P_S to $P_S + P_D$ development strategies

of inadequate input data, and to strengthen reliability of the model, several actions were conducted during model calibration and upscaling:

Monte Carlo simulation of effective heat exchange profile (Heff) accounts on maximum thickness a reinjection can interact with HEP through; obtained from tectonic model of the structure at highest probability rate P90(Δz)

- adjustment of reservoir parameters as function of temperature helps avoiding constants; fixes model logs within realistic conditions, easy to be subjected for future recalibration and history matching; and secures non-isothermal reservoir behavior, so that recovery logs can not exceed values at initial conditions
- use of sampled bottomhole and wellhead temperatures from exploration provides fixed margin boundary for recovery too
- mass-balance function is defined through (1) to (14) is now fixed at $Q_{prod} = Q_{inj} = 1{:}1$, as long as tracer tests are performed, yielding relevant data on effective connectivity between reinjector and producer, now securing 1-tank pressure regime

3.9.1.2 Production scheme

At a recent state, three wells are considered to contribute on geothermal energy production at a site, drilled during a hydrogeothermal exploration campaign in 1999 (Vranovská et al., 1999a,b). A distance between wells has been calculated for D = 800 m concerning deep reservoir position. Thus, thermal breakthrough and reservoir response and recovery algorithms calculate with the given horizontal distance. It is, however, ingenuous expecting new wells not to come, as long as technical installations are supposed to wear fast exposed to chemistry of local geothermal fluids. Some studies on decline curve analysis (Reyes et al., 2004) and economical capacity (Sanyal, 2005) have also been carried for the DDHS (Fričovský et al., 2020c), showing a need on new boreholes emplacement at a time not shorter than 24 yrs. Assuming position of new wells is unreal at now. Opting for new coordinates give a field operator a good chance to enlarge a horizontal distance between reinjection and production site, further increasing safety of a long-term production. A caution must be paid on geothermal settings at a new position.

3.9.1.3 Heat flow balance

Correction for temperature, i.e. wellhead T_{wh} or borehole inflow to represent a mean reservoir temperature T_{res} can reduce assumptions on relevant conductive and convective heat increment during production. Use of advective cooling ($Q_{inj}.c_{w,inj}.t_{prod}$) in thermal breakthrough and ALPMs accredits the magnitude of cooling dramatically (compared to a case where cooling is reduced to a diffuse). This is, however, balanced through introduction of convective (advective) heat increment (62) in a gross E_n (40) determination for both, the 1TIQ and 1TER model once the cold front arrives to production zone. Building-up the E_{CV} during production eases the effect of advective cooling as long as Γ_{CV} (58) increases with drop in $T_{CV,top} = T_{res,t}$. Starting the reclamation at t_{si} for scenarios where $t_B < t_{prod}$ and $T_{res,t} \leq T_{res}$ accounts for maxima in E_{CV} and Γ_{CV}, promoting recovery in early stage, while progressively decaying as long as $T_{res,r} \rightarrow \lim T_{res}$ in 1TER model. This allows a model to adjust towards reservoir dynamics that are function of change mean reservoir temperature.

Importance of conduction can not be questioned at local conditions. Convection is, however, assumed from indirect indices, such is local thermodynamics (e.g. Fričovský et al., 2018a) or linear stability analysis (e.g. Fričovský et al., 2018b,c; Vizi et al., 2020). To support the idea, several adiabatic boiling and phase stability models have also been carried (Fričovský et al., 2020c), limiting plausible

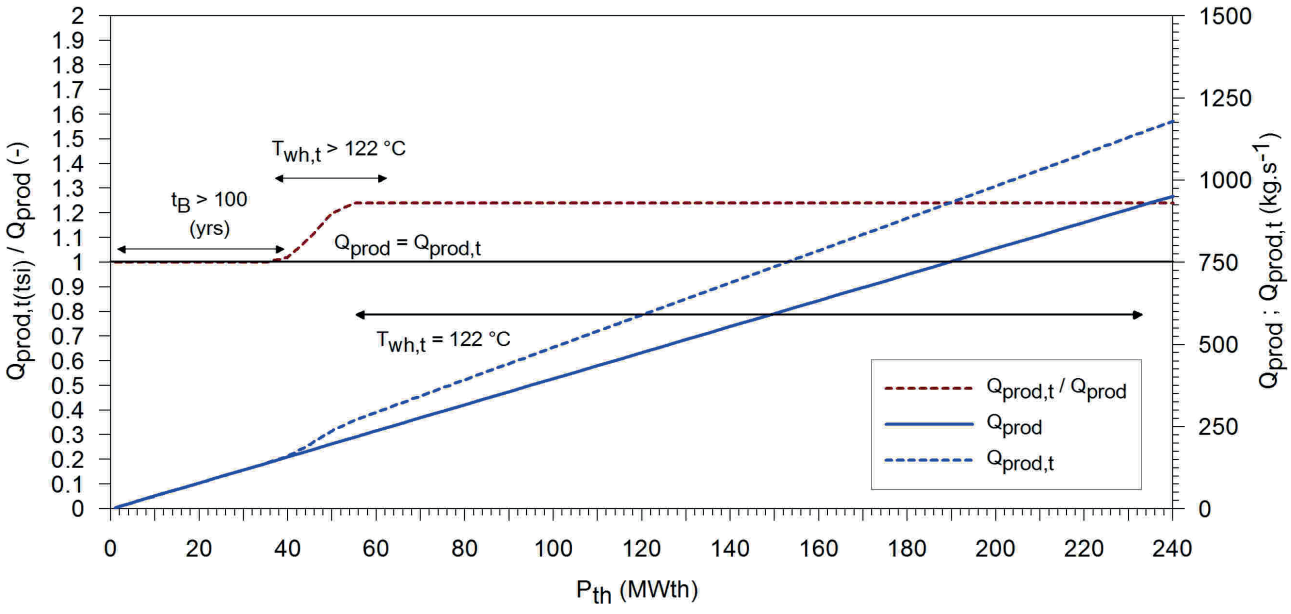

Fig. 3.26. *Preview on 1TIQ / 1TER reservoir response model estimaton for stepwise field reduction from $P_S + P_D$ to P_S strategies.*

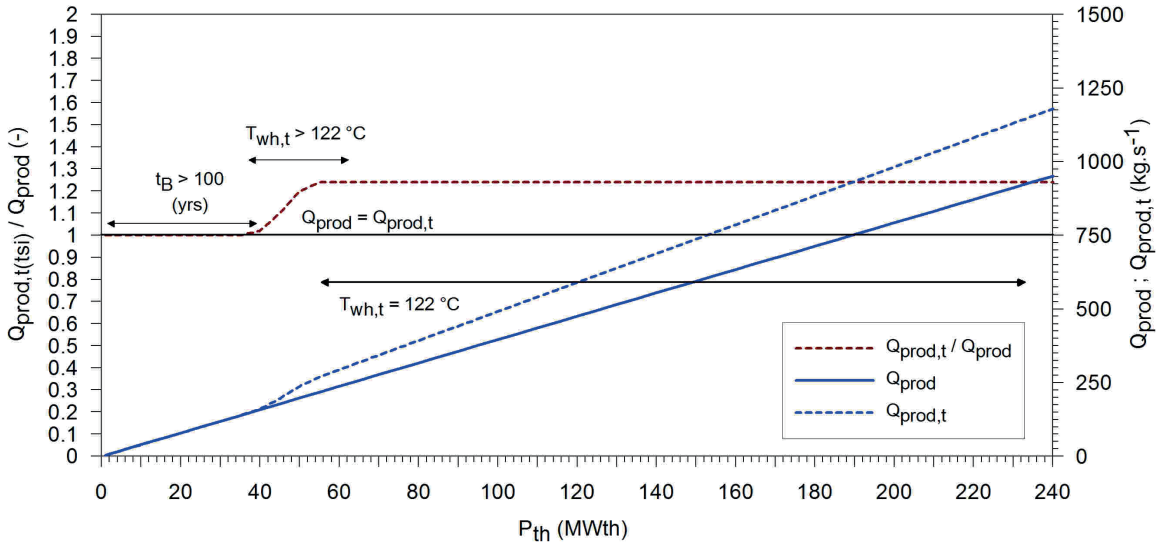

Fig. 3.27. *Desired yieldrates (Q_{prod}) at t_{si} for constant thermal output strategies.*

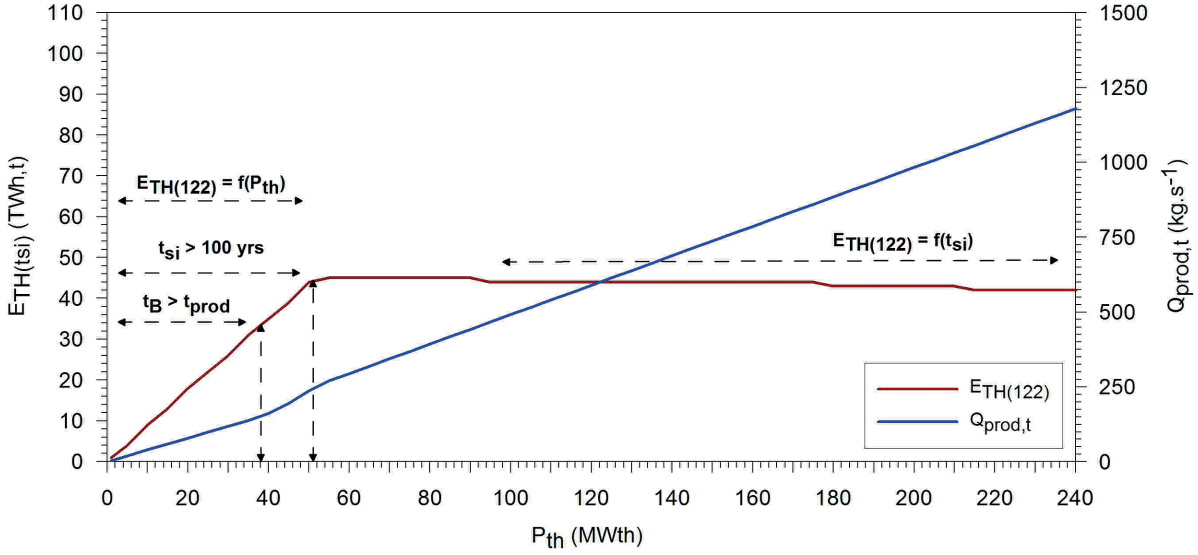

Fig. 3.28. *Cumulative geothermal energy production $E_{TH(122)}$ for constant thermal output strategies.*

convection as quiet at a steady-state in deepest parts of reservoir. However, more studies are required, such is use of geothermometry and mixing / boiling models, capable to address vertical geothermal brine movements in reservoir through thermal equilibrium recalibration.

3.9.2. Cumulative production of geothermal energy at sustainable conditions

One of most critical parameters when concerning a field development with consecutive investments into geothermal infrastructure, operation and maintenance costs etc. is a potential of energy that can be generated over a desired period of time, an operator can sell to the market. This is even more pronounced, as environmental subsidies from carbon dioxide mitigation can play a role in total investments – income balance.

The level of sustainable cumulative production of geothermal energy is approached introducing the $E_{TH(122)}$ parameter, representing ideal (theoretical) cumulative amount of energy produced at a time of shut-in (t_{si}), yet not including engineering considerations, such is thermal efficiency of heat exchange processes, assuming the thermal output constant in a model.

Any cooling calls for a necessary increase in yield to balance loss in $T_{res,t}$ and $T_{wh,t}$ paying an instant impact on deliverable energy at a wellhead through specific heat capacity of geothermal brine at the wellhead, i.e. $c_{w,wh} = f(T_{wh,t}, \rho_{w,wh})$, where $\rho_{w,wh} = f(T_{wh,t}, p_{wh})$, assuming constant wellhead pressure. As long as $Q_{prod} = Q_{inj} = 1{:}1$ is set in the 1TIQ model, the Q_{prod} or Q_{inj} rates increase up to 20 % depending on a decay in $T_{res,t}$ and $T_{wh,t}$ (Fig. 3.27), yet fixed through shut-in at $T_{wh,t} \leq T_{wh,t(crit)} = 122$ °C and $t_{si} = t_{Twh,t(crit)}$. As based on 1TIQ model, the boundary that corresponds to a maximum increase in desired productivity is, thus, $P_{th} \geq 51$ MWth. Following the boundary condition, a maximum sustainable thermal energy production that can be produced from a reservoir $E_{TH(122)} = 45 – 46$ TWh,th at $t_{si} = 100$ yrs (Fig. 3.28). Any constant thermal output

strategy above the threshold level of P_{th} = 51 MWth yields slow decay in $E_{TH(122)}$ as period of production shortens with t_{si} due to critical cooling rate boundary condition interception. The 1TIQ summation plot thus demonstrates a fair compromise between longevity of production and a cumulative energy recovery from a reservoir to turn investments reasonable.

Obviously, higher production rates can generate the same output in considerably shorter time, yet on considerable costs on a resource and reservoir environment. An example of such comparison is a constant management operating P_{th} = 49 MWth and P_{th} = 72 MWth. A first scenario generates $E_{TH(122)}$ = 43 Twh,th at $t_{si} = t_{prod}$ = 100 yrs, so that at such a rate, a system can be considered sustainable and renewable. The latter, maintained constant, does, however, generate $E_{TH(122)}$ = 45 TWh,th, yet a system terminates at t_{si} = 71 yrs, compromising a principle beyond what sustainability and sustainable development means. A total difference is, thus, 2 TWh,th between both, yet impact on a reservoir and production longevity is huge in a difference. At least for resources repeatedly considered "renewable" an income-only approach should not always be introduced.

3.10 Conclusions

A complete module on thermal breakthrough, production response and reclamation, is presented in this paper, providing theory beyond necessary for its reconstruction, upscaling and application. Assessing thermal breakthrough is approached through a doublet, advective cooling model with a diffuse / conductive retardation (e.g. Ungemach et al., 2005, 2009). Reservoir response to production forecasting is governed by analytical, pseudo lumped-parameter model 1TIQ (1-tank ALPM with heat flux and reinjection), set to run since beginning of production at D = 0 (position of reinjector), and since $t_B \leq t_{prod}$, i.e. if $t_{cool} \neq 0$ at D = 800 m (position of producers). A similar ALPM model is applied in simulation of reservoir reclamation after production shut-in with 1TER (1-tank closed energy recovery) model.

The entire model is precisely upscaled to local conditions, including reservoir geometry (e.g. simulation of HEP thickness, total "tank" thickness) and doublet scheme (e.g. D = 800 m), geothermal field (mean reservoir temperature, heat flux), and reservoir dynamics (convection contribution). A necessary mass balance (1 to 14) functions (e.g. Sarak et al., 2003a,b, 2005) secure a closed-tank (Axelsson, 1989) behavior of the model. Pressure is controlled through 1:1 production – injection ratio, i.e. $Q_{prod} = Q_{inj}$, assuming ideal connectivity within HEP as part of a reservoir profile, and no natural / induced recharge (Vranovská et al., 2015). The energy flux introduces the radiogenic heat production (64), conduction (54) and convection (61) into the balance (37). Given setup allows non-isothermal reservoir conditions during production and recovery, except constant radiogenic heat production E_{RG}, assumed stable at shallow crustal depths and given temperatures (Čermák et al., 1991). This reduces (40) impact of applied advective cooling on effective heat exchange profile in 1TIQ model (28 or 36) where convective Γ_{CV} and conductive Γ_{CD} gradients (65) are induced due to cooling ($T_{res,t} \rightarrow \lim T_{res,t(si)}$; $T_{top,t} \rightarrow \lim T_{top,crit}$) as long as there is some breakthrough i.e. $t_B < t_{prod}$. For recovery, the dynamic setup reduces heat flow density progressively as a reservoir reclaims (pseudo) initial conditions in 1TER model. Fixing the energy flux restrains exceeding initial, steady-state conditions during and after recovery from production. Analytical functions are adjusted rather to mean reservoir $T_{res,t}$, wellhead $T_{wh,t}$ or reinjection T_{inj} temperature, the less to the system geometry, i.e. depth (z) or thickness (H or Δz respectively). A given model does not include iterative techniques for history matching, such the least-square or Levenberg-Marquardt (Sarak et al., 2003), hence history matching is skipped in the model due to unreliable long-term monitoring data. However, the entire module can easily be equipped with history fitting function, depending on a parameter to match – yet Q_{prod} and T_{res} are the most likely.

Geothermal resources are repeatedly addressed as sustainable and renewable in once, presented to society as one of tools to approach sustainable development. Praxis has, however, repeatedly shown that both, sustainability and renewability can easily be compromised through depletive field management. It is, however, not a question of a geothermal fluid quantity. Instead, temperature, mobile phase stability and change, reservoir thermodynamics (exergy, enthalpy), and heat flux dynamics are frequently concerned. Each production that causes irreversible changes to a geothermal system is, thus, all but sustainable. To mitigate such a human impact, numerous approaches to study reservoir sustainability and renewability emerged in last decades, turning sustainability one of the most important issues of reservoir engineering. In fact, this topic has long been omitted in Slovakia, lacking any support in essential enactments, such is Act. No. 569/2007 Coll. (Geology act) and its related Regulation N. 51/2008 Coll., or Act. No. 364/2004 Coll. (Water Act). Neither balance based, nor analytical and numerical solutions on a resource sustainability in its energy capacity, potential and fluxes are set mandatory in hydrogeothermal assessments or prior field opening.

The Ďurkov Depression hydrogeothermal structure (DDHS) is considered one of the most perspective amongst geothermal systems in Slovakia. TOUGH2 code based model has been already carried to search for sustainable production (Giese, 1998, 1999), yielding several limits (purely conductive environment, orthogonal / regular grid atc.), however, assuming reinjection at T_{inj} = 25 °C. Under given geothermal fluid chemistry (e.g. Vranovská et al., 1999a,b, 2015; Bodiš & Vranovská, 2012), rather a fluid return at T_{inj} = 65 °C (Vranovská et al., 1999a) is more realistic. Multiple studies have also shown there is at least limited, quiet convection likely within deepest parts of a system that must be accounted. Authors also conclude, that at given thermal field setup, relying only on conductive cooling / heating balance becomes fairly optimistic assumption (local temperatures along effective heat exchange profile are simply too low).

Instead, a model on breakthrough, reservoir response and recovery has been adopted as part of a complex study

on reservoir sustainability at a site, funded by Ministry of Environment of the Slovak Republic (Fričovský et al., 2020c), balancing and modeling at a desired period of production equal to t_{prod} = 100 yrs according to a concept of sustainable reservoir production (Axelsson et al., 2001).

In cold-front progression analysis using advective breakthrough model with simultaneous conductive retardation, a thermal capacity of P_{th} = 38 MWth has been found a limit to avoid cooling within production zone during desired period of production (Fig. 3.16). At given conditions (T_{inj} = 65 °C and $Q_{prod} = Q_{inj}$ = 1:1 = const.), the capacity equals $Q_{prod} = Q_{inj}$ = 158 kg.s^{-1}. The model calculates with effective reservoir heat-exchange profile, assumed H_{eff} = 600 m as 90-th percentile of reservoir thickness simulation. As it is given by a theory beyond, reduction of return temperature increases the threshold value for a cold-front to arrive (e.g. P_{th} = 61 MWth for T_{inj} = 25 °C), and so an increase in H_{eff} does.

Thermal breakthrough is, however, frequently observed phenomena at geothermal fields, not necessarily terminating field production as long as there aren't changes in reservoir phase or quality, or, rather, if geothermal infrastructure has been optimized for some optional cooling. Several approaches have already been introduced to answer a rate of tolerable cooling that secures feasibility of a project and minimizes impact on a reservoir performance. For that case, the model adopts a 10 % tolerated cooling limit (Williams, 2004, 2007) prior shut-in. This allows temperature at a wellhead to be a principal boundary condition, i.e. $T_{wh,t(crit)} = 0.9T_{wh}$ = 122 °C (T_{wh} = 135 °C; Halás Sr et al., 2016), and so the 1TIQ model stops simulation at a time the drop in temperature intercepts the boundary condition, i.e. $t_{si} = t_{Twh,t(crit)}$. Each simulation has been run for a desired period of production, i.e. t_{prod} = 100 yrs to find out the realistic time of shut-in.

Plot of t_{si} development (Fig. 3.17) shows that for t_{prod} = 100 yrs, the critical thermal output is P_{th} = 51 MWth (Q_{prod} = 214 kg.s^{-1}) to maintain constant field operation. Because the model is not matched with the production history, production of P_{th} = 49 MWth is recommended. This is a value obtained from reserve capacity ratio application to geothermal reserves booking performed through Monte Carlo simulation of recoverable heat in place (Fig. 3.13). A given rate yields t_B = 79 yrs, so that t_{cool} = 21 yrs. At t_{prod} = 100 yrs, the wellhead temperature is expected above the critical, i.e. $T_{wh,t}$ = 124 °C, not intercepting introduced boundary condition, so $t_{si} = t_{prod}$ = 100 yrs. Due to t_{cool}, 1TIQ model assumes necessary increase in deliverability up to $Q_{prod,t} = Q_{inj}$ = 230 kg.s^{-1} at production termination (Fig. 3.23). The 1TER model for reclamation has been initiated as t_{reco} = 0 at $t_{prod} = t_{si}$, setting $Q_{prod} = Q_{inj}$ = 0 kg.s^{-1} in an algorithm. Obviously, a system is able to recover at $t_{reco} \leq t_{si}$, so that $\Delta t_{reco} = t_{si} - t_{reco} > 0$, classifying such strategy sustainable and of a renewable interaction with the reservoir. Generally, the reservoir (a geothermal system) is able to recover initial conditions nearby the production zone as long as $T_{res,t} \geq$ 138 °C and $t_{reco} \geq$ 60 yrs with $T_{top,crit} \geq$ 80 °C.

1TIQ model analysis also implicated that the conductive play-type of the DDGS, may only be generally preserved at initial state. A long term production and reinjection can, apparently, generate convective gradient through cooling high enough to make quiet, stable convection towards induced (D = 800 m) and unstable (D ≤ 600 m), optionally with convective regime prevailing over conductive close to reinjector (D ≤ 200 m). However, as long as a system is able to recover initial geothermal field, it is also able to return into quiet, conductive environment at a final stage of recovery.

The 1TIQ model has also been equipped with algorithm to calculate sustainable cumulative geothermal energy production – termed herein $E_{TH(122)}$, not accounting engineering efficiencies, such as optional heat exchanger station. The computation worked for a period between t_{prod} = 0 to t_{si} (Fig. 3.28). Obviously, a maximum amount of geothermal energy production under sustainable and renewable conditions may count no more than $E_{TH(122)}$ = 46 TWh,th, assuming constant production. It well represents an example of a compromise between maximizing long-term output and restraining irreversible or major risks posed onto reservoir.

Slovakia is still fossil-fuels oriented economics, though there is a political and social call on transition towards carbon-neutral primary energy mix. The DDHS is, obviously, amongst resources of contributable potential. Yet instead of excessive installments and depletion, concern must be acknowledged towards sustainability of geothermal energy production, the more, in case of sites of such energy potential. Obtained results must not be taken as absolute. Authors are aware of limits of the model, even constructed under precise upscaling to local conditions. Instead, gained analysis should provide background reliable enough to, first, open a field production at recommended limits (P_{th} = 49 MWth), followed by detailed field analysis, including tracer tests (assessing connectivity), production monitoring, model calibration (such using history matching), and transition towards complex numerical models. Just after yielding good certainty, the production should be increased, i.e. towards P_{th} = 72 MWth, as given by combination of sustainable (P_S) and developable (P_D) potential. Such a step-wise development is, indeed, a worldwide applied praxis, mitigating unexpected reservoir or production failure.

References

Agemar, T., Schellschmidt, R. & Schulz, R., 2012: Subsurface temperature distribution in Germany. Geothermics, 44, p. 65-77.

Alkan, H. & Satman, A., 1990: A new lumped parameter model for geothermal reservoirs in the presence of carbon dioxide. Geothermics, 19, p. 469-479.

Arevalo, A.S., 2003: Rapid environmental assessment tool for extended Berlin geothermal field project. In: Proceedings International Geothermal Conference, Reykjavik, Iceland, p. 1-7.

Axelsson, G., 1989: Simulation of pressure response data from geothermal reservoirs by lumped parameter models. Proceedings 14th Workshop on Geothermal Reservoir Engineering, Stanford University, CA, p. 1-7.

Axelsson, G., 2010: Sustainable geothermal utilization – Case histories; definitions; research issues and modelling. Geothermics, 39, p. 283-291.

Axelsson, G., 2011: Using long case histories to study hydrothermal renewability and sustainable utilization. Geothermal Resource Council Transactions, 35, p. 1393-1400.

Axelsson, G.., 2012a: Modelling sustainable geothermal energy utilization. Proceedings the 53rd Scandinavian Simulation and Modelling Society Conference, Reykjavik, Iceland, p. 1-14.

Axelsson, G., 2012b: The physics of geothermal energy. In: Sayigh, A. (Ed.) 2012: Comprehensive renewable energy. Elsevier Ltd., p. 1-52.

Axelsson, G., Bjornsson, G., Flovenz, O.G., Kristmansdóttir, H. & Sverrisdottir, G., 1995: Injection experiments in low-temperature geothermal areas in Iceland. Proceedings World Geothermal Congress 1995, Florenze, Italy, p. 1-5.

Axelsson, G., Gudmundsson, A., Steingrímsson, B., Palmasson, G., Armansson, H., Tilinius, H., Flovenz, O.G., Bjornsson, S. & Stefansson, V., 2001: Sustainable production of geothermal energy: suggested definition. International Geothermal Association News Quaterly, 43, p. 1-2.

Axelsson, G., Stefansson, V. & Xu, Y., 2002: Sustainable management of geothermal resources. Proceedings Beijing International Geothermal Symposium, Beijing, China, p. 277-283.

Axelsson, G., Stefansson, V. & Björnsson, G., 2004: Sustainable utilization of geothermal resources. Proceedings 29th Workshop on Geothermal Reservoir Engineering, Stanford University, CA, p. 1-8.

Baldwin, B. & Butler, C.O., 1985: Compaction curves. American Association of Petroleum Geologists Bulletin, 69 (4), p. 622-626.

Beardsmore, G.R., Rybach, L., Blackwell, D. & Baron, Ch., 2010: A protocol for estimaping and mapping global EGS potential. Geothermal Resource Council Transactions, 34, p. 301-312.

Bielik, M., 1999: Geophysical features of the Slovak Western Carpathians: a review. Geological Quaterly, 43 (3), p. 251-262.

Bjornsson, G., Axelsson, G., Flóvenz, O.G., 1994: Feasibility study for the Thelamork low-temperature system in Iceland. Proceedings 19th Workshop on Geothermal Reservoir Engineering, Stanford University, CA, p. 1-9.

Blöcher, M.G., Zimmermann, G., Moeck, I., Brandt, W., Hassanzadegan, A., Magri, F., 2010: 3D numerical modeling of hydrothermal processes during the lifetime of a deep geothermal reservoir. Geofluids, 10 (3), p. 406-421.

Bjarnadottir, R., 2010: Sustainability evaluation of geothermal systems in Iceland. Indicators for sustainable production [manuscript – Master's Thesis], Reykjavik Energy Graduate School of Sustainable Systems, Reykjavik.

Bodiš, D. & Vranovská, A., 2012: Genéza anomálneho obsahu arzénu v hydrogeotermálnej štruktúre Ďurkov [*Genesis of anomalous arsenic content in the hydrogeothermal structure of Ďurkov*]. Podzemná voda, XVIII (2), p. 123-136, in Slovak, English resume.

Brehme, M., Moeck, I., Kamah, Y., Zimmermann, G. & Sauter, M., 2014: A hydrotectonic model of a geothermal reservoir – A study in Lahedong, Indonesia. Geothermics, 51, p. 228-239.

Bromley, Ch., Rybach, L. & Mongillo, M., 2006: Sustainable utilization strategies and promotion of beneficial environmental effects: having your cake and eating it too. Proceedings New Zeeland Gegothermal Workshop.

Bujakowski, W., Tomaszewska, B. & Miecznik, M., 2016: The Podhale geothermal reservoir simulation for long-term sustainable production. Renewable Energy, 99, p. 420-430.

Burnell, J., O'Sullivan, M., O'Sullivan, J., Kissling, W.., Croucher, A., Pogacnik, J., Pearson, S., Caldwell, G., Ellis, S., Zarrouq, S. & Climo, M., 2015: Geothermal Supermodels: The next generation of integrated geophysical, chemical and flow simulation modelling tools. Proceedings World Geothermal Congress 2015, Melbourne, Australia, p. 1-7.

Clotworthy, A.W., Ussher, G.N.H., Lawless, J. V. & Randle, J.B., 2006: Towards an industry guideline for geothermal reserves determination. Geothermal Resource Council Transactions, 30, p. 852-859.

Čermák, V., Bodri, L. & Rybach, L., 1991: Radioactive heat production in the continental crust and its depth dependence. In: Čermák, V. – Rybach, L. (Eds.): Terrestrial Heat Flow and the Litosphere Structure. Springer – Verlag, Berlin Heidelberg, DE, p. 23-70.

Činčura, J. & Köhler, E., 1995: Paleoalpine karstification: the longest paleokarst period in the Western Carpathians (Slovakia). Geol. Carpathica, 46 (5), p. 343-347.

Deibert, L., Hjartarson, A., McDonald, I., McIlveen, J., Thompson, A., Toohey, B. & Yang, D., 2010: The Canadian geothermal code for public reporting – 2010 Edition. The Canadian Geothermal Code Committee, 34 p.

DiPippo, R., 2005: Geothermal power plants – principles, applications and case studies. Butterworth – Heinemann, New York, 445 p.

DiPippo, R., 2007: Ideal thermal efficiency for geothermal binary plants. Geothermics, 36, p. 276-285.

Doveri, M., Lelli, M., Marini, L. & Raco, B., 2010: Revision, calibration, and application of the volume method to evaluate the geothermal potential of some recent volcanic areas of Latium, Italy. Geothermics, 39, p. 260-269.

Falcone, G. & Beardsmore, G.R., 2015: Including geothermal energy within a consistent classification for renewable and non-renewable energy resources. Proceedings World Geothermal Congress 2015, Melbourne, Australia.

Falcone, G., Gnoni, A., Harrison, B. & Alimonti, C., 2013: Classification and reporting requirements for geothermal resources. Proceedings, European Geothermal Congress 2013, Pisa, Italy.

Fendek, M., Remšík, A. & Fendeková, M., 2005: Metodika vyhľadávania, hodnotenia a bilancovania množstva geotermálnej vody a geotermálnej energie [*Methodology of searching, evaluation and balancing of the amount of geothermal water and geothermal energy*]. Mineralia Slovaca, 37 (2), p. 117-121, [in Slovak, English summary].

Flóvenz, O.G., Árnason, F., Finnsson, M. & Axelsson, G., 1995: Direct utilization of geothermal water for space heating in Akureyri, N-Iceland. Proceedings World Geothermal Congress 1995, Firenze, Italy, p. 1-6.

Flóvenz, O.G., Arnason, F., Gautason, B., Axelsson, G., Egilson, T., Stendórsson, S.H. & Gunnarsson, H.S., 2010: Geothermal District Heating in Eyjafjördur, N-Iceland; Eighty Years of Problems, Solutions and Success. Proceedings World Geothermal Congress 2010, Bali, Indonesia, p. 1-8.

Fournier, R.O. & Potter, R.W. II., 1978: A magnesium correction for the Na-K-Ca chemical geothermometer. U.S. Geological Survey Open-File Report No. 78-986, 24 p.

Fournier, R.O. & Potter, R.W. II., 1979: Magnesium correction to the Na-K-Ca chemical geothermometer. Geochimica Cosmochimica Acta, 43, p. 1543-1550.

Fournier R.O. and Potter R.W.II., 1982: A revised and expanded silica (quartz) geothermometer. Geothermal Resources Council Bulletin 11, p. 3-12.

Fournier R.O., White D.E. & Trusdell A.H., 1974: Geochemical indicators of subsurface temperature - Part 1, basic assumptions. J. Res. U. S. Geol. Survey, 2, p. 259-261.

Fox, D.B., Sutter, D., Beckers, K.F., Lukawski, M.Z., Koch, D.L., Anderson, B.J. & Tester, J.W., 2013: Sustainable heat farming: modelin extraction and recovery in discretely fractured geothermal reservoirs. Geothermics, 46, p. 42-54.

Fričovský, B., Jacko, S. Jr., Popovičová, M. & Tometz, L., 2013: Substitution approach in cabron dioxide emission reduction evaluation: case study on geothermal power station project plan – Ďurkov (Košice Basin, Slovakia). International Journal of Environmental Science and Development, 4, 2, p. 124-129.

Fričovský, B., Tometz, L. & Fendek, M., 2016: Geothermometry techniques in reservoir temperature estimation and conceptual site models construction: principles, methods and application for the Bešeňová elevation hydrogeothermal structure, Slovakia. Mineralia Slovaca, 48, 1, p. 1-60.

Fričovský B., Vizi, L., Surový, M. & Mižák, J., 2018a: Numerical indices implications on reservoir convection for the Ďurkov Depression hydrogeothermal structure, Košice Basin. Geologické Práce, správy, 132, p. 3-30, in Slovak, extended English resume.

Fričovský B., Vizi, L. & Surový, M., 2018b: Vplyv segmentácie rezervoáru na formovanie priaznivých podmienok konvekcie: model ukloneného pórovitého prostredia; príklad hydrogeotermálnej štruktúry Ďurkovská depresia, Košická kotlina [*Influence of reservoir segmentation on the formation of favourable convection conditions: model of inclined porous medium; example of hydrogeothermal structure Ďurkov Depression,* Košice Basin]. Proceedings, 19. Slovak hydrogeological conference, Nimnica Spa, Slovakia, in Slovak.

Fričovský, B., Vizi, L., Gregor, M., Zlocha, M., Surový, M. & Černák, R., 2018c: Thermodynamic analysis and quality mapping of a geothermal resource at the Ďurkov hydrogeothermal structure, Košice depression, Eastern Slovakia. Proceedings 43rd Workshop on Geothermal Reservoir Engineering, Stanford University, CA, p. 1-9.

Fričovský, B., Vizi, L., Fordinál, K., Surový, M. & Marcin, D., 2019: A reviewed hydrogeothermal evaluation of the Ďurkov Depression hydrogeothermal structure: insights from probabilitstic assessment and sustainable production optimization. Proceedings 44rd Workshop on Geothermal Reservoir Engineering, Stanford University, CA, p. 1-14.

Fričovský, B., Černák, R., Marcin, D., Blanárová, V., Benková, K., Pelech, O., Fordinál, K., Bodiš, D. & Fendek, M., 2020a: Geothermal Energy Use – Country Update for Slovakia. Proceedings World Geothermal Congress 2020, Reykjavik, Iceland, p. 1-12 (fulltext accepted, in press).

Fričovský, B., Vizi, L., Marcin, D., Černák, R., Blanárová, V., Ujjobbágyová, Z., Bodiš, D., Benková, K., Pelech, O. & Fordinál, K., 2020b: Geothermal energy utilization in Slovakia: First insights from sustainability prospective. Proceedings World Geothermal Congress 2020, Reykjavik, Iceland, 1-12 (fulltext accepted, in press).

Fričovský, B., Vizi, L., Surový, M., Fordinál, K., Zlocha, M., Gregor, M. & Fričovská, J., 2020c: Hydrogeotermálne hodnotenie Ďurkovskej depresie: aplikácia princípov trvalo udržateľného rezervoárového manažmentu. Manuscript, Technical Report, SGIDŠ, Bratislava, 167 p. [in Slovak, in print].

Fridleifsson, I.B., Bertani, R., Huenges, E., Lund, J.W., Ragnarsson, A. & Rybach, L., 2008: The possible role and contribution of geothermal energy to the mitigation of climate change. In: Hohmeyer – Trittin (Eds): IPCC Scoping Meeting on Renewable Energy Sources Proceedings, Luebeck, Germany, p. 59-80.

Garg, S.K. & Kassoy, D.R., 1981: Convective heat and mass transfer in hydrothermal systems. In: Rybach, L., Muffler, L.J.P. (Eds.), Geothermal Systems. Principles and Case Histories. Wiley, p. 37–76.

Garg, S.K. & Combs, J., 2010: Appropriate use of USGS volumetric "heat in place" method and Monte Carlo simulations. Proceedings, 34th Workshop on Geothermal Reservoir Engineering, Stanford University, Stanford, California.

Garg, S.K. & Combs, J., 2015: A reformulation of USGS volumetric „heat in place" resource estimation method. Geothermics, 55, p. 150-158.

Giese, L., 1998: Report on the evaluation of well test data – geothermal well GTD-2, Ďurkov geothermal field, Košice Basin. Manuscript, Geothermia, Geochimica, Berlin.

Giese, L., 1999: Report on the evaluation of well test data – geothermal well GTD-3, Ďurkov geothermal field, Košice Basin. Manuscript, Geothermia, Geochimica, Berlin.

Giggenbach, W.F., 1988: Geothermal solute equilibria. Derivation of Na-K-Mg-Ca geoindicators. Geochimica Cosmochimica Acta, 52, p. 2749-2756.

González, Z., González, D. & Kretzchmar, T., 2015: First approach of Environmental Impact Assessment of Cerro Prieto geothermal power plant, BC, Mexico. In: Proceedings World Geothermal Congress 2015, Melbourne, Australia, p. 1-9.

Grant, M.A., 2000: Geothermal resource proving criteria. Proceedings World Geothermal Congress 2000, Kyushu-Tohoku, Japan.

Grant, M.A., 2014: Stored-heat assessments: a review in the light of field experience. Geothermal Energy Science, 2, p. 49-54.

Grant, M.A. & Bixley, P.F., 2011: Geothermal Reservoir Engineering, 2nd Edition. Elsevier – Academic Press, Amsterdam, NL, 359 p.

Gringarten, A.C., 1978: Reservoir lifetime and heat recovery factor in geothermal aquifers for urban heating. Pure and applied geophysics, 117, p. 297-308.

Gringarten, A.C. & Sauty, J.P., 1975: A theoretical study of heat extraction from aquifers with uniform regional flow. Journal of geophysical research, 80 (35), p. 4956-4962.

Gungor, A., Erbay, Z. & Hepbasli, A., 2011: Exergetic analysis and evaluation of a new application of gas-engine heat pumps (GEHPs) for food drying processes. Applied Energy, 88, p. 882-891.

Gutiérrez-Negrín, L.C.A., Maya-González, R. & Quijano-Leon, J.L., 2015: Present situation and perspectives of geothermal in Mexico. Proceedings World Geothermal Congress 2015, Melbourne, Australia, p. 1-10.

Haenel, R., Rybach, L. & Stegena, L., 1988: Fundamentals of geothermics. In: Haenel et al. (Eds.): Handbook of terrestrial heat-flow density determination with guidelines and recommendations of the International Heat Flow Commission. Kluwer Academic Publishers, Dordrecht, NL, p. 9-56.

Halás, O., Drozd, V. & Vranovská, A., 1999: Investigation of Ďurkov geothermal structure in Košice Basin for geothermal energy utilization. Proceedings XXIX IAH Congress: Hydrogeology and Land Use Management, Bratislava, Slovakia, p. 689-695.

Halás Sr. O., Halás Jr. O., Drozd, V. & Výboch, M., 2016: Košická kotlina – geotermálna energia: Čiastková záverečná správa a výpočet množstiev vôd [*Košice Basin - geothermal energy: Partial final report and calculation of water quanti-*

ties]. Manuscript – Technical report SLOVGEOTERM a.s., Bratislava, 58 p. In Slovak.

Holzbecher, E.O., 1998. Modeling Density-driven Flow in Porous Media: Principles, Numerics, and Software. Springer, Berlin, Germany.

Hosgor, F.B., Cinar, M., Kaklidir, F.T., Tureyen O.I. & Satman, A., 2013: A new lumped parameter (tank) model for reservoirs containing carbon dioxide. Proceedings 38th Workshop on Geothermal Reservoir Engineering, Stanford University, CA, p. 1-7.

Hyashi, K., Willis-Richards, J., Hopkirk, R.J. & Niibori, Y., 1999: Numerical models of HDR geothermal reservoirs – a review of current thinking and progress. Geothermics, 28, p. 507-518.

Ijäs, A., Kuitunen, M.T. & Jalava, K., 2008: Developing the RIAM method (rapid impact assessment matrix) in the context of impact significance assessment. Environmental Impact Assessment Review, 30, p. 82-89.

Jacko, S., Fričovský, B., Pachocká, K. & Vranovská, A., 2014. Reverse stationary temperature modeling and geothermal resource calibration for the Košice depression (eastern Slovakia). Geological exploration technology, geothermics, sustainable development, 1 (2014), p. 3 - 25.

Kassoy, D.R. & Zebib, A., 1975: Variable viscosity effects on the onset of convection in porous media. The Physics of Fluids, 18 (12), p. 1649-1651.

Kukurugyová, M., Jablonský, G., Nalevanková, J. & Dzurňák, R., 2015b: Production, profit and return of ORC-CHP geothermal power plant model at Ďurkov area, Slovakia. Proceedings, ISET 2015, Bratislava, Slovakia.

Lipsey, L., Pluymaekers, M., Goldberg, T., van Oversteeg, K., Ghazaryan, L., Cloetingh, S. & van Wees J.-D., 2016: Numerical modelling of thermal convection in the Luttelgeest carbonate platform, the Nederlands. Geothermics, 64, p. 135-151.

Lizoň, I. & Jančí J., 1979: Základný výskum priestorového rozloženia zemského tepla v Západných Karpatoch [*Basic research of spatial distribution of terrestrial heat in the Western Carpathians*]. Manuscript – Technical report. Bratislava: Geofyzika, Archív Geofond, 35 p. [in Slovak].

Majcin, D., Král, M., Bilčík, D., Šujan, M. & Vranovská, A., 2017: Deep geothermal sources for electricity production in Slovakia: thermal conditions, Contributions to Geophysics and Geodesy, 47 (1), p. 1-22.

Menjoz, A. & Sauty, J.P., 1982: Characteristics and effects of geothermal resource exploitation. Journal of Hydrogeology, 56, p. 49-59.

Moeck, I.S., 2014: Catalog of geothermal play types based on geologic controls. Geothermics, 37, p. 867-882.

Moeck, I. & Beardsmore, G., 2014: A new „Geothermal Play Type" catalog: streamlining exploration decision making. Proceedings 39th Workshop on Geothermal Reservoir Engineering, Stanford University, CA, USA, p. 1-10.

Muffler, L.P.J. & Cataldi, R., 1978: Methods for regional assessment of geothermal resources. Geothermics, 7, p. 53-89.

Neupane, G., Mattson, E., McLing, T., Palmer, D., Smith, R.W. & Wood, T.R., 2014: Deep Geothermal Reservoir Temperatures in the Eastern Snake River Plain, Idaho, using Multicomponent Geothermometry. In: Proceedings 39th Workshop on Geothermal Reservoir Engineering, Stanford University, California, p. 1-12.

O'Sullivan M.S., 2010: Geothermal fluid dynamics. Proceedings the 17th Australian Fluid Mechanics Conference, Auckland, New Zeeland, p. 1-6.

O'Sullivan, M.J., Bullivant, D.P., Follows, S.E. & Mannington, W.I., 1998: Modelling of the Wairakei – Tauhara geothermal system. Proceedings of the TOUGH Workshop '98, Lawrence Berkeley National Laboratory, California, USA, p. 1-6.

O'Sullivan, M.J., Pruess, K. & Lippmann, M.J., 2001: State of art of geothermal reservoir simulation. Geothermics, 30, p. 395-429.

Onur, M., Sarak, H., Tureyen, I., Cinar, M. & Satman, A., 2008: A new non-isothermal lumped-parameter model for low temperature, liquid dominated geothermal reservoirs and its application. Proceedings 33th Workshop on Geothermal Reservoir Engineering, Stanford University, CA, p. 1-10.

Ozgener, L., Hepbasli, A., Dincer, I. & Rosen, M.A., 2007: A key review on performance improvement aspects of geothermal district heating systems and applications. Renewable and Sustainable Energy Reviews, 11, p. 1675-1697.

Pachocká, K., Jacko, S. & Pachocki, M., 2010: 3D modeling of a geothermal reservoir in Eastern Slovakia. VDM Verlag Publ. Saarbrücken, 62 p.

Pasquale, V., Gola, G., Chiozzi, P. & Verdoya, M., 2011: Thermophysical properties of the Po Basin rocks. Geophysical Journal International, 186, p. 69-81.

Pastakia, C.M.R. & Jensen, A., 1998: The Rapid Impact Assessment Matrix (RIAM) for EIA. Environmental Impact Assessment Reviews, 18, p. 461-482.

Peiffer, L., Wanner, C., Spycher, N., Sonnenthal, E.L., Kennedy, B.M. & Iovenitti, J., 2014: Optimized multicomponent vs. classical geothermometry: Insights from modeling studies at the Dixie Valley geothermal area. Geothermics, 15, p. 154-169.

Pereszlenyi, M., Pereszlenyiova, A. & Masaryk, P., 1999: Geological setting of the Košice Basin in relation to geothermal energy resources. Bulletin d'Hydrogeologie, 17, p. 115-122.

Phillips, J., 2010a: The advancement of a mathematical model of sustainable development. Sustainable Science, 5, p. 127-142.

Phillips, J., 2010b: Evaluating the level and nature of sustainable development for a geothermal power plant. Renewable and Sustainable Energy Reviews, 14, p. 2414-2425.

Popovičová, M. & Holoubek, D., 2011: Binary geothermal power plant using n-pentane at Ďurkov, Slovakia. Acta Metallurgica Slovaca, 2, 1, p. 172-175.

Rabinowitz M., Sempéré J-Ch. & Genthon P., 1999: Thermal convection in a vertical permeable slot: Implications for hydrothermal circulation along mid-ocean ridges. Journal of Geophysical research, 104, B12, p. 29275-29292.

Reyes, J.L.P., Lee, K., Chen, Ch.Y. & Horne, R.N., 2004: Calculation of steam and water relative permeabilities using field production data, with laboratory verification. Geothermal Resource Council Transactions, 28, p. 1-12.

Rubinstein, R.Y. & Krosese, D.P., 1991: Simulation and Monte Carlo method, 2nd Edition. Wiley-Interscience, USA.

Rybach, L., 2007: Geothermal sustainability. Proceeding European Geothermal Congress 2007, Unterhaching, Germany, p. 1-5.

Rybach, L., 2010a: The future of geothermal energy and its challenges. Proceedings World Geothermal Congress 2010, Bali, Indonesia, 8 p.

Rybach, L., 2010b: Status and prospects of geothermal energy. Proceedings World Geothermal Congress 2010, Bali, Indonesia, 8 p .

Rybach, L., 2015: Classification of geothermal resources by potential. Geothermal Energy Science, 3, p. 13-17.

Rybach, L. & Mongillo, M., 2006: Geothermal sustainability – a review with identified research needs. Geothermal Resource Council Transactions, 30, p. 1083-1090.

Rybach, L., Mégel, T. & Eugster, W.J., 1999: How Renewable are Geothermal Resources? Geothermal Resources Council Transactions, 23, p. 563-567.

Sanyal, S.K., 2005: Sustainability and renewability of geothermal power capacity. Proceedings World Geothermal Congress 2005, Antalya, Turkey, p. 1-13.

Sanyal, S.K. & Sarmiento, Z.F., 2005: Booking geothermal energy reserves. Geothermal Resource Council Transactions, 29, p. 467-474.

Sarak, H., Onur, M. & Satman, A., 2003a: Application of lumped parameter models for simulation of low-temperature geothermal reservoirs. Proceedings 28th Workshop on Geothermal Reservoir Engineering, Stanford University, CA, 9 p.

Sarak, H., Onur, M. & Satman, A., 2003b: New lumped parameter models for simulation of low-temperature geothermal reservoirs. Proceedings 28th Workshop on Geothermal Reservoir Engineering, Stanford University, CA, 8 p.

Sarak, H., Onur, M. & Satman, A., 2005: Lumped-parameter models for low-temperature geothermal fields and their application. Geothermics, 34, 6, p. 728-755.

Sarmiento, Z.F., Steingrímsson, B. & Axelsson, G., 2013: Volumetric resource assessment. Proceedings, Short Course V on Conceptual Modelling of Geothermal Systems, UNU-GTP, Santa Tecla, El Salvador.

Satman, A., 2010: Sustainability of a geothermal reservoir. Proceedings World Geothermal Congress 2010, Bali, Indonesia, p. 1-13.

Satman, A., 2011: Sustainability of geothermal doublets. Proceedings 36th Workshop on Geothermal Reservoir Engineering, Stanford University, CA, p. 1-6.

Satman, A. & Tureyen, O.I., 2012: Sustainability factors for doublets and conventional geothermal systems. Proceedings 37th Workshop on Geothermal Reservoir Engineering, Stanford University, CA, p. 1-6.

Sauty, J.P., Gringarten, A.C., Landel, P.A. & Mejoz, A., 1980: Lifetime optimization of low enthalpy geothermal doublets. In: Strub A.S., Ungemach, P. (Eds.): Advances in European Geothermal Research. D. Reidel Publications Co., NL, p. 706-719.

Sclater, J.G. & Christie, P.A.F., 1980: Continental stretching: an explanation of the post Mid-Cretaceous subsidence of Central North Sea Basin. Journal of Geophysical Research, 85, p. 3711-3739.

Sheldon, H.A., Reid, L.B., Florio, B. & Kirkby, A.L., 2011: Convection or conduction? Interpreting temperature data from sedimentary basins. Proceedings Australian Geothermal Energy Conference, Melbourne, Australia, p. 1-4.

Shortall, R., Davidsdottir, B. & Axelsson, G., 2015a: Geothermal energy for sustainable development: A review of sustainability impacts and assessment frameworks. Renewable and Sustainable Energy Reviews, 44, p. 391-406.

Shortall, R., Davidsdottir, B. & Axelsson, G., 2015b: Methodology for designing a sustainability assessment framework for geothermal energy developments. Proceedings World Geothermal Congress 2015, Melbourne, Australia, p. 1-10.

Spycher, N., Peiffer, L., Sonnenthal, E.L., Saldi, G., Reed, M.H. & Kennedy, B.M., 2014: Integrated multicomponent solute geothermometry. Geothermics, 51, p. 113-123.

Stefansson, V., 2005: World Geothermal Assessment. Proceedings World Geothermal Congress 2005, Antalya, Turkey.

Stefansson, V. & Axelsson, G., 2005: Sustainable utilization of geothermal resources through stepwise development. Proceedings World Geothermal Congress 2005, Antalya, Turkey, p. 1-6.

Sutter, D., Fox, D.B., Anderson, B.J., Koch, D.L., von Rohr, P.R. & Tester, J.W., 2011: Sustainable Heat Farming of Geothermal Systems: a Case Study of Heat Extraction and Thermal Recovery in a Model EGS Fractured Reservoir. Proceedings 36th Workshop on Geothermal Reservoir Engineering, Stanford University, CA, USA, p. 1-11.

Takahashi, S. & Yoshida, S., 2016: Improvement of calculating formulas for volumetric resource assessment. Geothermics, 64, p. 187-195.

Tester, J.W., Anderson, B.J:, Batchelor, A.S., Blackwell, D.D., DiPippo, R., Drake, E.M., Garnish, J., Livesay, B., Moore, M.C., Nichols, K., Petty, S., Toksoz, M.N. & Veatch Jr., R.W., 2006: The future of geothermal energy. Massachusetts Institute of Technology, 372 p.

Tureyen, O.I. & Akyapi, E., 2011: A generalized non-isothermal tank model for liquid dominated geothermal reservoirs. Geothermics, 40, p. 50-57.

Tureyen, O.I., Onur, M. & Sarak, H., 2009: A generalized nonisothermal lumped-parameter model for liquid dominated geothermal reservoirs. Proceedings 34th Workshop on Geothermal Reservoir Engineering, Stanford University, CA, p. 1-10.

Tureyen, O.I., Kirmaci, A. & Onur, M., 2014: Assessment of uncertainty in future performance predictions by lumped-parameter models for single-phase liquid geothermal systems. Geothermics, 51, p. 300-311.

Ungemach, P., Antics, M. & Papachristou, M., 2005: Sustainable geothermal reservoir management. Proceedings, World Geothermal Congress Antalya, Turkey.

Ungemach, P., Papachristou, M. & Antics, M., 2007: Renewability versus Sustainability. A reservoir management approach. Proceedings, European Geothermal Congress 2007, Unterhaching, Germany.

Ungemach, P., Antics, M. & Lalos, P., 2009: Sustainable geothermal reservoir management practice, Geothermal Resources Council Transactions, 33, p. 885-891.

Utlu, Z. & Hepbasli, A., 2008: Energetic and exergetic of the industrial sector at varying dead (reference) state temperatures: A review with an illustrative example. Renewable and Sustainable Energy Reviews, 12, p. 1277-1301.

Vizi, L., Fričovský, B., Zlocha, M. & Surový, M., 2020: Use of geostatistical simulation in reservoir thermodynamics assessment and interpretation at the Ďurkov hydrogeothermal structure, Slovakia. Slovak Geological Magazine, 20 (1), [this issue].

Vranovská, A. & Bodiš, D., 1999: Survey for prospective utilization of geothermal energy in Košice Basin. Bulletin d'Hydrogeologie, 17, p. 106-113.

Vranovská, A., Bodiš, D. & Drozd, V., 1999a: Zhodnotenie hydrogeotermálnej štruktúry Ďurkov na základe vrtov GTD-1,2 a 3 [*Evaluation of hydrogeothermal structure Ďurkov based on wells GTD-1,2 and 3*]. Podzemná voda, V (2), p. 45-53.

Vranovská A., Bondarenková,Z., Král M. & Drozd, V., 1999b: Košická kotlina - štruktúra Ďurkov - hydrogeotermálne zhodnotenie, vyhľadávací prieskum. [*Košice Basin – Ďurkov structure, hydrogeothermal evaluation, exploratory survey*]. Manuscript – Technical report. Bratislava: SLOVGEOTERM, Geofond Archive, 90 p. [in Slovak].

Vranovská, A., Beňovský, V., Drozd, V., Halás, O. & Váňa, O., 2000: Investigation for geothermal energy utilization in the town Košice, Slovak Republic. Proceedings World Geothermal Congress 2000, Kyushu-Tohoku, Japan, p. 1-6.

Vranovská, A., Beňovský, V., Drozd, V., Halás, O. & Váňa, O., 2002: The results of pilot test in Ďurkov hydrogeotermal structure. Geol. Carpathica, 53 (2), p. 1-6.

Vranovská, A., Bodiš, D., Šráček, O. & Ženišová, Z., 2015: Anomalous arsenic concentrations in the Ďurkov carbonate

geothermal structure, eastern Slovakia. Environmental Earth Science, 73, p. 7103-7114.

Williams, C.F., 2007: Updated methods for estimating recovery factors for geothermal resources. Proceedings, 32nd Workshop on Geothermal Reservoir Engineering, Stanford University, CA.

Williams, C.F., 2014: Evaluating the volume method in the assessment of identified geothermal resources. Geothermal resource council transactions, 38, p. 967-974.

Williams, C.F., Lawless, J.V., Ward, M.A., Holgate, F.L. & Larking, A., 2010: A code for geothermal resources and reserves reporting. Proceedings world geothermal congress 2010, Bali, Indonesia.

Williams, C.F., Reed, M.J. & Anderson, A.F., 2011: Updating the classification of geothermal resources. Proceedings, 36th Workshop on Geothermal Reservoir Engineering, Stanford University, Stanford, California.

Yasukawa, K. & Sasada, M., 2015: Country update of Japan: Renewed Opportunities. Proceedings World Geothermal Congress 2015, Melbourne, Australia, p. 1-6.

Yousefi, H., Ehara, S., Yousefi, A. & Seiedi, F., 2009: Environmental impact assessment of Salaban geothermal power plant, NW Iran. In: Proceedings 34th Workshop on Geothermal Reservoir Engineering, Stanford University, CA, p. 1-9.